

**PROCESSING AND CHARACTERIZATION OF GLASS FLAKE
REINFORCED THERMOPLASTIC POLYMER MATRIX BIO-INSPIRED
BULK LAMELLAR COMPOSITES**

AYLİN GÜNEŞ

AUGUST 2014

PROCESSING AND CHARACTERIZATION OF GLASS FLAKE REINFORCED
THERMOPLASTIC POLYMER MATRIX BIO-INSPIRED BULK LAMELLAR
COMPOSITES

A THESIS SUBMITTED TO
THE GRADUATE SCHOOL OF NATURAL AND APPLIED SCIENCES
OF
MIDDLE EAST TECHNICAL UNIVERSITY

BY

AYLİN GÜNEŞ

IN PARTIAL FULFILLMENT OF THE REQUIREMENTS
FOR
THE DEGREE OF MASTER OF SCIENCE
IN
METALLURGICAL AND MATERIALS ENGINEERING

AUGUST 2014

Approval of the thesis:

**PROCESSING AND CHARACTERIZATION OF GLASS FLAKE
REINFORCED THERMOPLASTIC POLYMER MATRIX BIO-INSPIRED
BULK LAMELLAR COMPOSITES**

submitted by **AYLİN GÜNEŞ** in partial fulfillment of the requirements for the degree of **Master of Science in Metallurgical and Materials Engineering Department, Middle East Technical University** by,

Prof. Dr. Canan Özgen _____
Dean, Graduate School of **Natural and Applied Sciences**

Prof. Dr. C. Hakan Gür _____
Head of Department, **Metallurgical and Materials Engineering**

Assoc. Prof. Dr. Arcan Fehmi Dericioğlu _____
Supervisor, **Metallurgical and Materials Engineering Dept. METU**

Examining Committee Members:

Prof. Dr. Cevdet Kaynak _____
Metallurgical and Materials Eng. Dept., METU

Assoc. Prof. Dr. Arcan Fehmi Dericioğlu _____
Metallurgical and Materials Eng. Dept., METU

Prof. Dr. Cemil Hakan Gür _____
Metallurgical and Materials Eng. Dept., METU

Assist. Prof. Dr. Mert Efe _____
Metallurgical and Materials Eng. Dept., METU

Prof. Dr. Göknur Bayram _____
Chemical Engineering Dept., METU

Date:21.08.2014

I hereby declare that all information in this document has been obtained and presented in accordance with academic rules and ethical conduct. I also declare that, as required by these rules and conduct, I have fully cited and referenced all material and results that are not original to this work.

Name, Last name : Aylin Güneş

Signature :

ABSTRACT

PROCESSING AND CHARACTERIZATION OF GLASS FLAKE REINFORCED THERMOPLASTIC POLYMER MATRIX BIO-INSPIRED BULK LAMELLAR COMPOSITES

Güneş, Aylin

MSc., Department of Metallurgical and Materials Engineering

Supervisor: Assoc. Prof. Dr. Arcan F. Dericioğlu

August 2014, 104 pages

The aim of this study was to develop processing pathways to fabricate glass flake reinforced bio-inspired composites with microstructural architecture similar to that of nacre using two processing routes based on hot-pressing and magnetic field assistance. Glass flakes with different aspect ratios were used as inorganic reinforcement in two different thermoplastic matrices, polystyrene (PS) and acrylonitrile butadiene styrene (ABS). Correlation between inorganic content, microstructural architecture and mechanical property enhancement of the composites fabricated by various process combinations was examined. To investigate the effect of inorganic-organic phase interfacial interaction and adhesion on the mechanical properties of the fabricated composites, glass flakes surfaces were treated with an organofunctional silane called aminopropyltriethoxy silane. X-Ray Photoelectron Spectroscopy (XPS) was used to analyze the adsorption of silane molecules on the inorganic reinforcement surfaces. Mechanical properties of the fabricated composites were examined using three point bending, micro hardness and work of fracture tests.

Results indicated that hot-pressing and magnetic field assistance based methods are easy and effective pathways to fabricate nacre-like bulk inorganic-organic composites with brick and mortar microstructural architecture. Composites fabricated by these two different pathways reinforced by glass flakes exhibited improved mechanical characteristics such as higher flexural strength, stiffness and hardness. Treatment of the glass flake surfaces by silane further enhanced the mechanical properties of the fabricated composites, where it provided simultaneous improvement in both strength and fracture resistance of the composites, which is the main challenging task to be achieved in the field of materials science from a structural point of view.

Keywords: Bio-inspired composites, Artificial nacre, Hot-pressing based methods, Magnetic Field Assistance based methods, Silane coupling

ÖZ

CAM PLAKA TAKVİYELİ TERMOPLASTİK POLİMER MATRİSLİ DOĞADAN ESİNLENİLMİŞ HACİMLİ KOMPOZİT ÜRETİMİ VE KARAKTERİZASYONU

Güneş, Aylın

Yüksek Lisans, Metalurji ve Malzeme Mühendisliği Bölümü

Tez Yöneticisi: Doç. Dr. Arcan Fehmi Dericioğlu

Ağustos 2014, 104 sayfa

Bu çalışma kapsamında, sıcak presleme ve manyetik alanla destekleme tabanlı yöntemler kullanılarak mikroyapısı itibarıyla doğal sedefe benzeyen cam plaka takviyeli kompozitlerin üretimi amaçlanmıştır. Polistren (PS) ve akrilonitril butadiyen stiren (ABS) olmak üzere iki farklı termoplastik matris malzemesi ve en-boy oranı farklı cam plaka takviye malzemesi kullanılmıştır. Çeşitli yöntemlerle üretilen kompozitlerde farklı miktardaki inorganik malzemenin mikroyapısı ve mekanik özelliklere etkileri araştırılmıştır. İnorganik ve organik fazlar arasındaki arayüzey etkileşimi ve tutunmanın üretilen kompozitlerin mekanik özelliklerine etkilerini araştırmak amacıyla cam plaka yüzeyleri aminopropiltrioksil silan olarak adlandırılan bir organofonksiyonel silan ajanıyla modifiye edilmiştir. Modifiye edilmiş inorganik takviye malzeme yüzeyleri X-Işınları Fotoelektron Spektroskopisi (XPS) yöntemi ile karakterize edilerek silan ajan malzemesinin yüzeye tutunup tutunmadığı incelenmiştir. Üretilen kompozitlerin mekanik özellikleri üç noktadan bükülme, mikro sertlik ve kırılma testleri kullanılarak belirlenmiştir.

Elde edilen sonuçlar, sıcak presleme ve manyetik alanla destekleme tabanlı yöntemlerin sedef benzeri tuğla-ve-harç mikroyapı mimarisine sahip hacimli inorganik-organik kompozit malzemelerin üretiminde kullanılacak kolay ve efektif bir üretim metodu olduğunu göstermiştir. İki farklı tabana dayalı üretim metodlarıyla üretilen ve cam plaka takviye malzemesiyle güçlendirilen kompozitler eğme mukavemeti, eğilmezlik ve sertlik özelliklerinde gelişme göstermiştir. Silanlama ile yüzeyleri modifiye edilen cam plakalarla takviye edilmiş kompozitler yapısal malzeme alanındaki asıl amaç olan eş zamanlı olarak yüksek mukavemet ve kırılma dayanımına sahip olma yönünde mekanik özelliklerinde gelişme göstermiştir.

Anahtar Kelimeler: Doğadan esinlenen kompozitler, Yapay sedef, Sıcak presleme destekleme tabanlı yöntemler, Manyetik alan destekleme tabanlı yöntemler, Silanlama.

To My Family

ACKNOWLEDGEMENTS

Foremost, I would like to thank Assoc. Prof. Arcan Fehmi Dericiođlu for tremendous guidance, incredible patience, support, extraordinary encouragement and trust. Moreover, I would thank Prof. Dr. Őakir Bor for his indebted guidance, tremendous help and support.

I am thankful to my previous and current lab mates: Eda Aydođan, Őzgür Hamat, Güney Dalođlu, Dr. Selen Nimet Gürbüz Güner, Simge Tülbez and Seray Kaya and to my friends: Murat Yalçın, Őzgür Başkan Tařtan and especially to Emin Erkan Ařık, Dr. Gül İpek Nakař and Benu Tunca and I am grateful for precious love and support to Bođaç Karçıka.

I am also grateful to all the staff of the Department of Metallurgical and Materials Engineering, Res. Assoc. Serkan Yılmaz, Őnder Őahin and Yusuf Yıldırım.

I owe a debt to my dear family for their endless love, support and encouragement throughout my life.

TABLE OF CONTENTS

ABSTRACT.....	v
ÖZ.....	vi
ACKNOWLEDGEMENTS.....	viii
TABLE OF CONTENTS.....	ix
LIST OF TABLES.....	xii
LIST OF FIGURES.....	xiii
CHAPTERS	
1. INTRODUCTION.....	1
2. LITERATURE REVIEW.....	5
2.1 Natural Materials.....	5
2.2 Composite Materials.....	6
2.3 Bio-inspired Materials.....	7
2.4 Nacre.....	9
2.4.1 Mechanical Behavior of Nacre.....	13
2.4.2 Hierarchical Structure of Nacre.....	16
2.4.3 Organic Phase in Mollusc Shell Structure.....	21
2.4.4 Possible Fabrication Methods of Composite Materials Inspired by Nacre.....	26
2.5 Inorganic Surface Functionalization with Organofunctional Silane.....	31

2.6 Applied Surface Characterization Techniques	32
2.6.1 X-Ray Photoelectron Spectroscopy	32
2.6.2 Fourier Transformed Infrared Spectroscopy.....	32
3. EXPERIMENTAL PROCEDURE.....	33
3.1 Raw Materials.....	36
3.2. Fabrication of Nacre-Like Polystyrene or Acrylonitrile Butadiene Styrene Matrices Bulk Lamellar Composites Using As Received Glass Flakes.....	41
3.3 Fabrication of Nacre-Like Bulk Lamellar Thermoplastic Matrix Composites Using Surface Modified Glass Flakes	46
3.3.1 Surface Modification of Glass Flakes with Aminopropyltriethoxy Silane	46
3.3.2 Surface Modification Cationic Magnetite Nanoparticle Solution	47
3.3.3 Fabrication of Polystyrene Matrix Composites Reinforced by Surface Modified Glass Flakes.....	48
3.4 Characterization.....	49
3.4.1 Determination of Inorganic Reinforcement Content and Density	49
3.4.2 Microstructural Characterization	50
3.4.3 Mechanical Characterization	50
3.4.3.1 Hardness Measurement	50
3.4.3.2 Three-Point Bending Tests.....	51
3.4.3.3 Work of Fracture Tests.....	51

3.4.4 X-Ray Photoelectron Spectroscopy (XPS).....	52
3.4.5 Fourier Transform Infrared Spectroscopy (FTIR).....	52
4. RESULTS AND DISCUSSION	53
4.1 Fabrication of Nacre like Bulk Lamellar Thermoplastic Polymer Matrix Composite Materials	53
4.2 Magnetite Nanoparticle Attached Gkass Flake Reinforced Nacre-Like Bulk Lamellar Composites Fabricated by Magnetic Field Assistance	80
5. CONCUSION.....	93
REFERENCES	97

LIST OF TABLES

TABLES

Table 3.1. Properties of glass flakes used in this dissertation	36
Table 3.2. Chemical Analysis of glass flakes	37
Table 4.1. Inorganic content, density, relative density (%) and hardness obtained by four different process combinations in ABS or PS matrix composites	59
Table 4.2. Inorganic content, density, relative density (%) and hardness of AC+HASC processed ABS or PS matrix composites reinforced by as-received or silane treated glass flakes	75
Table 4.3. Density, relative density (%) and hardness of the fabricated composites for three different initial polymer contents (wt% PS	85

LIST OF FIGURES

FIGURES

Figure 2.1 (a) water strider, (b) sem images of a water strider leg covered by numerous oriented needle-shaped microsetae, (c) sem image of grooved nanostructure on the seta surface [39], (d) bio inspired au/tio ₂ photocatalyst derived from butterfly wing (papilio paris) [40]	8
Figure 2.2 Overall view of hierarchical structure of abalone shell, showing mesolayers, mineral tiles, tile pullout in a fracture region [41].....	9
Figure 2.3 The hierarchical structure of nacre (Growth line image from Menig et al. (2000), Nanograins from Rousseau et al. (2005)) [2]	10
Figure 2.4 Strength vs density of natural materials [4]	11
Figure 2.5 Comparison of mollusc shell with other natural materials in terms of toughness –modulus diagram [4].....	12
Figure 2.6 (a) Stress-strain curve of nacre in tension along the tablets, (b) schematic showing tablet sliding [42].....	14
Figure 2.7 (a) Stress – strain curves of simple shear (s-s) and shear compression (s-c) responses of dried and hydrated nacre, (b) transverse strain as function of shear strain [42].....	15
Figure 2.8 Strength of nacre under different loading directions [44].....	15

Figure 2.9 Hierarchical structure of nacre [50-54]	17
Figure 2.10 Interlocking mechanisms in nacre [19].....	18
Figure 2.11 (a) Schematic illustration showing interlocks between platelets of nacre showing that rotation of levels of platelets is essential for the formation of platelet interlocks, (b) schematic illustration showing the mechanism of loading through a cross-section cut across platelets and (c) through the interlocks [19]	19
Figure 2.12 Stress-strain plots of nacre with interlocks as obtained from 3D finite element simulations with failure sequence of interlocks superimposed. The stress-strain plot shows good strength as well as high toughness which is proportional the area under the curve [19].....	20
Figure 2.13 Various views of organic layer in nacre subjected to tensile test (Field-emission SEM); (a, b) layers hanging between two tiles (marked with arrow); (c, d) top view of tile surface with organic layer networks [41].....	22
Figure 2.14 Increase of modulus of elasticity of nacre as a function of the Poisson's ratio of the organic matrix [18].....	23
Figure 2.15 (a) Stress-strain curves measured in tensile test of dried and hydrated nacre. The insets illustrate the deformation behavior during loading, (b) deformation behavior in the work-hardening stage in the stress-strain curve(SEM image). Platelets are progressively pulled out in an accumulative manner [8]	24
Figure 2.16 Schematic diagram of deformation behavior of proteins with modular structures [8].....	25

Figure 2.17 Hierarchical toughening mechanism of nacre. Toughening can be classified according to the operating dimension, from an inter-platelet mechanism operating at the sub micrometer scale, to an intra-platelet mechanism of the order of several tens of nanometers, down to individual organic molecules (nm scale) [8].....	25
Figure 2.18 Schematic illustration for the fabrication of artificial nacre (a) LBL, self-assembly of DAR/PAA multilayered film via the alternating deposition method; (b) preparation of CaCO ₃ nanolaminated structure on the DAR/PAA multilayered films by CO ₂ gas diffusion method; (c) preparation of the multilayer organic/inorganic hybrid composite by alternately repeating steps (a) and (b) [60].....	27
Figure 2.19 Bottom up colloidal assembly of multilayered hybrid films. Surface modified platelets are assembled at the air-water interface to produce a highly oriented layer of platelets after ultrasonication. The 2D assembled platelets are transferred to a flat substrate and afterwards covered with a polymer layer by conventional spin coating [61].....	28
Figure 2.20 Schematic Illustration of Hot press Assisted Slip Casting (HASC) Method [13].....	29
Figure 2.21 Processing route for the production of platelet-reinforced composites with tailored architectures using mechanical and magnetic stimuli. Solenoids are used to keep the alignment of the ultrahigh magnetic response (UHMR) -platelets while curing the composites inside an oven at 60°C [15].....	30
Figure 2.22 Silane treatment reactions [65]	31

Figure 3.1 Flow chart of the fabrication procedures applied in this study (a) Hot-Pressing based methods, (b) Magnetic Field Assistance based method.....	34
Figure 3.2 Scanning electron microscope images a) Micronised glass flakes, b) Unmilled glass flakes.....	37
Figure 3.3 Polystyrene a) structure of monomer and polymer b) structure of syndiotactic Polystyrene (PS) in highly crystalline form	39
Figure 3.4 Different chemical structures in ABS.....	40
Figure 3.5 Chemical structure of Acrylonitrile Butadiene Styrene.....	40
Figure 3.6 Chemical Structure of Aminopropyltriethoxy silane.....	41
Figure 3.7 Schematic representation of Tape Casting (TC) method.....	45
Figure 3.8 Schematic representation of Hot press Assisted Slip Casting (HASC) method.....	45
Figure 3.9 Silane treatment reactions.....	47
Figure 4.1. Fracture surfaces of TC+HASC processed PS matrix composites composed of different glass flake mixtures containing (a) 10 wt%, (b) 20 wt%, (c) 5 wt%, (d) 80 wt% and (e) 90 wt% high aspect ratio glass flakes (GF 750).....	55
Figure 4.2. Scanning electron microscope images of the a) ABS matrix and b) PS matrix composites fabricated by AC+HP process where the pores are shown by arrows.....	60

Figure 4.3. Scanning electron microscope images of composites fabricated by TC+HASC route (a) presence of spherical pores, (b) adhesion of the polymer matrix on the glass flake surfaces.	61
Figure 4.4. Schematic representation of the simple mixed and tape casted films into steel die before hot press assisted slip casting solution.....	63
Figure 4.5. Flowing of polymer solution like plug between flakes [21].....	64
Figure 4.6. Restitution in a viscoelastic fluid [21].....	65
Figure 4.7. Scanning electron microscope images of the fracture surfaces of the three point bending tested PS matrix composites fabricated by (a) AC+HASC, (b) TC+HASC, (c) TC+HP and (d) AC+HP.....	66
Figure 4.8. Scanning electron microscope images of the fracture surfaces of the three point bending tested ABS matrix composites fabricated by (a) AC+HASC, (b) TC+HASC, (c) TC+HP and (d) AC+HP.....	67
Figure 4.9. Flexural stress vs. strain curves of PS matrix composites fabricated by the four process combinations.....	69
Figure 4.10. Flexural stress vs. strain curves of ABS matrix composites fabricated by the four process combinations.....	69
Figure 4.11. Variation in mechanical properties of acrylonitrile butadiene styrene and polystyrene polymer matrices composites fabricated by AC+HASC method.....	71
Figure 4.12. XPS spectra of (a) as-received and (b) silane treated glass flakes.....	73

Figure 4.13. Fracture surfaces of three point bending tested AC+HASC processed PS matrix composites reinforced by (a) and (c) as-received and (b) and (d) silane treated glass flakes.....	76
Figure 4.14. Fracture surfaces of three point bending tested AC+HASC processed ABS matrix composites reinforced by (a) and (c) as-received and (b) and (d) silane treated glass flakes.....	77
Figure 4.15. Flexural stress vs. strain curves of AC+HASC processed PS and ABS matrix composites reinforced by as-received and silane treated glass flakes.....	78
Figure 4.16. Schematic representation of the interaction between aminoproyltriethoxy silane and polymer chains [23].....	79
Figure 4.17. Load- extension curves of SENB specimens of AC+HASC processed PS and ABS matrix composites reinforced by as-received and silane treated glass flakes.....	80
Figure 4.18. Color difference between as-received and nanoparticle attached glass flakes before and after filtering the processing solution.....	81
Figure 4.19 Optical microscope image of the surface modified glass flakes aligned on the hard magnet.....	82
Figure 4.20 FTIR spectra of (a) as-received and (b) magnetite nanoparticle attached glass flakes.....	83

Figure 4.21 Fracture surfaces of the three point bending tested composites fabricated by magnetic field assistance and HP containing (a) 38 wt %, (b) 43 wt % and (c) 53 wt % PS matrix	86
Figure 4.22. Three point bending test data of composites fabricated by magnetic field assistance followed by HP having different amounts of polymer matrix.....	87
Figure 4.23. Schematic representation of the chemical interaction between the magnetite nanoparticles attached on the glass flake surfaces with polystyrene molecules.....	88
Figure 4.24. Fracture surfaces of the three point bending tested 53 wt% PS matrix containing composites fabricated by magnetic field assistance and HP reinforced by (a) only magnetite nanoparticle attached glass flakes and (b) magnetite nanoparticle attached and then silane treated glass flakes.....	89
Figure 4.25. Three point bending test data of composites fabricated by magnetic field assistance followed by HP having different amounts of polymer matrix also including the silane treated one.....	90
Figure 4.26. Load vs. extension curves of WOF tested composites fabricated by magnetic field assistance followed by HP process having different amounts of polymer matrix also including the silane treated one.....	91

CHAPTER 1

INTRODUCTION

In the last few years, needs of mankind has increased extremely, and hence, people need to innovative new structural materials especially for energy, defense and aerospace applications. Materials to be fabricated or redesigned should not only supply basic requirements for a specific life time but also should be energy efficient and environment friendly during their production and service. As a result of these, scientists have been focusing on the natural materials, which have excellent microstructural architectures and designs leading to extraordinary mechanical property combinations, creating a new scientific area called “Bio- inspired” materials [1-5].

Nature has extraordinary composite materials that have unique designs and properties. Among most of the natural composites, nacre demonstrates high strength along with high fracture resistance based on its unique architectural design. Nacre, the mother-of-pearl, located on the interior surface of the mollusc shell is a natural composite composed of an inorganic and organic component (95 vol% CaCO_3 and 5 vol% protein) [6-10] efficiently combining these components providing unique mechanical properties.

Although there are successful results reporting on the brick and mortar architecture composed of thermoset polymers as the organic component and CaCO_3 , alumina or glass platelets as inorganic component [11,12-21], mechanical test results illustrated low fracture resistance due to the inherent brittleness of the thermoset polymers used in the structure. Therefore, to overcome this limitation changing the polymer type to thermoplastics could

be a solution to reach improvement in the mechanical behavior. In this research, use of thermoplastic polymers namely polystyrene and acrylonitrile butadiene styrene and glass flakes with different dimensions in nacre-like bio-inspired composites has been proposed.

In the last years, there are numerous studies about bio-inspired materials, and especially for nacre structure both thin film and bulk composite production methods improve rapidly [16-18]. However, recently nanocomposite and nano materials are popular research areas as a result of which most of the studies in this field concentrate on thin film formed bio-inspired materials rather than bulk ones. Among the processing methods of thin film formed bio-materials most frequently studied ones are self-assembly, layer by layer deposition, physical vapor deposition, chemical vapor deposition, self-deposition and centrifugal deposition [13-19]. All of these methods and the others could be helpful to create nacre-like thin film structures. However, there are also some efficient methods for fabricating nacre-like bulk lamellar composites which aim to obtain alignment of flake or platelet formed inorganic reinforcements in the composite structure.

In this context, the main aim of this study is to develop new processing pathways to control inorganic phase orientation in the bulk formed bio-inspired composites. For this purpose, one of the methods used is Hot Press Assisted Slip Casting (HASC), which was one of the processes applied in this study using different thermoplastic polymer matrices [11]. In addition to this, tape casting and magnetic field assistance were also incorporated to potential processing combinations to achieve brick-and-mortar structure similar to that of nacre yet in a bulk composite.

In this dissertation, different from the popular approaches leading to thin film formed bio-inspired composites, efforts have been focused on fabricating bulk nacre-like composites as potential structural materials. Furthermore, most of the previous studies report on the fabrication of nacre-like thermoset polymer matrix composites, especially epoxy matrix; on the

contrary to these thermoplastic polymers namely polystyrene and acrylonitrile butadiene styrene were used in this study as the matrix of the nacre-like composites because of their biodegradable nature and recyclability. Each polymers has own characteristic properties and depend on these properties, by changing some parameters such as temperature or pressure and keeping same methodology, it is demonstrated that Hot press Assisted Slip Casting method and tape casting method are two beneficial techniques to fabricate nacre-like bulk laminar polymer matrix composite materials.

One of the possible approaches to further enhance the mechanical properties of organic-inorganic composites is to use a coupling agent between these phases which is an organofunctional silane. Silane treatment is a common procedure especially for industrial composite production. Silane is an important chemical substance and the most important feature of silane is to provide the interaction between the inorganic and organic components. It functions like a chemical bridge at the interface enhancing the bonding, and hence the mechanical qualification of the composite materials. There are different kinds of silanes available for different applications. Selection of proper silane and its treatment on inorganic surfaces and resulting polymer-surface interaction properties are important features defining the overall success of the silanization. In the scope of this study, aminopropyltriethoxy silane (APTES) has been used to modify the glass flake surfaces so that they can interact with the polystyrene and acrylonitrile butadiene styrene matrices more effectively.

To conclude, there are different kinds of techniques present to fabricate nacre-like bulk lamellar composites, yet different combinations of hot press assisted slip casting, tape casting and magnetic field assistance are being proposed as alternative routes to create nacre-like bulk composites available for structural applications. Replacing the thermoset matrix frequently used in such composites with a thermoplastic one and further improving its

mechanical properties with possible surface treatments, environment friendly composites can be presented as alternative structural materials.

This thesis is composed of five chapters. In Chapter 2 general information about natural materials and composites, especially about nacre, and processing methods of nacre-like bio-inspired composites have been introduced. Specifically, structure and mechanical property vs. structure relationship of nacre has been mentioned. Chapter comprises the raw materials, details of the different processing pathways used during the fabrication of the nacre-like composites as well as the methods used for their characterization. In Chapter 4, results obtained results have been presented and discussed. Conclusions have been pointed out in Chapter 5.

CHAPTER 2

LITERATURE REVIEW

2.1 Natural Materials

Before the beginning of human creation and after human beings, nature has indisputable rules. The relationship between nature and human beings and interpretation of nature leads to the basic rules of science. Consequently, nature is a big source to understand the creatures and universe. Dependently, all of the scientists have observed, inferred and inspired from nature. Especially to be inspired by nature, there are lots of examples such as seashell, spider silk, butterfly wings, bamboos, seaweeds, coconuts etc [22-24]. All of these natural materials have great material properties chemically, mechanically or structurally.

One of these magnificent materials is nacre in other words the inner layer of mollusc shell. It is composed of inorganic and organic components. As inorganic phase, nacre includes 95 vol % CaCO_3 and as organic phase, it contains 5 vol % protein (as lustrins and β -chitin) [6-10, 22-24]. The extraordinary point in nacre structure is that it is composed of mostly inorganic part; however mechanical behavior of this natural composite is excellent when compared to other highly inorganic containing composites. This behavior could clarify not only the chemical interaction between inorganic and organic phase but also the geometrical arrangement in nacre (mother of pearl) structure. These exceptions of nacre make it desirable to be mimicked and to fabricate versatile materials in nacre like arrangement.

Following subheadings include detailed information about mimicking of natural materials and structural and chemical mechanism of mother of pearl.

2.2 Composite Materials

Composite materials are formed the combine the physical and chemical properties of two or more materials to create new superior materials. Some composite materials, which were found in nature, have been used by people ever since prehistorically [24]. However, by developing the technological arguments with new material requirements generated the need to more advantageous materials. As a result of many studies after Second World War there has been a rapid increase in producing and discovering new materials and new substances [25-29]. There is a huge spectrum for composite materials. However, most recognized composite materials are in nature. In addition to that, natural composite materials have superior material properties, such as high strength, stiffness and robustness. So, these results have also affected the composite material research area, and by inspiring and mimicking nature, composite production has changed and improved.

Following the investigation of new polymers, which are more applicable for industrial applications, and evolved knowledge about composite materials, there has been a division in composite material production as polymer matrix composites, ceramic matrix composites and metal matrix composites [26, 27, 30]. All these groups include their own material properties, and now in the world there is a high number of application areas of all these different types of composites.

Polymer matrix composite structures are used in industry for improved strength and stiffness of the composites where generally as reinforcement fibers are being used [27,28,29]. However, the aim of this dissertation is the fabrication of polymer matrix composites by using glass flakes in different aspect ratios as reinforcement materials.

2.3 Bio-inspired Materials

Nature has remarkable materials with intriguing hierarchical arrangement, design and mechanical properties. Analyzing natural materials has provided the reason why natural materials have higher mechanical and structural properties, which has led to a new research area called ‘‘Bio-inspired materials.’’ In the world, there are huge research laboratories and many articles about bio-inspired materials [25, 26, 30-37]. Now, there are many investigations on natural materials, to imitate natural compounds by using different types of substances. Although resulting materials have not revealed higher toughness values compared to natural ones, imitating the hierarchical architecture of these natural materials has led to improved structural and mechanical results [38]. In Figure 2.1 some sources of bio-inspiration studies are shown.

One of the main reasons to produce materials similar to natural materials is their excellent mechanical properties. In the new world conditions, there is a trend to use less energy to fabricate yet to obtain good results. However, under natural conditions, there is very long time to create excellent structures. So, by applying scientific improvements, producing bio-inspired materials with properties closer to those of natural ones has been the aim of this research area.

With the aspect of producing mechanically reliable materials relatively easy, most of the natural materials such as nacre, bone, wood, spider silk, bamboo etc. have been used as sources of bioinspiration, and scientists could develop easy processing methods [25, 26, 30-37]. This material processing method have been improving day by day, and with the investigation of new material properties found in nature creation of new processing methods has been possible. Therefore, bioinspired materials have attracted growing attention in scientific world supplying effective results both industrially and scientifically.

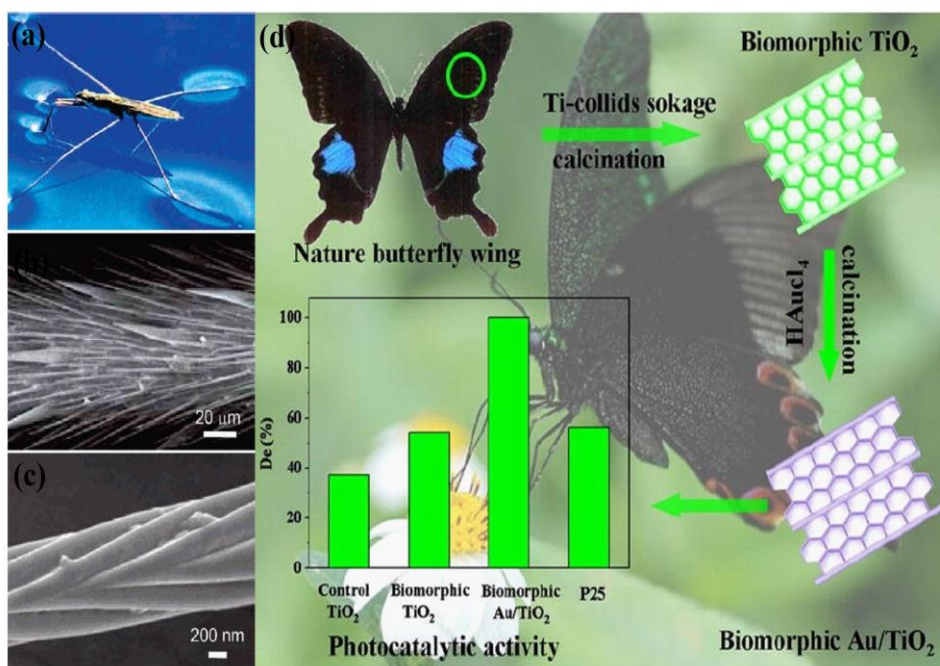


Figure 2.1 (a) Water Strider, (b) SEM images of a water strider leg covered by numerous oriented needle-shaped microsetae, (c) SEM image of grooved nanostructure on the seta surface [39], (d) Bio inspired Au/TiO₂ photocatalyst derived from butterfly wing (Papilio Paris) [40].

Long time ago, getting inspiration from nature has proven itself to be successful to fulfill the needs. Still nature teaches and shows scientists lots of exciting behaviors and scientific ideas. There are lots of studies on bioinspiration, however; this study especially focuses on bio-inspiration from nacre, i.e. mother of pearl. In Figure 2.2 microstructure of nacre is demonstrated.

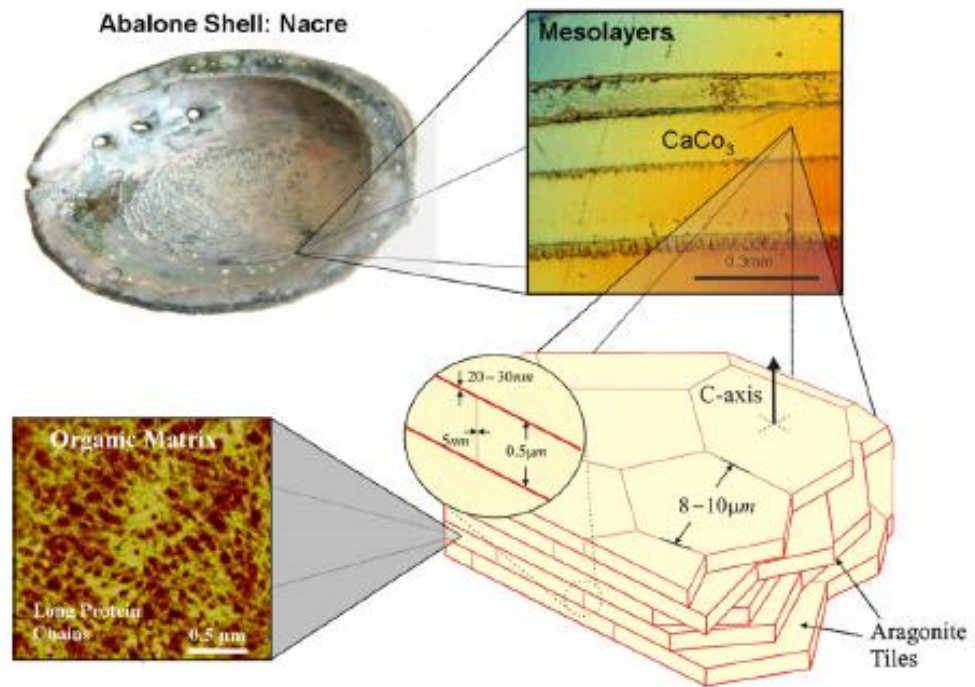


Figure 2.2 Overall view of hierarchical structure of abalone shell, showing mesolayers, mineral tiles, tile pullout in a fracture region [41].

2.4 Nacre

Nacre is one of the natural composite materials that have special structure. It contains 95 vol % inorganic phase (CaCO_3) and 5 vol % organic phase (proteins such as lustrins and β -chitin) [16-20]. Nacre, i.e. mother of pearl, has extraordinary mechanical behavior even though it has very high inorganic content. Containing 95 vol % inorganic phase nacre is almost a ceramic, yet the difference of mother of pearl from the ceramic materials is to have superior toughness and strength by superimposing the components [1-10, 16, 17, 18, 34, 41, 42]. As a result of these specific properties nacre could be a special case to be investigated scientifically, and most of the scientists are inspired by this natural composite to fabricate strains and tough composite materials. Figure 2.3 shows the hierarchical arrangement of nacre from macro to nano scale nacre structure.

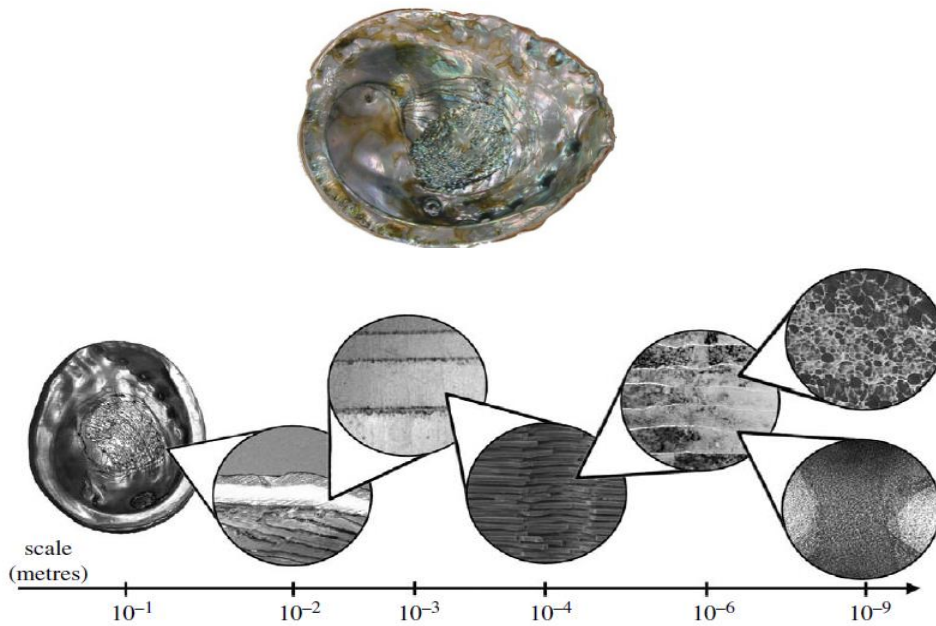


Figure 2.3 The hierarchical structure of nacre (Growth line image from Menig et al. (2000), Nanograins from Rousseau et al. (2005)) [2].

There are numerous natural composite materials and each of them shows different type of superior behavior. Mother of pearl reveals excellent mechanical behavior when compared to most of the natural materials. The main phase in nacre is aragonite which is a crystalline polymorph of calcium carbonate. In Figure 2.4, the comparison between aragonite and other natural materials is presented. This specific strength graph shows that aragonite has a remarkable specific strength. This helps to increase the strength of the mother of pearl. However, as the natural composite materials are combinations of different materials with varying interactions, they show nonuniform strength distribution, even though the average strengths might be considerably high.

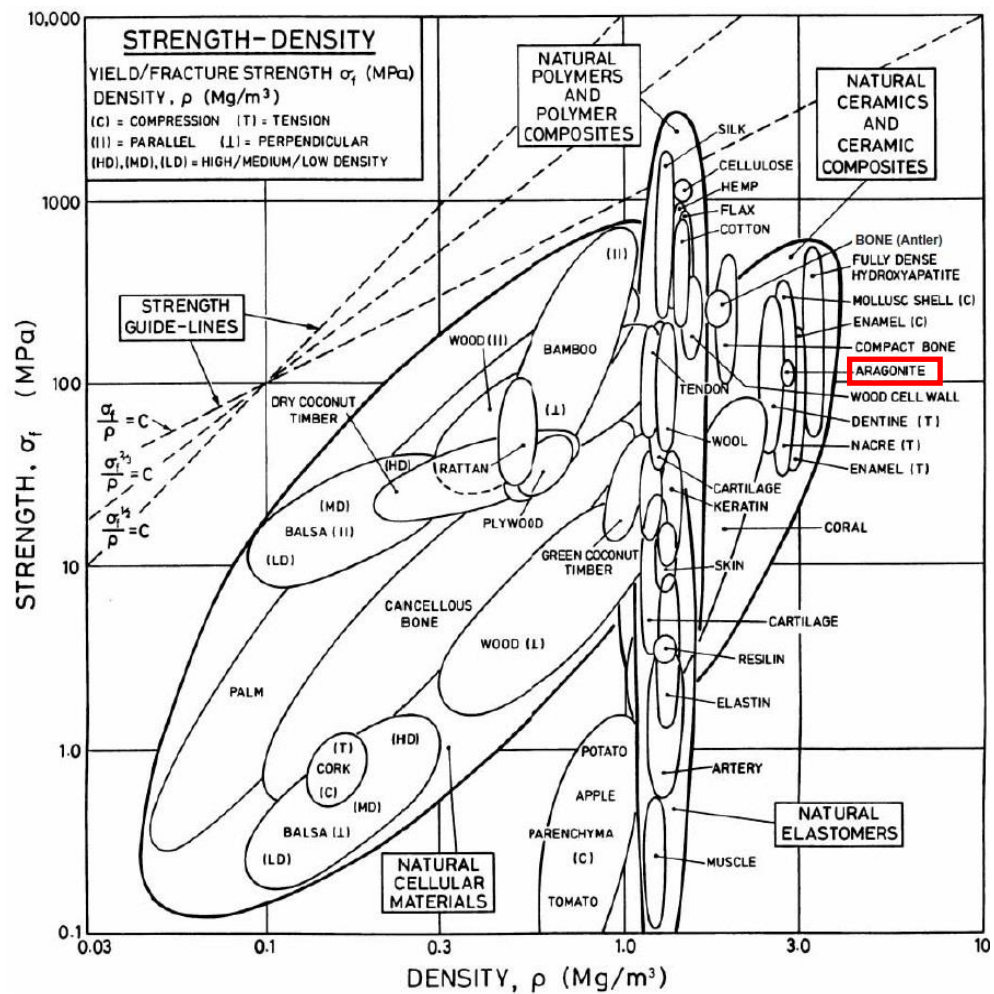


Figure 2.4 Strength vs density of natural materials [4].

High strength and toughness of nacre is based on two main reasons which are the hierarchical structure of mother of pearl and the intrinsic mechanical characteristics of its inorganic and organic phases.

Mollusc shell is formed according to possible pathways to defend itself from natural predators, and structure of this animal directly illustrates an armor behavior. The outer part of the shell is the hardest part in the structure and inner layer of the structure is tough meaning that it is one of the most excellent armor to provide survival in the nature [4, 42]. The comparison of

toughness and modulus of the mollusc shell with those of the other natural materials is given in Figure 2.5.

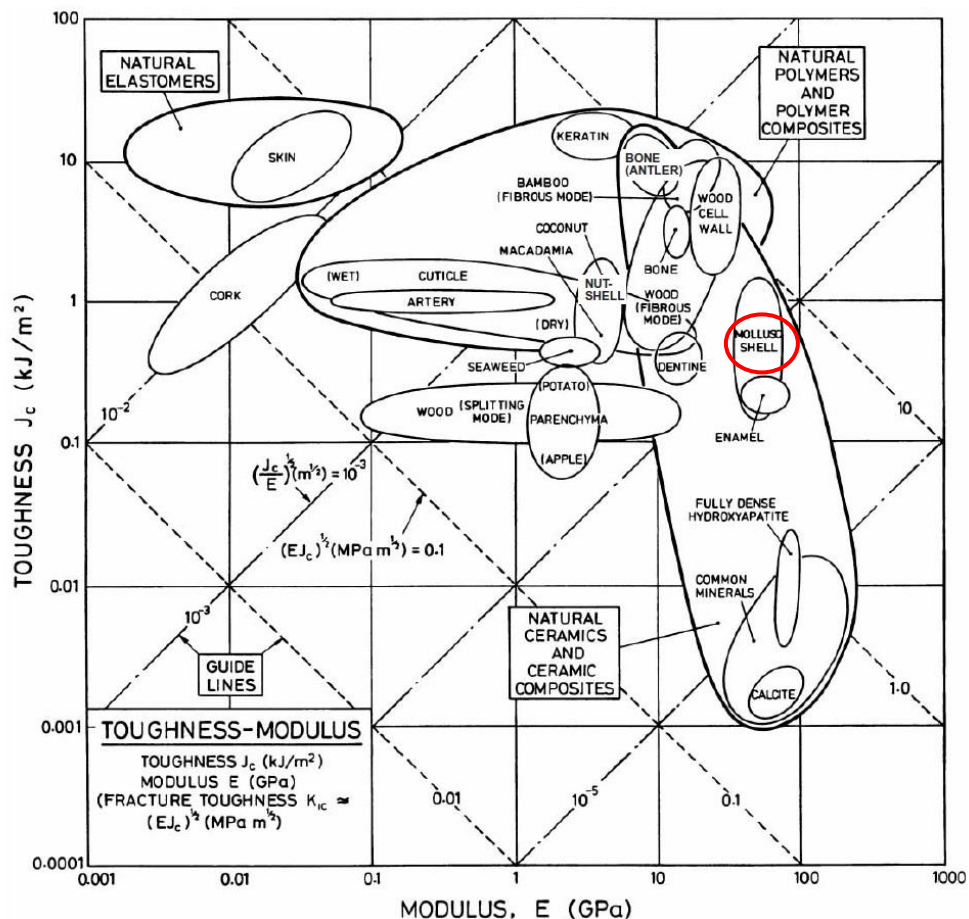


Figure 2.5 Comparison of mollusc shell with other natural materials in terms of toughness and modulus [4].

Nacre has a complex mechanical behavior mechanism. Inorganic phase nucleation, mineral bridging, nanoasperities, waviness, arrangement, organic phase defolding play crucial role to get the unique properties. Detailed information about all of these parameters are given in the following section.

2.4.1 Mechanical Properties of Nacre

Materials have some advantages and disadvantages according to their type which are ceramics, metals and polymer. While investigating these materials separately, each of them reveals superior behavior in terms of different aspects. According to this division, polymers show more elastic behavior than others while ceramics show more brittle behavior than others. Looking at these general rules, nacre should reveal brittle behavior. Nevertheless, although nacre contains large inorganic content, it demonstrates high strength and toughness. Therefore, mechanical behavior of nacre is composed of some exceptional mechanical cases.

The main advantage of nacre is its high compressive and tensile strength. In addition to these it also shows high toughness and high elastic modulus which depend on both the friction mechanism between aragonite platelets and the waviness of platelets that are based on the arrangement of the platelets and organic matrix behavior in the structure.

The investigation of nacre started with its behavior under tension. The reason is that a probable attack in the natural medium of mother of pearl directly causes tensile stress [42, 43]. Tensile properties of nacre are different in dry and wet condition. According to the tensile test results of the nacre, wet condition possesses superior mechanical properties than dried. In Figure 2.6, tensile behavior of mother of pearl in two different physical conditions is given. The main difference of nacre in tension arises from the inorganic-organic phase interaction governed by sliding and friction between aragonites. According to these results, dried nacre behaves like a monolithic ceramic, however; hydrated nacre shows more inelastic behavior. In tension, tablets slide and void content increases, and it is directly the reason of failure in the structure.

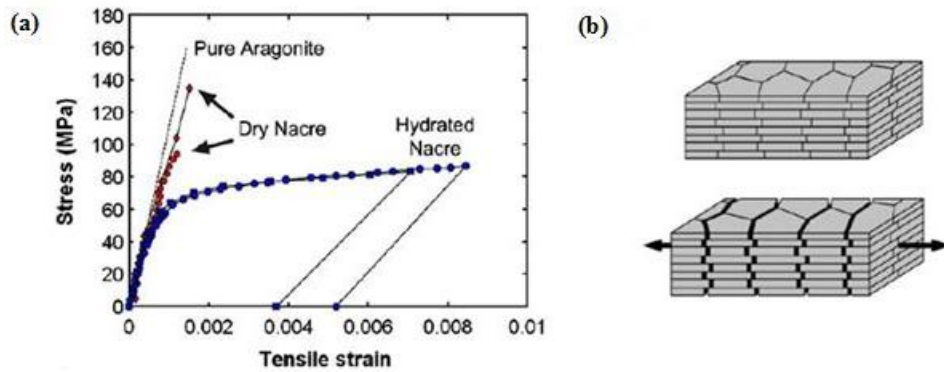


Figure 2.6 (a) Stress-strain curve of nacre in tension along the tablets, (b) schematic showing tablet sliding [42].

However, the tensile response reverses in shear. In tension most probably caused by the organic matrix, hydrated nacre is higher in strength than the dried nacre. While investigating the shear properties, dried nacre is stronger than hydrated one. This mechanical result brings out the more complex mechanical approach, the shear strength measurement reveals that the organic bridging between tablets could provide a limited compensation in compression and shear. The important mechanical features in the structure are waviness and friction force between platelets that are higher in dried condition.

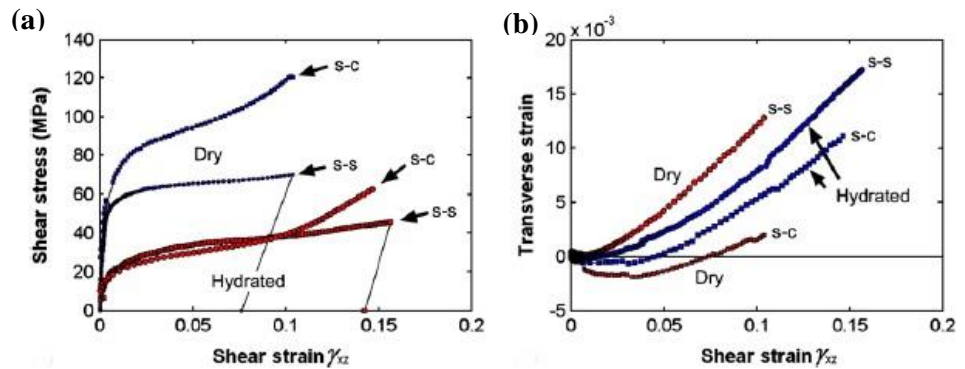


Figure 2.7 (a) Stress – strain curves of simple shear (s-s) and shear compression (s-c) responses of dried and hydrated nacre, (b) transverse strain as function of shear strain [42].

All of these mechanical behaviors could be summarized in Figure 2.7. Nacre is strong, tough and stiff and its shear, compression and bending response can be observed in the following microstructural sketch.

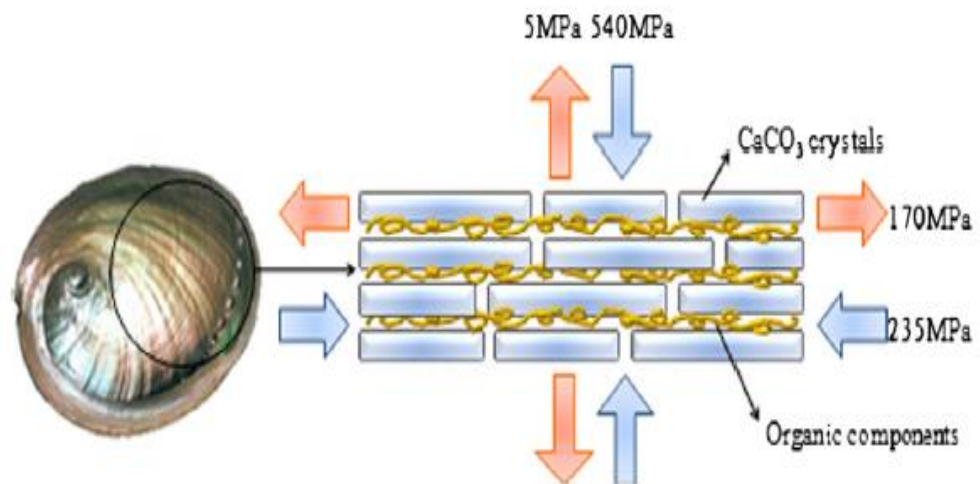


Figure 2.8 Strength of nacre under different loading directions [44].

Mechanical behavior of the mother of pearl principally depends on the toughening mechanism. Scientists investigate the nacre structure deeply, yet

even they observe the nacre structure at nano scale, they could not understand its mechanical behavior completely [6-8,18,42]. However in the micrometer scale hierarchical structure of the inorganic phase and the interaction of the organic phase with the inorganic phase show the excellent properties in terms of mechanical strength [1, 2, 6-10, 16, 18, ,41-45]. The toughening mechanism could be explained as when the load is applied to the nacre, the sliding of platelets occurs. Normally, there should be huge friction energy on weak platelets; however, because of the excellent interaction between phases, the friction energy formed due to sliding is distributed. Distribution of the energy behaves like work hardening mechanism so by means of energy distribution applied load increases up to deforming the structure. This work hardening mechanism in the polymeric structure leads to whitening, and it is similar to metal work hardening behavior [2, 4, 6-10, 18, 41-45]. All of these mechanical processes form an efficient energy dissipating system in the structure. In the sub- micrometer scale, the crucial part is caused from the interaction between nano grains and the organic phase. In this part, organic phase provides the resilience, and mechanism due to the viscoelasticity of the organic component the energy dissipating reaches to an efficient state [2, 4, 6-10, 18, 41-45]. At the last part of the structure molecular domains are considered, and toughening mechanism in this part is based on the refolding and unfolding of the molecular domains [18, 42]. The refolding and unfolding of protein domains is observed when load is applied. While the work hardening behavior is observed, the refolding of domain happens; however, deformation is seen when protein domain is unfolded. Consequently, this special toughening mechanism induces the inspiration form nature.

2.4.2 Hierarchical Structure of Nacre

Hierarchical structure of nacre is another key point. This impressive structural arrangement is also the reason behind the high mechanical qualifications of nacre. The structure is defined as ‘brick and mortar’ architecture, and in Figure 2.9 brick and mortar structure of nacre can be

observed. The important approach about the nacre hierarchical structure is called Voronoi model. Voronoi model explains the inorganic phase nucleation based on a systematic. The nucleation starts between platelets and according to the nucleated platelets, the shape of growing platelet structure is like stairs [46]. Therefore, it causes a variation in mechanical behavior. The mechanical behavior of the part of lap-streak platelets termed as core is different than the other part [46-49].

Alignment of CaCO_3 platelets, which possess brick and mortar structure, provides the efficient mechanical result. In addition to this, it is an explanation of how this high inorganic content composite material could show extremely remarkable toughness and strength combination.

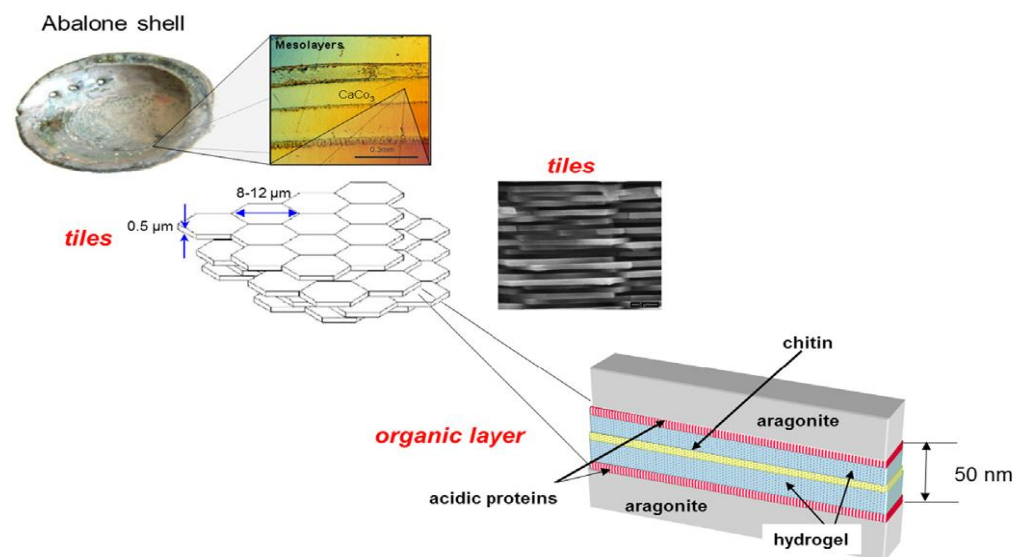


Figure 2.9 Hierarchical structure of nacre [50-54].

The special architecture of nacre leads to an efficient energy dissipating system. This means that applying load on nacre energy could disperse in an effective way, and it results in high loading capacity. Another crucial point in this structure and in energy dissipating system of nacre is the interlocking mechanism. Interlocking mechanism shows penetration of platelets between

each other, and this penetration between platelets is not a disadvantage; on the contrary, it could be one of the best structural means to improve mechanical properties. This beneficial interlocking behavior provides distribution of energy leading to high toughness [9-18]. In Figure 2.10, interlocking mechanism can clearly be seen.

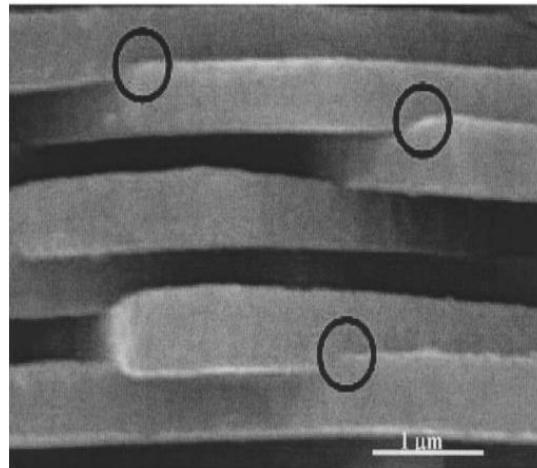


Figure 2.10 Interlocking mechanisms in nacre [9].

Penetration of upper platelet to lower platelet results in a rotation between platelets, and this interlocking mechanism occurs after the rotation. One of the crucial reasons to get high toughness and strength values of mother of pearl is to have this geometrical deformation. First deformation mechanism in the interlocking platelets is observed in the organic phase of the structure. The deformation can be calculated by applying load to these platelets in two dimensions. It is like a shear mechanism so the first expected deformation is observed between platelet and organic layer, as organic layer has lower elastic modulus than platelets (Figure 2.11). This interfacial response is a sign of the strength of the platelets as well. After the organic phase deforms the interlocking zone damages, and these steps are directly related with each other.

Scientists have been studying especially the effect of interlocking mechanism of platelets on the strength of nacre. To demonstrate and clarify interlocking mechanism some of the finite element method have been used, and 3D observation could have been achieved from the modelling efforts [9].

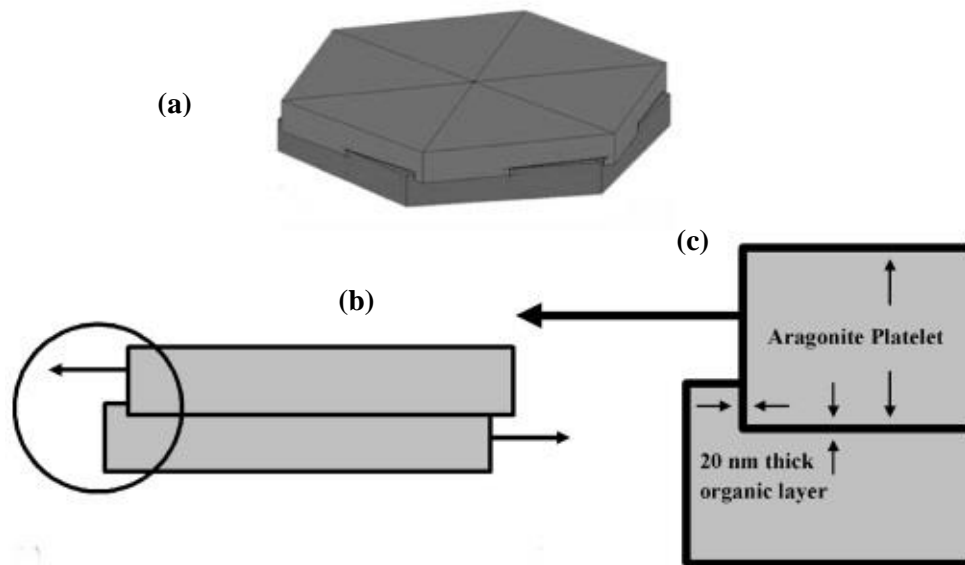


Figure 2.11 (a) Schematic illustration showing interlocks between platelets of nacre showing that rotation of levels of platelets is essential for the formation of platelet interlocks, (b) schematic illustration showing the mechanism of loading through a cross-section cut across platelets and (c) through the interlocks [9].

Scientists who study the simulation of nacre structure and effect of interlocks investigate the two different conditions such as forming interlocking between platelets and non-forming interlocking. It is an essential investigation to understand the importance of interlocking. Moreover, results showed that without interlocking formation, organic phase in mother of pearl structure exhibits plastic behavior and in 14 MPa this plastic deformation leads to the failure of nacre. When the interlocks are

introduced to nacre structure, it takes time to fail all interlocks and it could be thought like work hardening mechanism. The applied load for failure of all interlocks in nacre reaches up to 50 MPa [6-9]. Therefore, results and demonstrations clearly showed the effect of interlocking on the mechanical properties of nacre and the significant development of mechanical strength. The mechanical behavior of interlocking platelets could be observed in Figure 2.12. In this Figure the effect of failure, and how it provides the increase in the applied load for failure can be followed.

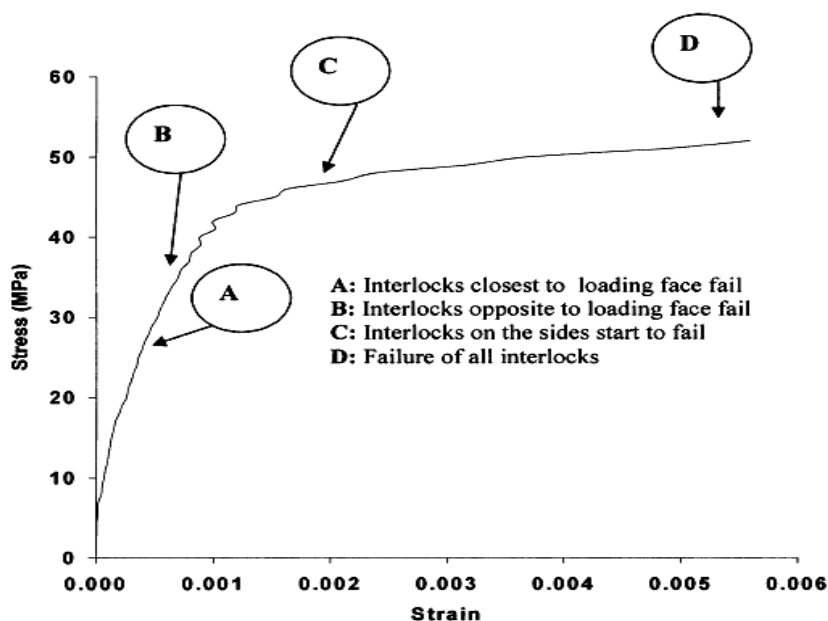


Figure 2.12 Stress-strain plots of nacre with interlocks as obtained from 3D finite element simulations with failure sequence of interlocks superimposed. The stress-strain plot shows good strength as well as high toughness which is proportional the area under the curve [19].

Consequently, the geometry of structure during formation and the mechanic changes in the structure could supply higher toughness and strength. Among most of the feasible natural composite materials, nacre has a great advantage and exception to have high inorganic content. Therefore, to overcome the disadvantages of highly inorganic composition and to survive in nature,

nacre enhances its structural and mechanical properties. In recent years, although influential explanations on the mechanical properties of mother of pearl have been provided, still there are huge unknown aspects in the mechanical properties of nacre. One of the understood mechanical behaviors is the interlocking mechanism, and this mechanism acts like work hardening mechanism rising the mechanical strength nacre.

2.4.3 Organic Phase in Mollusc Shell Structure

The organic phase of the nacre structure is one of the beneficial parts of this extraordinary composite material. Organic part in the nacre structure is a protein which is called β -chitin [1-6, 16 -56]. Although the organic content in nacre is quite low when compared to inorganic content (95 vol % aragonite -5 vol %protein), it has a very crucial role in the mechanical behavior of the mother of pearl. The most important contribution of the organic phase in the mechanical properties is elasticity. This small part in the composite material and its contribution on elasticity leads to improved mechanical properties. However, it is also effective on the stiffness. According to Hooke's Law, longitudinal strain decreases while increasing transverse stress. Therefore, relationship between elasticity and Hooke's law could be satisfied. The result of this interaction shows that the organic content increment at some point could show effective results in terms of stiffness and poisson's ratio. Studies on organic phase of nacre structure and simulations have shown that the organic phase ensures crucial results on stiffness of material [8]. According to the results of strength and strain values, the factors of mineral bridging and asperities have a crucial role in mechanical behavior especially for fracture. While fracture happens in nacre structure, mineral bridging and asperities behave as obstacles leading to increased applied loads [18, 41]. In Figure 2.13, mineral bridging and organic phase in nacre structure are shown clearly.

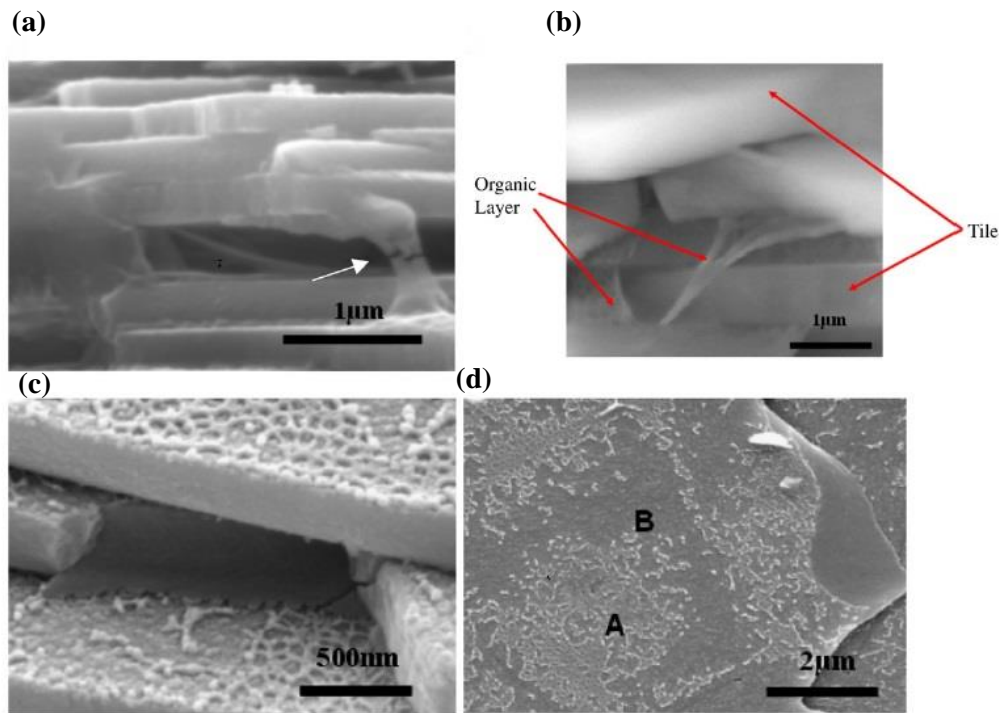


Figure 2.13 Various views of organic layer in nacre subjected to tensile test (Field-emission SEM); (a, b) layers hanging between two tiles (marked with arrow); (c, d) top view of tile surface with organic layer networks [41].

Organic phase in the structure creates elastic behavior, and it affects directly the force distribution i.e. mechanical results of this impressive structure. This small amount in mother of pearl leads to magnificent results in terms of stiffness. In Figure 2.14 effect of organic matrix on modulus of elasticity of nacre is shown.

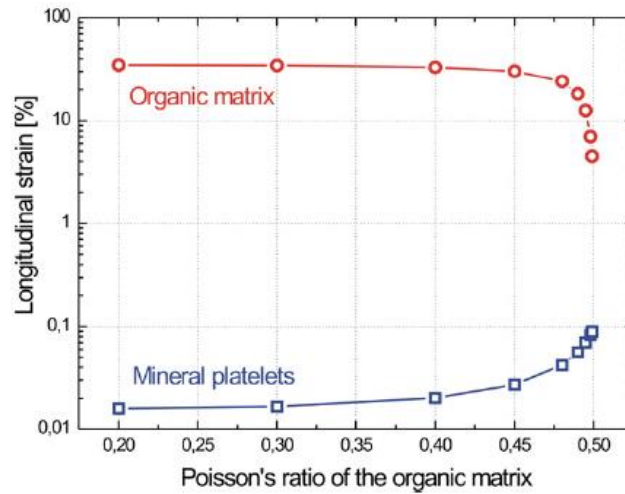


Figure 2.14 Increase of modulus of elasticity of nacre as a function of the Poisson's ratio of the organic matrix [18].

One of the effects of the organic phase on mechanical behavior depends on the hydration of the polymer. There are two different behaviors of nacre, one of them includes dry organic phase, and the other is in the case of hydrated proteins. These two cases show different mechanical properties. When the structure is hydrated, this basically creates more flexibility. Actually, these properties are related with the interfacial interactions however; they could also lead to brittle behavior. Macro scale composite behavior shows clearly the importance and contribution of organic phase in the viscoelastic property and resilience of the material [18]. In Figure 2.15, stress-strain differences between hydrated nacre and dried nacre are demonstrated.

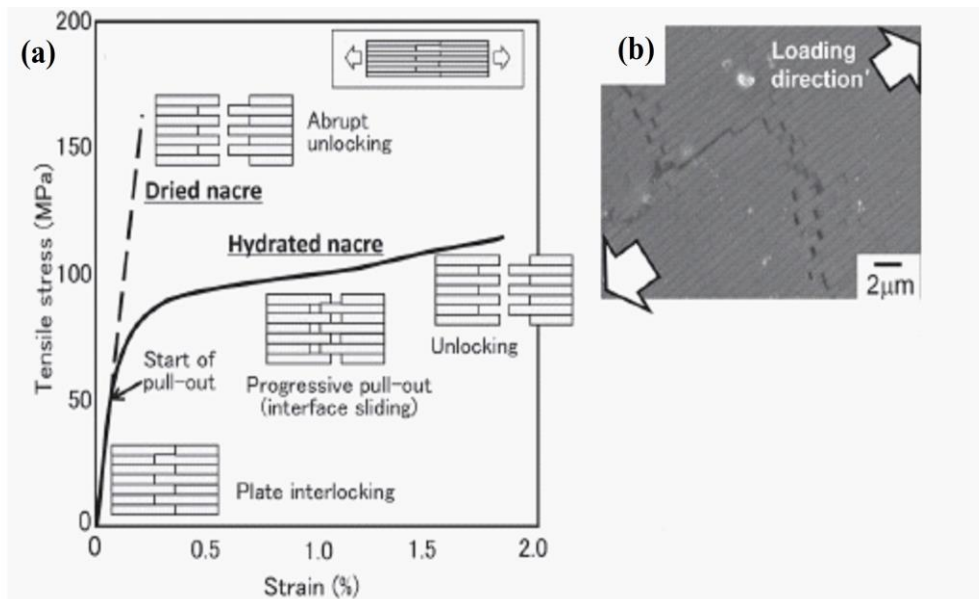


Figure 2.15 (a) Stress-strain curves measured in tensile test of dried and hydrated nacre. The insets illustrate the deformation behavior during loading, (b) deformation behavior in the work-hardening stage in the stress-strain curve (SEM image). Platelets are progressively pulled out in an accumulative manner [18].

One of the interesting parts in nacre behavior about organic phase is observed in the nanoscale. In this part, nano grain and organic bridging are main part of the structure, while deep in the structure molecular toughening mechanism is operative. This mechanism is composed of folding and unfolding of proteins. These folding and unfolding reinforces the work hardening mechanism, so it has control on toughness increment directly [18]. Mechanical effects of folding and unfolding are shown in Figure 2.16.

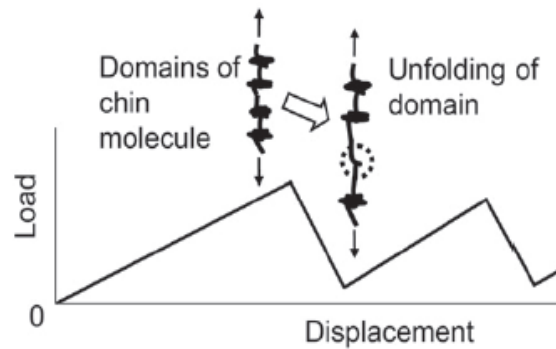


Figure 2.16 Schematic diagram of deformation behavior of proteins with modular structures [8].

In Figure 2.17, there is scale about nacre structure and observation of organic phase. In this chart, structure of nacre, toughening mechanism of nacre and the role of organic phase has been clarify.

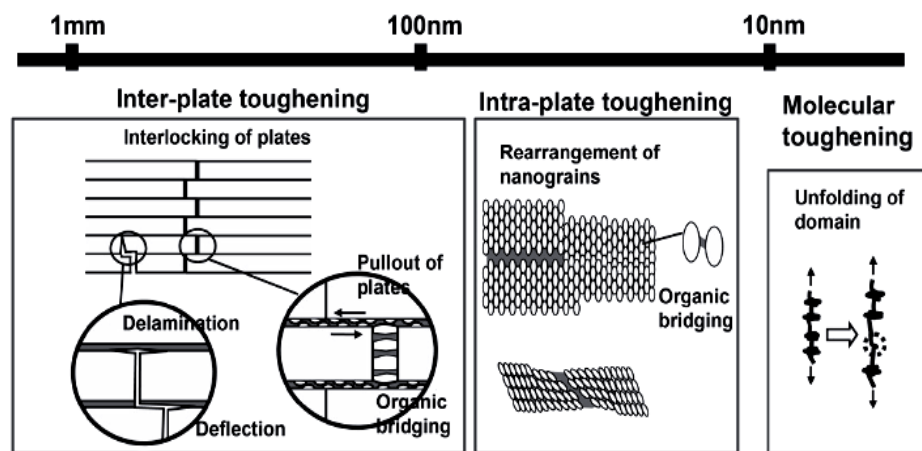


Figure 2.17 Hierarchical toughening mechanism of nacre. Toughening can be classified according to the operating dimension, from an inter-platelet mechanism operating at the sub micrometer scale, to an intra-platelet mechanism of the order of several tens of nanometers, down to individual organic molecules (nm scale) [18].

2.4.4 Possible Fabrication Methods of Composite Materials Inspired by Nacre

After the discovery of superior behavior in terms of high strength and toughness of nacre, scientists started to look at possible fabrication methods for composite materials inspired by nacre. Investigations of nacre hierarchical structure and mechanical behavior have triggered the efforts to develop some fabrication pathways. Some of these production methods are well-known now such as layer by layer (LBL), Self-Assembly, Thin Film Coating, Hot press Assisted Slip Casting (HASC), Tape Casting, Magnetic Field Interaction etc. These methods are being discussed below showing the production of nacre like architecture with achieved mechanical results.

Layer by layer assembly method is one of the general methods to create organic-inorganic composites by imitating nacre structure [20, 57-60]. Wei and his collaborators have studied fabrication of nacre-like nanocomposite using layer by layer assembly. This bottom up approach is applied using polymer thin films of diazo resins (DAR) and polyacrylic acids (PAA) as organic phase with CaCO_3 strata as inorganic constituent. The aim of that study is to ensure hierarchical structure of nacre in nanoscale. The procedure of this method and effective organic and inorganic interaction can be observed in Figure 2.18.

Wei and his collaborates pointed out to the attraction of interfaces where the interaction between interfaces is helpful to provide one of the main properties of nacre, which is its hierarchical structure in other words brick and mortar arrangement. Thanks to these useful structural strategies of mother of pearl, layer by layer method could be improved and Wei's study is one of the examples of this effective method using different components than nature. Article proposes that combining of necessary amount of chemicals and supplying efficient temperature, diffusion and nucleation could be observed and the brick and mortar arrangement can be reached.

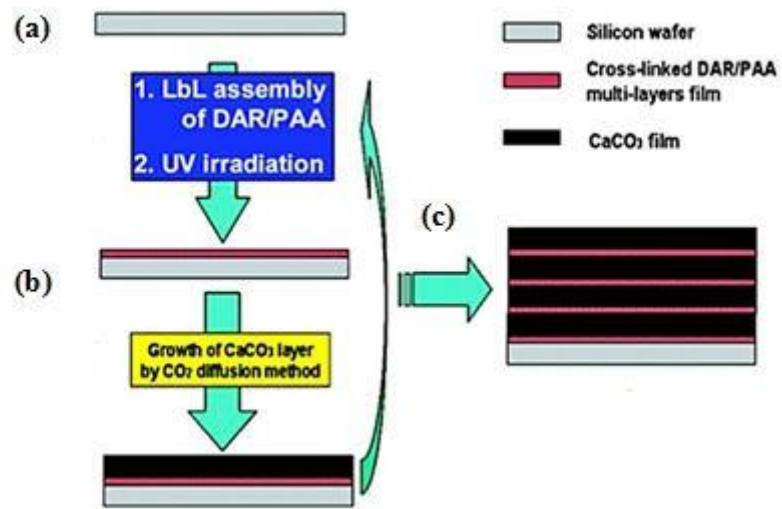


Figure 2.18 Schematic illustration for the fabrication of artificial nacre (a) LBL, self-assembly of DAR/PAA multilayered film via the alternating deposition method; (b) preparation of CaCO₃ nanolaminated structure on the DAR/PAA multilayered films by CO₂ gas diffusion method; (c) preparation of the multilayer organic/inorganic hybrid composite by alternately repeating steps (a) and (b) [60].

Self-assembly is one of the common processing methods to reach nacre like architecture [19, 61-63]. This technique is one of the examples to provide one of the main properties of mother of pearl, which is its hierarchical structure. After the investigation of this excellent arrangement as mentioned above, the crucial part is control the interaction of two chemically different phases. There are various ways and chemical reactions, to control this interaction. One of them is very common, and this is widely used in industry which is silane treatment. Bonderer et al. used this chemical treatment to get superior mechanical properties.

Silane is a different type of chemical. It is called as coupling agent generally, and the main property of this coupling agent is to supply the

interfacial bonding between inorganic and organic phases. It behaves like a bridge so its composition directly affects the mechanical behavior of the material. Bonderer et al. explained the contribution of the silane application on mechanical results. Bonderer's study showed that while using alumina platelets with CaCO_3 and applying silane treatment on them, the effect of reinforcement on the mechanical properties could be observed clearly [61]. In Figure 2.19, silane application on alumina platelets and the procedure applied in that study is shown.

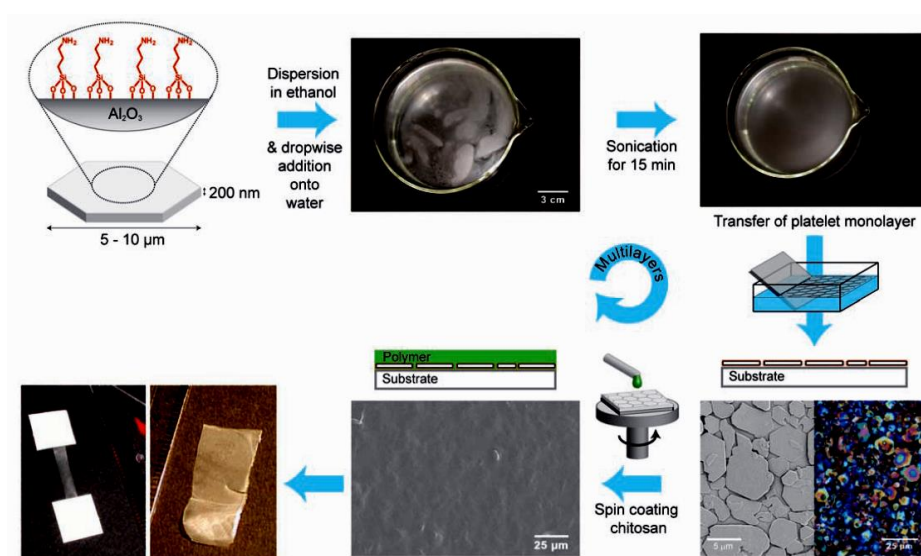


Figure 2.19 Bottom up colloidal assembly of multilayered hybrid films. Surface modified platelets are assembled at the air-water interface to produce a highly oriented layer of platelets after ultrasonication. The 2D assembled platelets are transferred to a flat substrate and afterwards covered with a polymer layer by conventional spin coating [61].

This study demonstrated that the artificial bioinspired material could reach relatively to high elastic modulus which is 10 GPa for alumina platelet-chitosan films, being comparable to those of with teeth and bone. Another remarkable result is that artificial film has approximately 300 MPa tensile strength which is quite high for a polymer based artificial material.

Another new approach was proposed to fabricate bio-inspired bulk composites. Ekiz et al. studied on the nanocomposite using epoxy as organic phase and alumina platelets as inorganic phase, and this new approach was called Hot Press Assisted Slip Casting (HASC) [11]. Steel die is used for shaping the composite structure and plaster mold is used for filtration of excess polymer. This method is useful to create hierarchical structure like nacre, and the work of fracture test results were 254 J/m^2 which is a comparable to that of natural nacre [11]. Figure 2.20 shows the assembly of Hot Press Assisted Slip Casting (HASC) Method schematically.

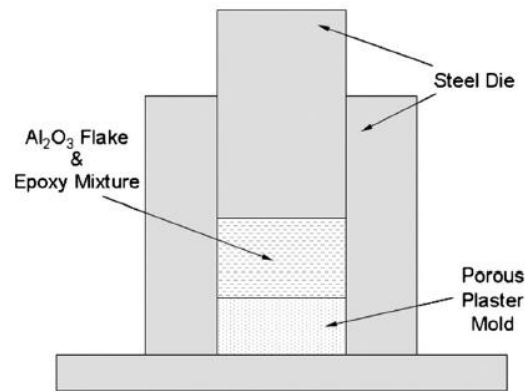


Figure 2.20 Schematic illustration of Hot press Assisted Slip Casting (HASC) Method assembly[13].

The improvement of this approach was achieved by Gürbüz. Gürbüz et al. studied on different types of silanes to treat alumina platelets. They tried the same fabrication approach while using surface modification with silane, where, work of fracture test result was 178 J/m^2 [12].

The other new approach proposed to fabricate nacre-like composite is Tape Casting or Doctor Blading. Libanori et al. produced nacre-like composites using alumina platelets as inorganic reinforcement and polyurethane as organic matrix. To improve the interaction between alumina platelets and matrix, aminopropyltriethoxy silane (APTES) and polyvinylpyrrolidone was

used in this study, where the main point was to reinforce reinforced the matrix with laponite. Mechanical results revealed that thermoplastic matrix reinforced by laponite showed increase in strength and elastic modulus substantially, being 91.7 MPa and 6.97 GPa, respectively [64].

One of the new approaches to supply hierarchical structure of mother of pearl is to align flakes with magnetic and mechanic stimulus. Nonmagnetic flakes can interact with the magnetic field by attaching magnetite particles on their surface. Magnetite particle attached alumina platelets were used as inorganic phase and epoxy matrix was used as organic phase. Aligned platelets were put into epoxy matrix, and mechanical results showed that this magnetic alignment causes an increase in flexural modulus being 1.4 fold higher than that of the as cast composite [15]. Related procedure is shown in Figure 2.21. The drawback in this study was the need to a relatively strong magnetic field.

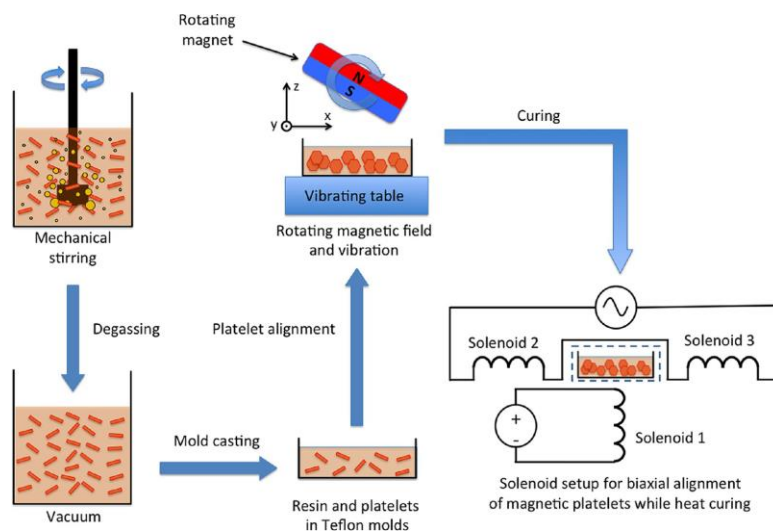


Figure 2.21 Processing route for the production of platelet-reinforced composites with tailored architectures using mechanical and magnetic stimuli. Solenoids are used to keep the alignment of the ultrahigh magnetic response (UHMR)-platelets while curing the composites inside an oven at 60°C [15].

2.5 Inorganic Surface Functionalization with Organofunctional Silane

Silane is a chemical compound used to supply the interaction between organic and inorganic phases. This interaction is provided by two different chemical reactions. First reaction is called hydrolysis that means $-OH$ groups are introduced to the inorganic phase, and at the end of the reaction alcohol groups remove. Second reaction is called condensation reaction. Condensation reaction is necessary to achieve binding between silane group and inorganic phase, and water removes from the structure by improving the attachment with increasing temperature. These reactions are illustrated in Figure 2.22.

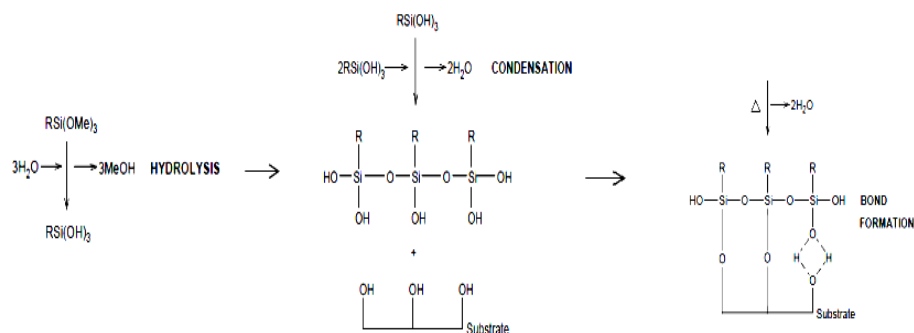


Figure 2.22 Silane treatment reactions [65].

Silane treatment is a common procedure used in industry for coupling agents. Both for thermoset and thermoplastic polymer matrices there are various types of silane coupling agents available [65-67]. Although silane coupling agent is used to improve interaction between inorganic and organic surfaces directly leading to strength enhancement, silane and polymer interaction could also be used to reduce dewetting in the structure [68].

2.6 Applied Surface Characterization techniques

2.6.1 X-Ray Photoelectron Spectroscopy

X-Ray photoelectron spectroscopy (XPS) is a quantitative and qualitative analytical technique. XPS provides information about surface elemental composition and chemical and electronic state. This technique is used for determining all elements other than hydrogen and helium [69]. The analyzed depth of the sample in XPS technique is on the order of 5-10 nm [70].

XPS technique is based on the photoelectric effect. Each surface atom has core electrons, and for all surface atoms there is a characteristic binding energy. XPS technique makes use of the removal of these electrons where the ionization energy is recorded. Therefore, this technique mainly determines the surface chemical composition of specimens by detecting the kinetic energy of the ejected photoelectrons from surface atoms. Photoelectron counts vs binding energy graph gives the information about elements present at the very surface of the material [71].

2.6.2 Fourier Transformed Infrared Spectroscopy

Fourier Transformed Infrared Spectroscopy (FTIR) is a spectroscopic technique used to determine chemical compounds. FTIR mainly depends on the vibration of atoms that changes the binding of elements in different directions. Molecular vibrations should be detected by FTIR to determine the presence of chemical compounds. Therefore, molecular geometry is important [72-73].

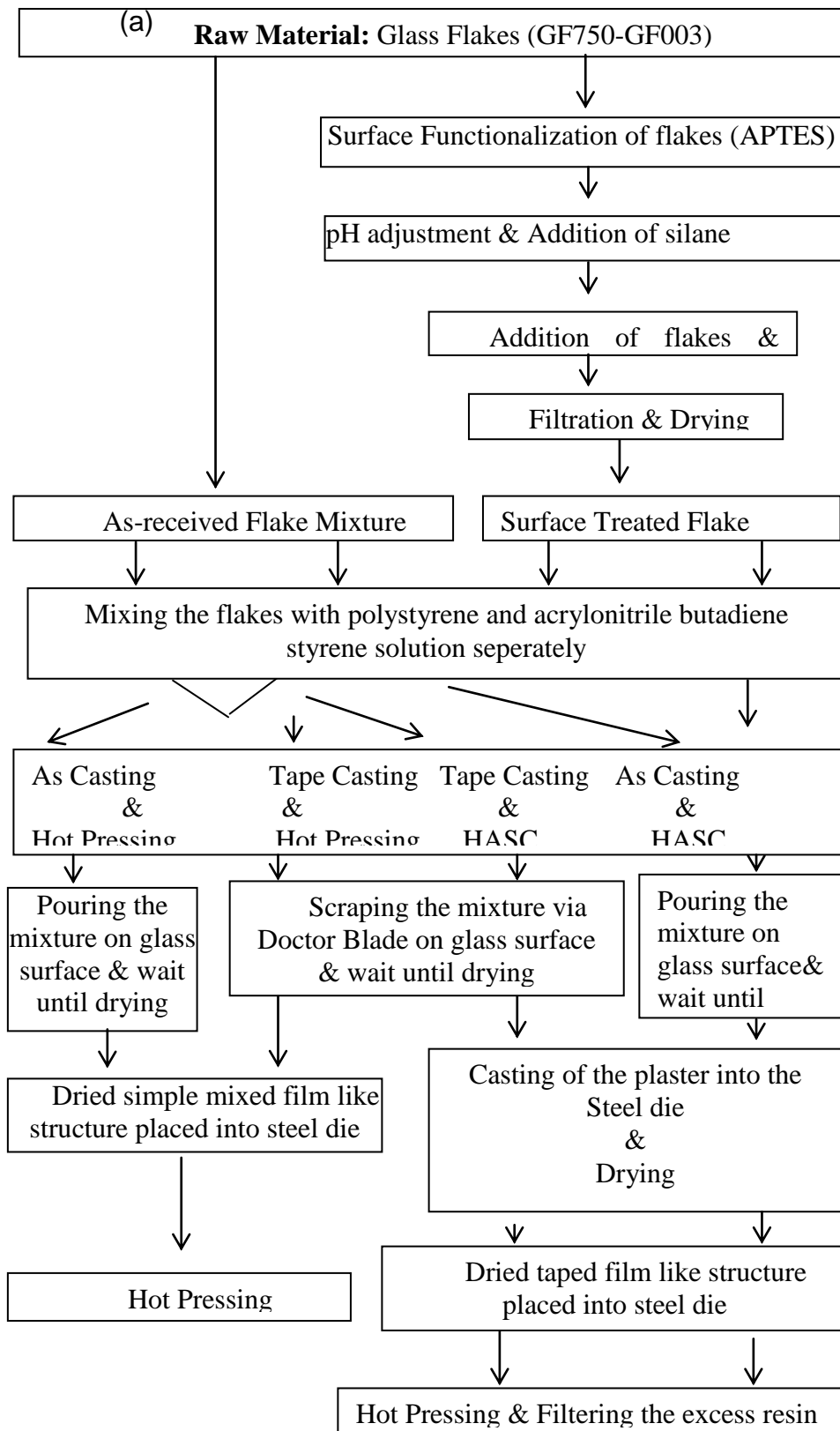
The vibration of atoms results in the oscillation of electric charge, and oscillating molecular dipole interacts with the electromagnetic radiation being put into resonance. This behavior provides determination of chemical compounds. [72-73].

CHAPTER 3

EXPERIMENTAL PROCEDURE

In the scope of this study, fabrication of bio-inspired nacre-like bulk lamellar composite materials will be investigated containing both low and high aspect ratio glass flakes as the reinforcing phase and fabricated by “Hot press Assisted Slip Casting Procedure”(HASC), “Tape Casting”(TC) and “Magnetic Field Assistance” techniques. One of the significant points in this study is the investigation of different thermoplastic polymers as the matrix material in composite structures.

In this chapter, hot press assisted slip casting procedure, tape casting and magnetic field assistance procedures were explained where raw materials were also identified. Microstructural and mechanical characterization methods utilized were demonstrated. Fabrication procedures applied throughout this study are summarized in the form of a flow chart and presented in Figure 3.1.



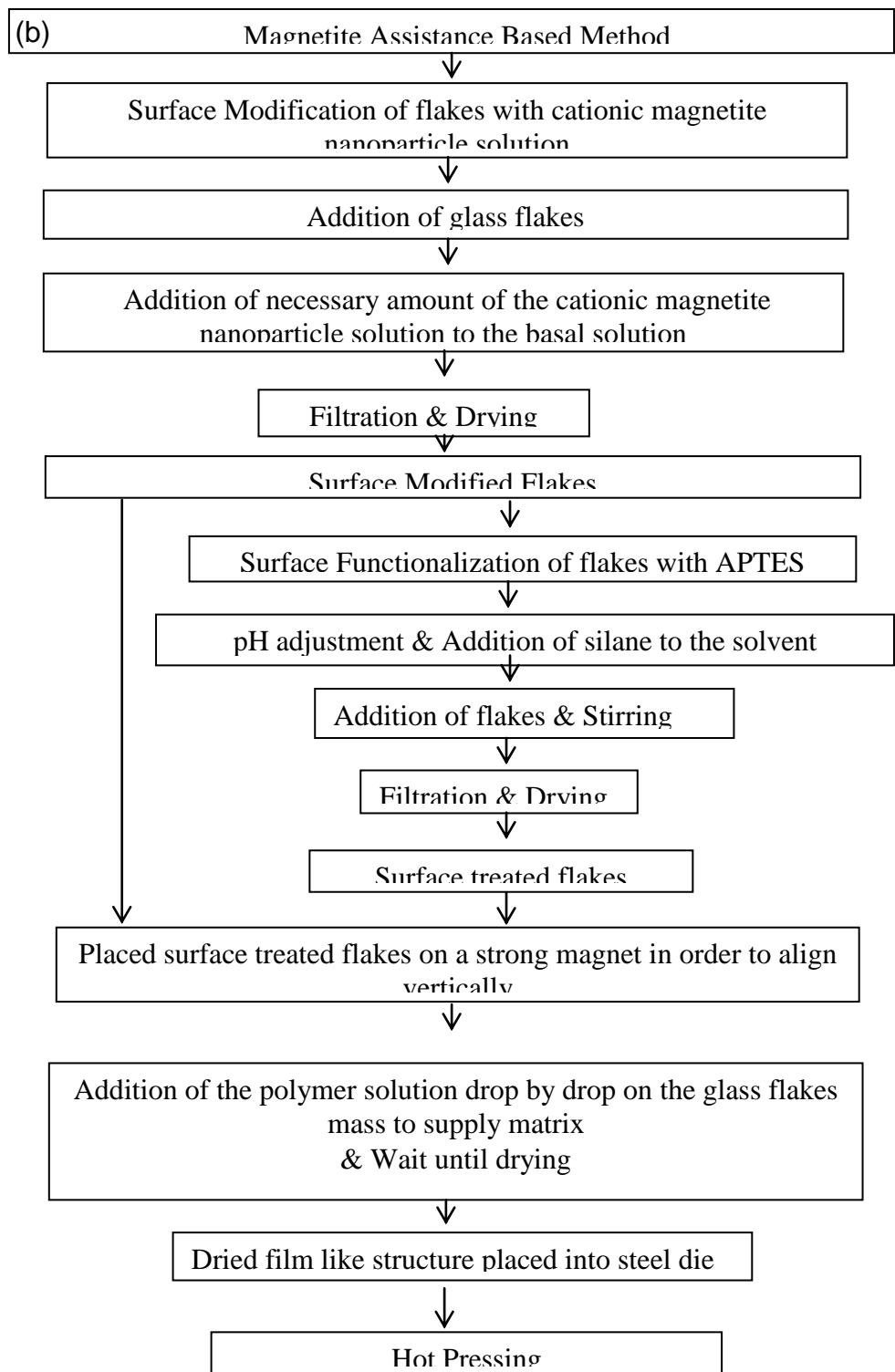


Figure 3.1 Flow chart of the fabrication procedures applied in this study (a) Hot-Pressing based methods, (b) Magnetic Field Assistance based methods.

3.1 Raw Materials

Bio-inspired nacre-like bulk lamellar thermoplastic polymer matrix composite materials were fabricated using polystyrene and acrylonitrile butadiene styrene as organic matrix phase and glass flake as inorganic reinforcing phase. Indication and aspect ratio of two different types of glass flakes used are demonstrated in Table 3.1. One of the inorganic phases used in this dissertation is called as unmilled glass flake and the other one is micronized, where these differences result from the production methods of the glass flakes. Particle size distribution of micronized glass flakes (GF 003) is such that 2% or less is $> 150\mu\text{m}$, 10% or less is between $50\text{-}150\mu\text{m}$ and 88% or more is $< 50\mu\text{m}$. The average diameter of GF 003 micronized glass flakes is less than $50\mu\text{m}$ and the thickness of these flakes is $2.3\text{-}3.3\mu\text{m}$ (Glass Flake Ltd., Leeds, UK). Particle size distribution of unmilled glass flakes (GF 750) is such that 80% or more is $1700\text{-}150\mu\text{m}$ and 20% or less is $<150\mu\text{m}$. The average diameter of unmilled glass flakes GF 750 is between $1700\text{-}150\mu\text{m}$ and the thickness of these flakes is between $5.5\text{-}9.5\mu\text{m}$ (Glass Flake Ltd., Leeds). Both of the glass flakes are made of C type glass as a result of which they are extra corrosion resistant. Microstructural observation of these glass flakes has been conducted using scanning electron microscope (SEM), and the SEM images are given in Figure 3.1. The chemical content of these glass flakes are shown in Table 3.2.

Table 3.1 Properties of glass flakes used in this dissertation.

Indication	Type	Morpholog	Density (g/cm^3)	Aspect Ratio
GF 003	Micronized	Flake	2.6	~15-20
GF 750	Unmilled	Flake	2.6	~73

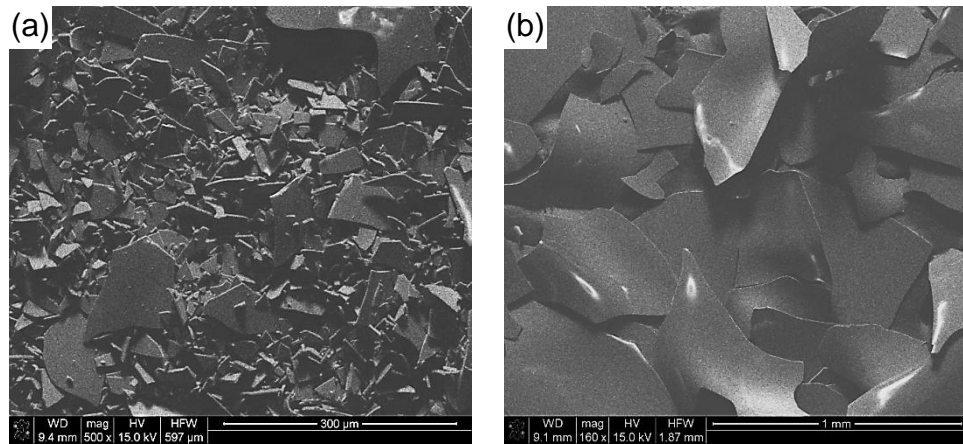


Figure 3.2 Scanning electron microscope images of a) Micronized glass flakes GF 003, b) Unmilled glass flakes GF 750.

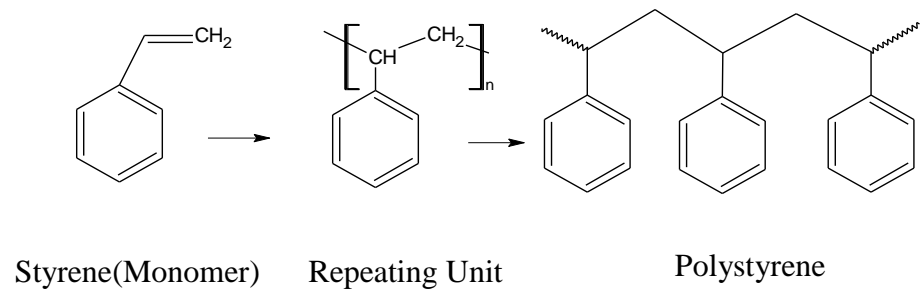
Table 3.2 Chemical analysis of the glass flakes.

Chemical Analysis (GF003 and GF750)	
SiO ₂	64-70%
K ₂ O	0-3%
B ₂ O ₃	2-5%
ZnO	1-5%
Na ₂ O	8-13%
MgO	1-4%
CaO	3-7%
Al ₂ O ₃	3-6%
TiO ₂	0-3%

Fabrication of nacre-like composite materials was conducted using thermoplastic polymers as matrix materials. These thermoplastic polymers are Polystyrene (PS) and Acrylonitrile Butadiene Styrene (ABS). Initially the polymers had granular form and the matrix formation from these polymers were achieved by solving efficient amount of polymers granules in a proper solvent. Typical properties of these thermoplastic polymers was obtained by the help of gel permeation chromatography, and the number average molecular weight of PS was determined to be 64946 g/mole while that of the ABS was determined to be 28309 g/mole. Polymer solutions were prepared using chloroform and dimethyl formamide (99% Merck, Sigma-Aldrich, USA) as solvents for PS and ABS, respectively.

The reason of choosing PS and ABS as thermoplastic polymer matrices was that there are quite a number of common industrial applications of these polymers, and they could be comparable with the results of other studies on nacre-like composites especially having thermoset matrix. In this study crystalline polystyrene and amorphous acrylonitrile butadiene granules were used as initial polymer materials. The difference of polymer structure in crystalline form of PS and monomer of PS can be seen in Figure 3.3. Furthermore, ABS is a terpolymer which means that it is a combination of three different chemical units. These chemicals units and ABS structure are shown in Figure 3.4 and Figure 3.5, respectively.

a)



b)

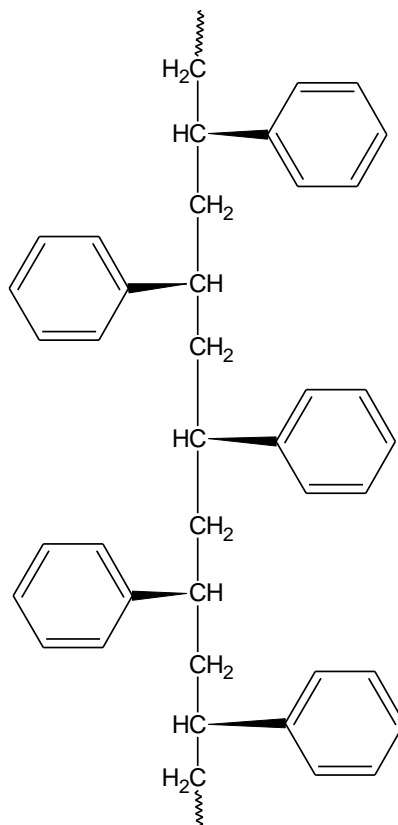


Figure 3.3 Polystyrene a) structure of monomer and polymer b) structure of syndiotactic Polystyrene (PS) in highly crystalline form.

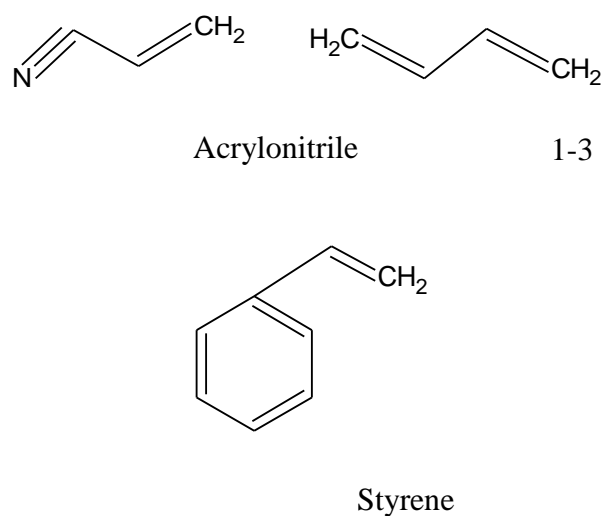


Figure 3.4 Different chemical units in ABS.

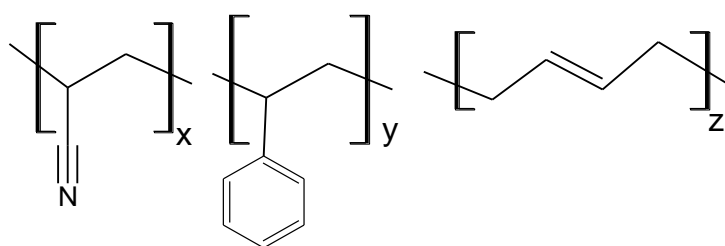


Figure 3.5 Chemical structure of Acrylonitrile Butadiene Styrene (ABS).

In this study, glass flakes surfaces were also modified according to the processes described below. Two different types of surface applications were applied. One of them is the application of a coupling agent which is called silane. There are different types of silanes used as coupling agents, where in this study an organofunctional silane, namely aminopropyltriethoxy silane (APTES, Silquest A-1100, Momentive Performance Materials Inc., Ohio, USA) was used. The aim of using this coupling agent was to achieve a better bonding between the organic and inorganic phases of the composites. Chemical structure of APTES is given in Figure 3.6.

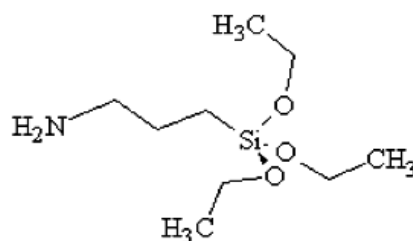


Figure 3.6 Chemical structure of Aminopropyltriethoxy silane (APTES).

The other surface modification applied was the attachment of cationic magnetite nanoparticles (EMG series-605, FerroTec Corp., Santa Clara, USA) on the glass flake surfaces. The reason of using cationic magnetite nanoparticle solutions was to provide an effect of magnetic field on glass flakes for alignment control. For both of the surface modification procedures, these chemical solutions could be active in particular solutions. Therefore, ethanol-distilled water mixture and distilled water were used as basal solvents for organofunctional silane and cationic magnetite nanoparticle solutions, respectively. For surface functionalization with APTES, reagent grade acetic acid and ethanol were used.

3.2. Fabrication of Nacre-like Polystyrene or Acrylonitrile Butadiene Styrene Matrix Bulk Lamellar Composites Using As-Received Glass Flakes

The aim of this study is to fabricate nacre-like bulk lamellar composites using glass flake as the inorganic reinforcing component and thermoplastic polymer as the organic matrix. There are various methods proposed in the literature to achieve nacre-like architecture [6, 16, 20]; however, in the scope of this study mainly four different combinations were used to obtain the alignment of flakes. These combinations were composed of four

different techniques which are As Casting (AC), Tape Casting (TC), Hot Pressing (HP) and lastly Hot press Assisted Slip Casting (HASC). Combinations of these techniques were investigated to determine especially the effect of TC and HASC methods on glass flake alignment. On the other hand, AC and HP methods were used to differentiate TC and HASC processes and to demonstrate the variation in the alignment of flakes deeply. Consequently, four different types of combinations used in this study can be indicated as AC+HASC, AC+HP, TC+HASC, TC+HP.

For all of these methods, there was a common procedure to prepare the polymer solutions containing 10 g of the corresponding polymer granules. Polystyrene and acrylonitrile butadiene styrene granules were dissolved in efficient solvents that are chloroform and dimethyl formamide, respectively. Proper amount of polymer solutions were prepared with 80 ml of either of the solvents and 10 g of the corresponding polymer granules.

Following the preparation of the polymer solutions, 30 ml from each polymer solution was taken and mixed with 3 g of glass flakes mixture to prepare the suspensions which were used in as casting or tape casting procedures. 3 g of glass flakes was determined to be the efficient flake amount. A mixture of two different types of glass flakes with different sizes was used throughout this study as the reinforcing phase. This glass flake mixture contained 80 wt% GF 750 and 20 wt% GF 003. The mixture content was determined by trying different glass flake proportions changing from 100 wt% GF 750 to 0 wt% GF 750 where the mixtures were observed to reveal a microstructure similar to that of nacre structure. Later on, mixture of flakes was added to 30 ml polymer solution and stirred with magnetic stirrer for approximately 5 min. Finally, as casting or tape casting procedure was applied.

After mixing step the mixture was poured on a glass surface which was kept in as-cast condition in the case of as casting or was doctor bladed in the case of tape casting. For the as casting method, the mixture poured on the glass

surface has been kept approximately one day in the as-cast condition to dry. After that, dried film like structure was removed from the glass surface by cutting square shaped specimens using a fresh knife.

The second method used was tape casting. Tape casting process in other words knife coating or Doctor Blading is based on scraping a particle containing mixture via blade on a substrate. There is a blade in tape casting machine which is called doctor blade, and there are calipers to adjust the height of the blade from the substrate to control the final thickness of the tapes. In this particular case, polymer solution-glass flake mixture was poured in the tape casting chamber after adjusting the blade to 50 μm height, and then the chamber was moved with a speed of 20 cm/s to scrape the mixture on the glass substrate surface. Scraped tapes were kept on the glass substrate for several days to dry, after which they were removed by cutting them as square shaped specimens using a fresh knife. Schematic representation of the tape casting equipment and the applied procedure are shown in Figure 3.7.

The two initial shaping methods (AC and TC) were followed by two other methods called HASC and HP to consolidate dried initial films or tapes to form bulk composites. Both AC and TC procedures were followed by putting the films or tapes into a steel die for compaction. A 20 x 20 mm square cross sectioned steel die has been used as a mold for the processing of the composites. After placing dried films or tapes into the steel die HASC or HP processes were applied on both as-cast or tape cast specimens both of which included application of heat and pressure simultaneously.

In the case of the HASC process, the lower exit of the steel die was closed with plaster as a porous filter through which excess liquid resin can flow under the action of the applied pressure, and hence can be drained while providing alignment to the glass flakes with their basal surfaces perpendicular to the hot-pressing direction. Porous plaster was cast into the lower exit of the square cross sectioned steel die. Following the melting of

the polymer by the applied pressure liquid polymer started to flow in the mold leading to the removal of the excess polymer increasing the reinforcement content in the composite structure in HASC process. Schematic representation of the HASC process is shown in Figure 3.8. HASC process was applied on both as-cast or tape cast initial materials. HASC operation temperature was set to 170 and 155 °C in the case of PS and ABS matrices, respectively. Pressure for both of the polymers was increased up to 87.5 MPa and applied for 45 min.

Last method used in this study for consolidation of the composites was hot-pressing (HP), which is a conventional process conducted at elevated temperature with the application of uniaxial pressure. After placing dried films or tapes into the square cross sectioned steel die, initial pressure that was less than 10 MPa, was applied for compaction and temperature started to increase at the same time. Maximum hot-pressing temperature values were changed according to the polymer matrix. For PS maximum operation temperature was adjusted to 200 °C while it was adjusted to 170 °C in the case of ABS.

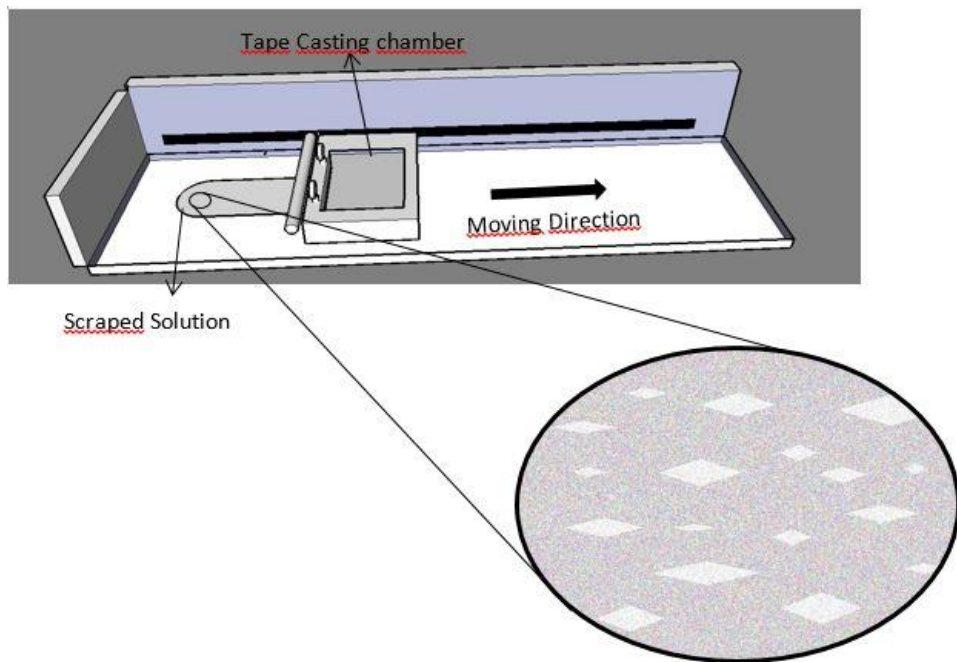


Figure 3.7 Schematic representation of the Tape Casting (TC) method.

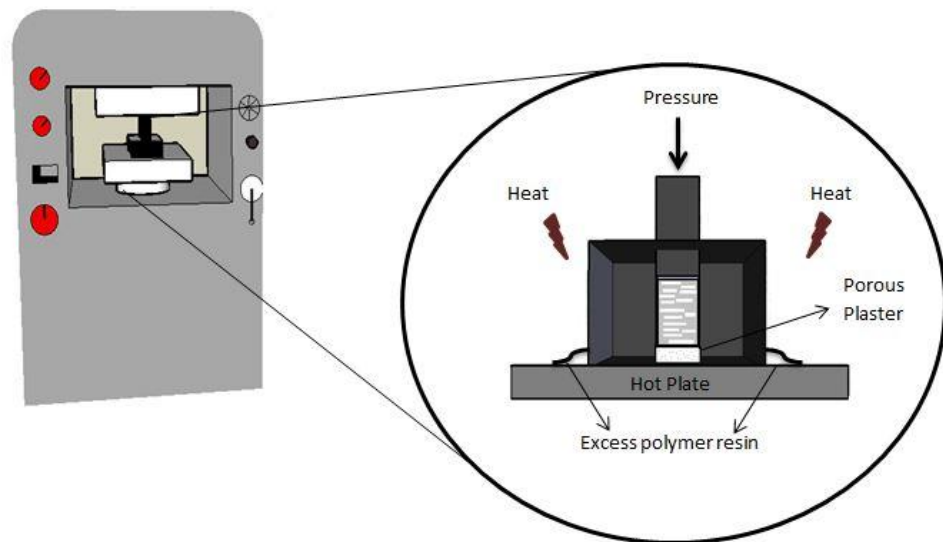


Figure 3.8 Schematic representation of the Hot press Assisted Slip Casting (HASC) method.

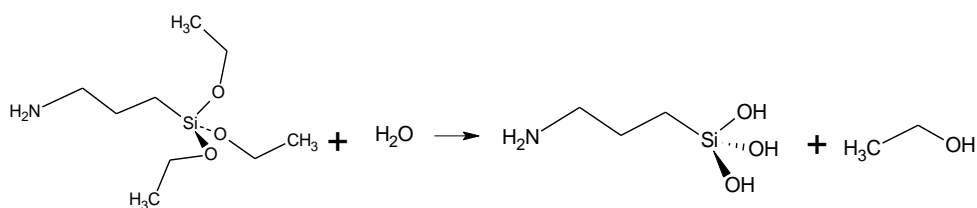
3.3 Fabrication of Nacre-Like Bulk Lamellar Thermoplastic Matrix Composites Using Surface Modified Glass Flakes

Two different surface modification procedures the details of which were explained below are used to modify the glass flake surfaces in this study. For the fabrication of the nacre-like bulk lamellar PS matrix composites reinforced by these surface treated glass flakes AC+HASC process combination was chosen among the four previously described combinations, as it has been determined to reveal the best microstructural architecture along with the maximum mechanical property enhancement.

3.3.1 Surface Modification of Glass Flakes with Aminopropyltriethoxy Silane

To observe convenience and interfacial bonding between the inorganic and organic components of the desired composites, surfaces of the glass flakes were modified by functionalization using a silane coupling agent. Surface functionalization procedure was applied in a basal solution based on reagent grade acetic acid and ethanol. In this procedure solution should have specific pH range to provide hydrolysis reaction that is first compulsory reaction for silane application. After providing appropriate pH value (4.5-5.5), silane solution was added to the basal solution and stirred on a magnetic stirrer for 90 min. Then, glass flakes were added to the resulting clear solution and mixed for an additional 30 min. Following this, the excess solution was filtered off using a filter paper. Second and last compulsory reaction of the silane treatment is the condensation which was supplied by keeping the filtered glass flakes in a drying oven at 120 °C for 60 min. Detailed representation of the silane treatment reactions are shown in Figure 3.9.

Hydrolysis Reaction



Aminopropyltriethoxy

Condensation Reactions

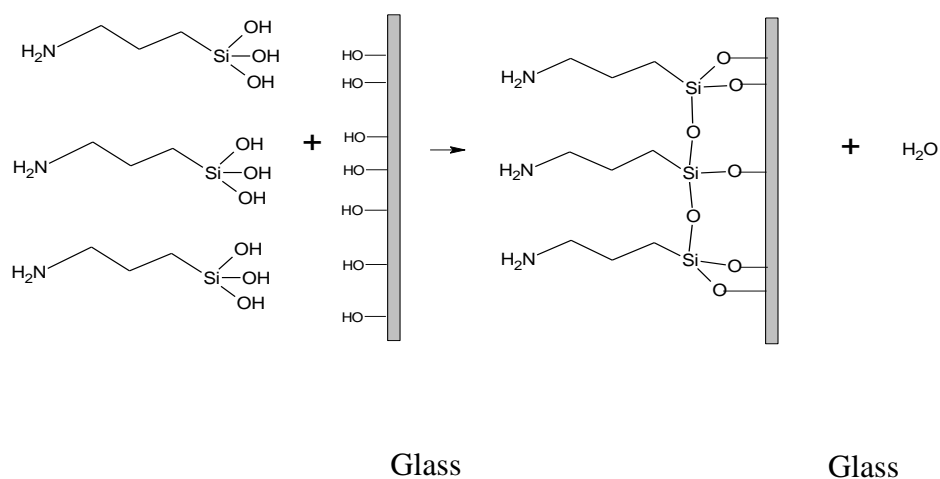


Figure 3.9 Silane treatment reactions.

3.3.2 Surface Modification with Cationic Magnetite Nanoparticle Solution

Cationic magnetite nanoparticle solution is a ferromagnetic water based solution. As solution is cationic, pH of the solution is critical. For magnetite nanoparticle attachment only GF 750 type glass flakes were used. The basal solution for attachment of magnetite nanoparticles was distilled water (pH≈6.5). By adding 5 g of glass flakes into 80 ml distilled water, the solution pH reached up to 9.5 which is enough to attach magnetite nanoparticles from the cationic solution. 0.5μl (ca. 20 vol%) of the cationic nanoparticle suspension was added to the basal solution containing the glass

flakes. The mixture was stirred on a magnetic stirrer for 90 min after which the excess liquid was filtered off using filter paper. At this step, the filtered excess solution was colorless; however, the color of the glass flakes turned into brown. After the filtration, magnetite nanoparticle attached flakes were put in an oven to dry at 120 °C for 1.5 h.

Magnetite nanoparticle attached glass flake surfaces were additionally treated with silane application. After drying magnetite nanoparticle attached glass flakes were added to the prescribed basal solution that was prepared for organofunctional silane application. pH range to activate silane and the amount of silane were not changed. After addition of the glass flakes, the mixture was stirred for 60 min and the excess solution was filtered off. After the filtration, double surface treated glass flakes were kept in a drying oven at 120 °C for 60 min.

3.3.3 Fabrication of the Polystyrene Matrix Composites Reinforced by Surface Modified Glass Flakes

There are various methods to mimic mollusc shell architecture. One of the newest methods to fabricate nacre-like structure includes assisting the inorganic flake alignment by magnetic field application. The scope of this study is to achieve brick and mortar architecture with the help of various pathways to fabricate nacre-like bulk lamellar thermoplastic matrix composites. In this context, magnetic field application to magnetite nanoparticle attached glass flakes was one of the alignment methods studied within this dissertation.

To supply the effect of magnetic field on the non-magnetic inorganic reinforcements, magnetite nanoparticles were attached on glass flake surfaces were modified with cationic magnetite nanoparticle solution. Magnetite nanoparticle attached and also additionally silane treated glass flakes were placed on a niobium hard magnet to orientate them with the magnetic field being their basal surfaces perpendicular to the magnet

surface. The polymer matrix was provided by pouring the prescribed polystyrene solution on the magnetically oriented glass flakes carefully and keeping them on the magnet until the solvents evaporate to obtain complete drying. The important point in this application is the area of magnet surface. Magnetite nanoparticle attached glass flakes should properly cover the magnet surface to effectively couple with the magnetic field. Hence, just 1 g of glass flakes was put on the surface of the magnet and three different matrix amounts was obtained by adding three different amounts of the polymer solution as 5, 6 and 9 ml. Following drying the film like structure was removed from the magnet and placed into the aforementioned steel die and hot pressing procedure was applied to three different matrix amount containing composites as described previously.

3.4 Characterization

3.4.1 Determination of Inorganic Reinforcement Content and Density

The determination of the inorganic reinforcement content of the composites was conducted by burning off at least three specimens fabricated by each method at 600°C for 60 min under air atmosphere applying a heating rate of 4°C/min. Thermoplastic polymers, PS and ABS were removed by combustion and the residues were used to calculate inorganic content for each composite. Volume percentage of the inorganic phase (V_R %) was determined using the following equation;

$$V_R \% = \frac{W_R \times \rho_M}{(1 - W_R) \times \rho_R + W_R \times \rho_M} \times 100 \quad (3.1)$$

where W_R is determined weight of the reinforcement, ρ_R is the theoretical density of the glass flakes and ρ_M is the theoretical density of the corresponding polymer matrix.

Densities of the specimens were determined by means of Archimedes' principle. Equation 3.2 describes Archimedes' principle. By the help of an

immersion medium that is water and measuring dry weight (W_{dry}), saturated weight (W_{sat}) and suspension weight (W_{sus}) of the specimen, density of the fabricated composites was calculated.

$$\rho = \frac{W_{dry}}{W_{sat} - W_{sus}} \quad (3.2)$$

3.4.2 Microstructural Characterization

Specimens cut from composites fabricated by different process combinations were mounted in epoxy resin. To get an appropriate specimen surface, specimens were ground with silicon carbide emery papers according to metallographic surface preparation standards. Ground specimen surfaces were polished with 1 μm and 0.3 μm diamond suspensions. Fracture surfaces of the three-point bending specimens and as polished composite surfaces were examined for microstructural characterization with the help of a scanning electron microscope (SEM) (FEI Nova Nano SEM 430).

3.4.3 Mechanical Characterization

Mechanical characterization of the fabricated nacre-like bulk lamellar composites was executed by hardness, three-point bending and work of fracture tests (WOF). Applied loading direction was parallel to hot-pressing direction for all cases.

3.4.3.1 Hardness Measurement

Vickers micro hardness measurement of fabricated nacre-like bulk lamellar thermoplastic polymer matrix composites was conducted on as polished surfaces using micro hardness tester (Shimadzu HV 0.2) with an applied maximum load of 1.92 N for 10 s.

3.4.3.2 Three-Point Bending Tests

Flexural stress and strain of the fabricated composites were measured by three-point bending tests. Three-point bending specimen dimensions that are Length (l), width (b) and thickness (d) were 20, 1 and 5 mm, respectively. A screw-driven type testing machine (Instron 5565A) was used to carry out three point bending tests. The support span was 16 mm and cross-head speed was 0.4 mm/min. Load (P) vs. deflection (D) data was used to calculate flexural strength (σ_f) and strain values (ε_f) of fabricated composites using following equations.

$$\sigma_f = \frac{3PL}{bd^2} \quad (3.3)$$

$$\varepsilon_f = \frac{6Dd}{L^2} \quad (3.4)$$

All the dimensions are in mm. P is the load at a given point on the load deflection curve, D is defined as maximum deflection of the center of the beam, L is the support span, b is the width of the beam tested and d is depth (thickness) of the beam.

3.4.3.3 Work of Fracture Tests

To investigate the energy requirement for fracture and crack growth in the composite structure, work of fracture test was executed on composites fabricated by AC+HASC process combination. Screw-driven type testing machine mentioned in three point bending test was used again and the same support span (16 mm) and cross head speed (0.4 mm/min) were used. Single edge notch beam (SENB) geometry was used to conduct work of fracture test. Length (l) of the specimens was 20 mm, width (b) of the specimens was

4 mm and thickness (d) of the specimens was 3 mm. To provide stable fracture span (L)/width (b) ratio should be as 4 [49]. The notch size 0.45b-0.55b was supplied with a diamond saw and a sharp pre-crack was supplied with the help of sliding a fresh razor blade across the notch. At the end of the tests, area under the load-displacement curves (E) and fracture surface areas (A) were calculated to determine work of fracture (WOF) values of all specimens. The formula to calculate WOF values is as follows.

$$WOF = \frac{2A}{E} \quad (3.5)$$

3.4.4 X-Ray Photoelectron Spectroscopy (XPS)

The efficiency of surface functionalization treatment applied on inorganic reinforcements with aminopropyltriethoxy silane was investigated using X-ray photoelectron spectroscopy (XPS) (PHI 5000 Versa Probe). As-received and silane-treated glass flake surfaces were analyzed with a monochromatic Al K α radiation source. The pass energy of XPS survey spectra was 187.85 eV at a photoelectron take-off angle of 45°. High resolution XPS spectra of Si2p and N1s core levels were acquired with pass energy of 55 and 58.70 eV. Peak deconvolution of N1s core levels was carried out using mixed Gaussian-Lorentzian function.

3.4.5 Fourier Transform Infrared Spectroscopy (FTIR)

Success of the applied surface treatment procedures including both magnetite nanoparticle attachment and silanization of the inorganic reinforcements nanoparticle was investigated by Fourier Transform Infrared Spectroscopy (FTIR) (Bruker IFS 66/S). As-received, magnetite nanoparticle attached and silanized (after magnetite nanoparticle attachment) glass flakes were analyzed in mid-wavelength infrared range whose spectrum range is between 400 and 4000 cm⁻¹.

CHAPTER 4

RESULTS AND DISCUSSION

In this study, effectiveness of various processing method combinations in fabricating nacre-like bulk lamellar thermoplastic polymer matrix composites has been investigated. Alignment of glass flakes in two different thermoplastic polymer matrices, polystyrene and acrylonitrile butadiene styrene was tried to be achieved by as casting or tape casting processes which were followed by two different consolidation processes namely hot press assisted slip casting or hot pressing. As an alternative approach, magnetite nano particle attached glass flakes were aligned in polystyrene matrix with the action of an applied magnetic field, after which bulk composites have been achieved by consolidation via hot pressing. In this chapter, the results gathered based on the effects of different process combinations in revealing nacre-like bulk lamellar composites have been discussed. All results composed of the correlation between the applied process parameters, and resulting microstructural and mechanical characteristics have been summarized in this chapter.

4.1 Fabrication of Nacre like Bulk Lamellar Thermoplastic Polymer Matrix Composite Materials

In this study, primarily effectiveness of a hybrid conventional method called hot-press assisted slip casting (HASC) and hot-pressing (HP) in fabricating thermoplastic matrix bio-inspired bulk composites having brick and mortar microstructure was investigated. Even though, both of the consolidation

processes involve melting of the polymer by heating, the major difference is the flow of the molten polymer from the structure through a porous filter in the case of the HASC process. Initial materials to be consolidated by either of these processes were prepared by two different methods namely by as-casting (AC) or tape casting (TC). As described in the previous chapter, both of the initial materials were in a dried film or tape like form before consolidation. The tape-cast film had uniform thickness around 40 μm , while the as-cast film was relatively thicker with a non-uniform thickness. Consequently, microstructural architecture-controlled mechanical properties of PS and ABS matrix bulk bio-inspired composites fabricated by four different process combinations, namely by AC+HASC, by AC+HP, by TC+HASC or by TC+HP, have been discussed.

All the procedures started with polymer solution and glass flake mixture preparation. Content of the glass flake mixture was determined to achieve architecture similar to that of nacre based on microstructural observations. Initially, there were two types of glass flakes as the reinforcing materials different in terms of their production method and size. Various mixtures of the two different glass flakes were prepared in which their amounts changed from 0 wt% to 100 wt% systematically with 10% increment of one type. Based on the microstructural observations conducted on the polystyrene matrix composites fabricated by TC+HASC process containing different glass flake mixtures (Figure 4.1), the composite containing 80 wt% high aspect ratio (GF 750) and 20 wt% low aspect ratio (GF 003) glass flake mixture was determined to reveal a microstructure closest to that of nacre. As a result of this, throughout this study this specific reinforcement mixture has been utilized for the fabrication of the nacre-like bio-inspired composites.

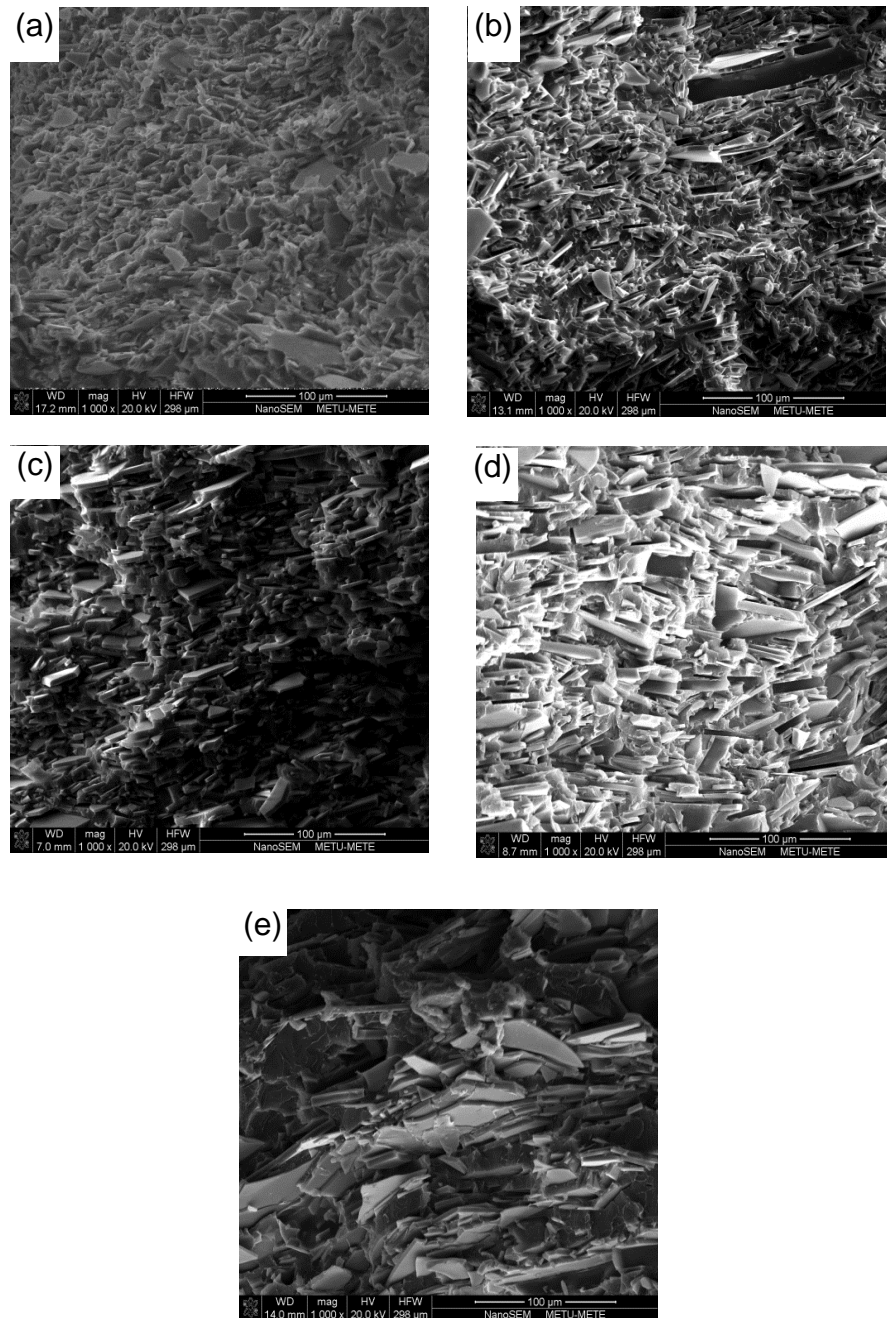


Figure 4.1 Fracture surfaces of TC+HASC processed PS matrix composites composed of different glass flake mixtures containing (a) 10 wt%, (b) 20 wt%, (c) 50 wt%, (d) 80 wt% and (e) 90 wt% high aspect ratio glass flakes (GF 750).

According to Flory-Huggins theory that describes the dissolution of the polymer to form a solution, the interaction between polymer and solvent molecules could clarify in a unit cell and the molecular interaction could be shown by demonstrating solvent and polymer molecules separately. In the unit cell, there could be three types of possible interactions between the solvent and polymer molecules, which are solvent-solvent, solvent-polymer and polymer-polymer interactions. The determination of which type of the interaction is favorable is based on the volume content of the polymer in the solvent.

In this study, to determine the volume concentration into the solvent and to indicate the differences between PS and ABS polymer activity and polymer fluidity into the solvents, gel permeation chromatography (GPC) was conducted. According to GPC results, PS granules had 541941 g/mole weight average molecular weight and ABS granules had 323169 g/mole weight average molecular weight. In addition to this, calculated densities of PS and ABS were 1.01 g/cm³ and 1.02 g /cm³, respectively. Dissolution of the polymer granules was achieved by using the same amount of solvent and same amount of polymer granules for both of the thermoplastic polymer matrices. Therefore, the volume content of the polymer was nearly the same for both of the polymers yet according to the results for each polymer average molecular weights, mixing entropies and relative internal energies were different.

The investigation of the mixing entropy was crucial to follow the dissolution of the polymer granules, since presence of solvent – solvent and polymer – solvent interaction may lead to some mechanical and chemical drawbacks in the final composite structure resulting from the phase variation in polymer solutions. As a result of these reasons, in the scope of this study, mixing entropy could be calculated with Flory-Huggins theorem. The following equation was used to determine the mixing of entropy, ΔS_{mix} , where k_B , n_{site} , ϕ and N are Boltzman constant, number of site (monomer of the polymer or

a solvent molecule), volume fraction and occupied polymer chain sites, respectively.

$$\frac{-\Delta S_{mix}}{k_B n_{site}} = \frac{\phi}{N} \ln \phi + (1-\phi) \ln(1-\phi) \quad (4.1)$$

Calculated ΔS_{mix} is equal to 0.86 J/K and 0.90 J/K for PS and ABS, respectively. These results were demonstrated that the change of the entropy in the polymer granules after dissolution is efficient to adsorb the polymer to the glass flake surface by minimizing the interaction between the solvent molecules as the calculated entropy changes are less than 1 [74-76].

Calculating intrinsic viscosities of the polymers, which define the polymer viscosity in the solvent, could be as crucial as Flory- Huggins theorem to describe especially the polymer behavior in the solution. In this case, Mark Houwink equation (Equation 4.2) was used to demonstrate the behavior of the polymer chain, where η , M, K, and a are intrinsic viscosity, molecular weight and Mark-Houwink parameters depend on the polymer-solvent system respectively.

$$[\eta] = KM^a \quad (4.2)$$

According to GPC results, inherent viscosity values of number average molecular weight of polymers defined as $[\eta]$ in Mark Houwink equation are 0.585 and 0.406 for PS and ABS, respectively. ‘a’ in the Mark Houwink equation was determined to be equal to 0.7 and 0.8 for PS and ABS, respectively, showing the extent of the flexibility of these polymers.

Another thermodynamically explanation about the adsorption of the polymer on different surfaces is the simple model of Cohen Stuart et al [77]. It depends on the Flory-Huggins theorem yet the model provides a simple calculation method for the energy interaction of different surfaces. In this study, chloroform was used as the solvent for PS and dimethylformamide (DMF) was used for ABS. DMF is a generally well-accepted, harmless and

widely used solvent for ABS. However, there could be a drawback about chloroform such that it could react like an acid deactivating the polymer at the end of this reaction. However, Cohen Stuart et al. observed that the energy between chloroform and polystyrene was efficient to provide the adsorption of the polymer by the inorganic surface. Polystyrene dissolved in chloroform was shown to be adsorbed on an inorganic surface with the energy considerations conducted [77].

In this study, these four different routes were applied to two different thermoplastic polymers, and both composites with these two different thermoplastic polymers demonstrated superior mechanical performance when fabricated by AC+HASC. According to inorganic content, density, relative density % and hardness results given in Table 4.1, inorganic content of the composites changed between 45-52 % for ABS and 44-55% for PS matrix composites. For both of the polymer matrices, standard deviation of the presented inorganic content values change between around 2 and 3%. Hardness of the composites fabricated by four different pathways were proportional to the inorganic content, which contributes to the increase of density and is directly based on the flow of polymer out of the structure. Consequently, AC+HASC processed composites indicated superior hardness results for both polymer matrices. For both of the polymer matrices, densification and the porosity results revealed that AC+HASC method is superior to the other methods. The densification and porosity content presented in Table 1 demonstrates that ABS polymer matrix composites reveal the lowest porosity. The reasons of lower porosity in ABS polymer matrix composites compared to PS polymer matrix ones, except the one fabricated by AC+HP route, are the lower viscosity and restitution of the molten ABS as well as its amorphous structure and lower weight average molecular weight leading to more efficient consolidation.

Table 4 1. Inorganic content, density, relative density (%) and hardness obtained by four different process combinations in ABS or PS matrix composites.

	Inorganic Content (wt%)	Density (g/cm ³)	Relative Density (%)	Hardness (HV0.2)
ABS Matrix				
AC+HASC	52	1.47 ± 0.1	100	15 ± 1.7
TC+HASC	49	1.43 ± 0.1	97	14 ± 1.4
TC+HP	48	1.11 ± 0.2	78	11 ± 2.0
AC+HP	45	0.68 ± 0.3	49	10 ± 1.4
PS Matrix				
AC+HASC	55	1.39 ± 0.2	93	20 ± 2.3
TC+HASC	54	1.32 ± 0.2	89	16 ± 1.6
TC+HP	46	1.19 ± 0.2	86	14 ± 2.4
AC+HP	44	0.93 ± 0.3	68	7 ± 1.8

Presence of porosity in the microstructure was observed in PS matrix composites for all of the processing routes applied. However, difference between density and relative density indicates that AC+HP processed composite included more porosity than the others. The reason why porosity content was specifically higher in AC+HP processed composites is the weak interaction between the molten polymer and the flake surfaces along with the absence of a pressure increase to distribute the molten polymer in all directions, where the process does not involve the flow of the molten polymer in the system. In Figure 4.2 (a) and (b) show the excessive porosity in the AC+HP processed ABS and PS matrix composites, respectively. Microstructural observation indicates that there is no interaction between flake surfaces and the polymer matrices such that the surfaces of the glass flakes are almost clean leading to the high porosity contents observed.

However, in the case of the HASC process, the flow of the molten polymer leads to the increase in the interaction between glass flake surfaces and the polymer matrices. Therefore, HASC process was more effective than HP in terms of consolidation efficiency. Moreover, according to the flow mechanism of the molten polymer, the shape of the pores in composites

consolidated by HASC or HP process is different. In the AC+HP processed composites the pores elongated entrapped in between individual flakes (shown by arrows in Figure 4.2), while they are in spherical form in the case of TC+HASC or AC+HASC processed composites (Figure 4.3) due to the friction building up on the molten polymer during its flow. Since the fluidity of ABS is higher compared to that of the PS, relative densities of the ABS matrix composites were superior to those of the PS matrix ones especially in the case of the HASC including routes.

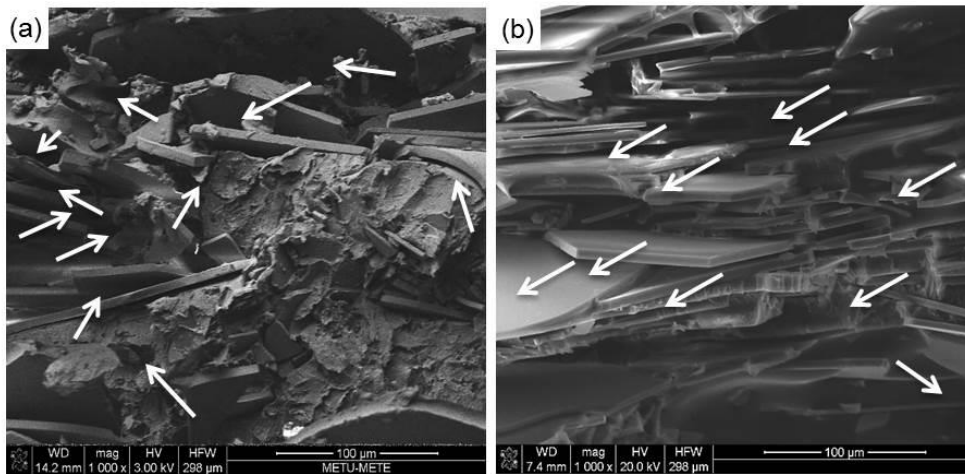


Figure 4.2. Scanning electron microscope images of the a) ABS matrix and b) PS matrix composites fabricated by AC+HP process where the pores are shown by arrows.

Even though the HASC including process combinations involve the flow of the molten polymer in the system, there still exist porosities in the resulting composites. Especially in the case of TC+HASC processed composites, relatively higher amount of porosity points out to the negative effect of the higher amount of air gaps present in between the initial tapes to be consolidated as well as the non-Newtonian flow behavior of the molten polymer. In Figure 4.3 (a) spherical pores present in TC+HASC processed

composites can be seen. Moreover, better interaction between the glass flake surfaces and the polymer matrix in the case of the HASC including routes compared to HP process including combinations are evident by the polymer layers adhered on the glass flake surfaces shown by arrows in Figure 4.3 (b).

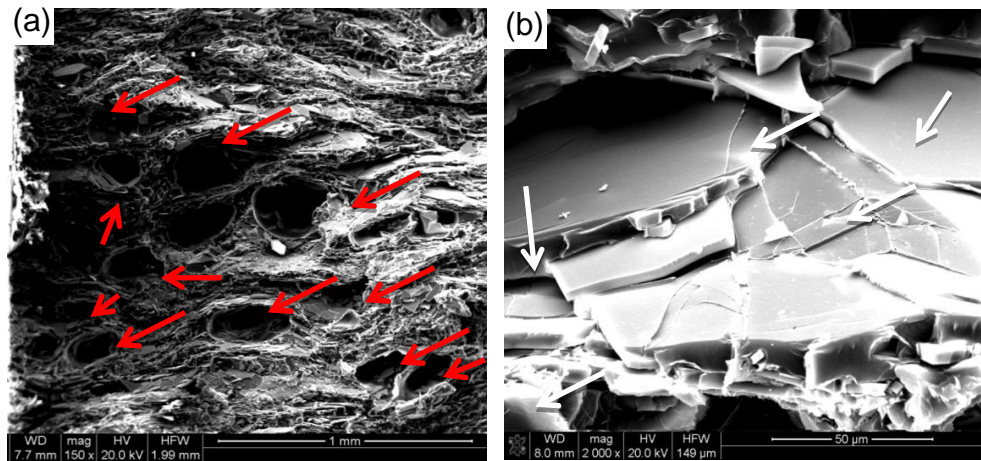


Figure 4.3. Scanning electron microscope images of composites fabricated by TC+HASC route (a) presence of spherical pores, (b) adhesion of the polymer matrix on the glass flake surfaces.

To consolidate the material and to obtain bulk a composite with brick and mortar architecture, heat was applied on the initially film or tape formed structures that were schematically illustrated in Figure 4.4. According to the procedure that was described in Chapter 3, temperature has been increased during both HASC and HP processes. While increasing temperature, organic component in the structure started to melt in both cases where it also started to flow during HASC process following melting. Polymer started to melt in the regions closer to the die wall, since first the wall of the steel die reached the adjusted temperature then the center of the structure could reach the same temperature. Therefore, flow of the molten polymer started from the

regions near the steel die wall and proceeded to the inner parts of the structure where it started to flow on the glass flake surfaces.

During the flow of the molten polymer, different friction mechanisms became operative where friction was acting on the molten polymer by both the glass flake surfaces and the wall of the steel die, which was the primary drawback to remove the excess organic matrix from the structure during HASC process. However, although increasing pressure during the HASC process was enforcing the friction, it was helpful to remove the excess liquid polymer matrix, and hence to increase the inorganic content of the composite. During this action, a significant amount of glass flakes was also lost with the flowing liquid polymer. Nevertheless, the amount of drained polymer during HASC process was different depending on whether the initial dried material was formed by AC or TC process. In the case of the dried initial tapes formed by TC process amount of the drained polymer was lower, since the scraping action during tape casting leaves lower amount of polymer in the tapes compared to the films formed by AC process (Figure 4.4).

In AC+HASC process, the flow mechanism of the molten polymer was different than that of the TC+HASC combination. In Figure 4.4 (b), the structure of the as-cast initial film is schematically illustrated. According to this following the AC process there was a random flake orientation and a relatively higher initial polymer amount in the film to be consolidated. In this relatively loose and randomly oriented body heat and pressure induced liquid polymer flow was more effective in removing the excess organic matrix leading to higher inorganic content, while it was also more efficient in forming the brick and mortar architecture due to the better flow of the polymer achieved in the structure. In the case of the TC formed initial material to be consolidated, the body confined in the steel die contains relatively lower amount of the organic phase with highly aligned inorganic phase. This is to say that in this structure there is a thin layer of polymer available between the glass flakes, and a relatively high interfacial area

between the phases. As a result of this, higher frictional force acts on the flowing molten polymer by the glass flake surfaces hindering its efficient flow out of the system. Consequently, TC+HASC processed composites reveal lower inorganic contents as well as lower densification with respect to AC+HASC processed ones.

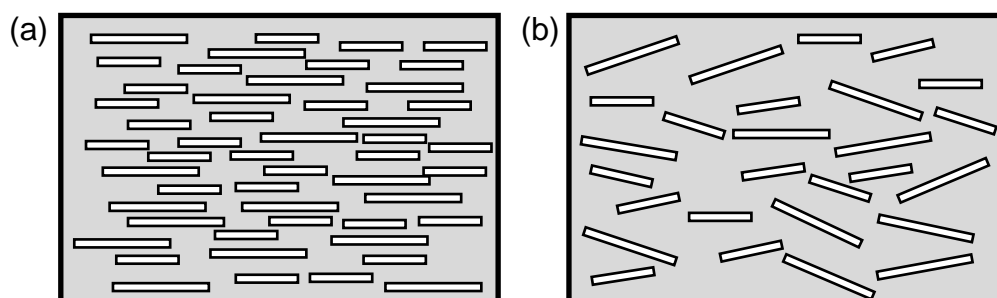


Figure 4.4. Schematic representation of the simple mixed and tape casted films into steel die before hot press assisted slip casting solution.

As already mentioned, porosity contents of the HASC processed composites differ based on whether their initial materials were formed by AC or TC process. This can be explained by the difference in the flow of the molten polymer in AC or TC initial dried film or tape cases. Reason of the difference is the amount of the polymer and the initial orientation of the glass flakes in the initial dried films or tapes. Dried film or tape like structures start to melt with increasing temperature. In this case, fluid behavior of the molten polymer is of significant importance. Generally, polymer solutions have non-Newtonian fluid behavior. However, non-Newtonian fluid mechanism divides into two as shear thinning and shear thickening. Most of the polymer solutions show shear-thinning mechanism [78]. This mechanism can be explained based on the flowing behavior of a polymer solution in a tube where it is related to the friction applied on the polymer by the interior walls of the tube (Figure 4.5). There develops a

pressure difference between the interior and exterior ($P_A > P_B$) of the polymer solution affecting its fluidity, and the friction applied by the contact surfaces controls flow front of the polymer.

In this study, motion of the molten polymer between the glass flakes is similar to the previously described mechanism on shear thinning. Local differences in the amount of polymer in the initial AC or TC formed dried films or tapes leads to the development of pressure and friction variations on the flowing polymer upon melting. In terms of the fluid mechanism, flow of the molten polymer in AC+HASC processed composite is easier due to higher local pressure differences along with lower friction applied on the polymer by the glass flake surface. In the case of the TC+HASC processed composites this situation is just the opposite where the previously mention lower amount of initial polymer with larger interfacial area results in lower local pressure differences and higher frictional forces, respectively.

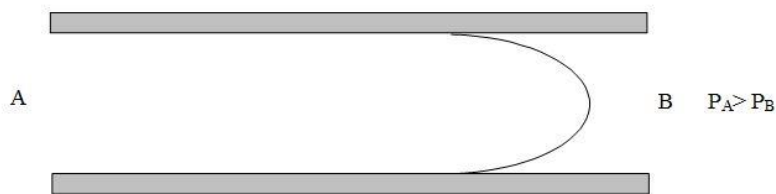


Figure 4.5. Flowing of polymer solution like plug between flakes [78].

Additionally, the flow mechanism of polymer includes restitution pointing out to the withdrawal of the flow front (material line) of the molten polymer upon the balance of the interior and exterior pressures. Following restitution curved and stationary polymer front leads to the formation of spherical pores. The schematic representation of restitution in a viscoelastic fluid is demonstrated in Figure 4.6. Both AC+HASC and TC+HASC process combinations resulted in the formation of spherical porosity the amount of which is higher in the case of TC+HASC processed composites due to

higher frictional forces involved that was evidenced by the microstructural observations.

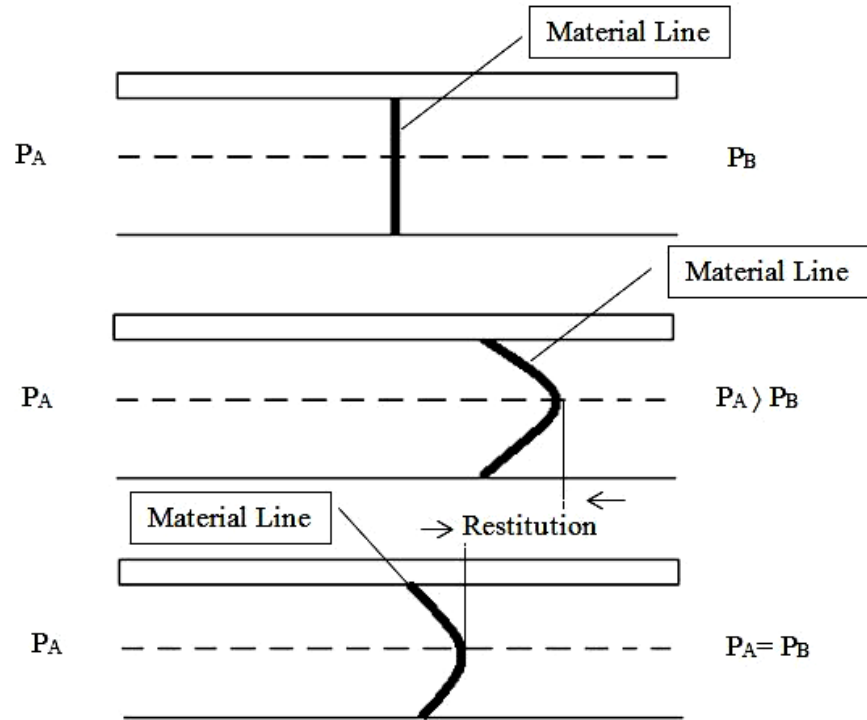


Figure 4.6. Restitution in a viscoelastic fluid [78].

All these factors could be taken into consideration as they have significant effects on the alignment of the glass flakes in the composites, and hence achievement of the desired brick and mortar architecture. Microstructural examination of the composites fabricated by the four different process combinations has been conducted on their fracture surfaces obtained after three point bending tests. Figures 4.7 and 4.8 show the SEM images of the fracture surfaces of PS and ABS matrix composites respectively fabricated by each process combination. The images clearly illustrate that especially HASC process provided the alignment of the glass flakes by means of simultaneous heat and pressure application which involves the flow of the

molten polymer during the process. The HASC processed composites reveal considerable interaction between the polymer matrix and the glass flake surfaces with uniform distribution of the polymer in the structure. The brick and mortar architecture was achieved especially by the HASC method rather than HP. Independent of the consolidation process applied usage of initial tapes formed by TC process supplied remarkable nacre-like alignment, as doctor blading action on the glass flake containing suspension provides alignment of the flakes even before the consolidation step.

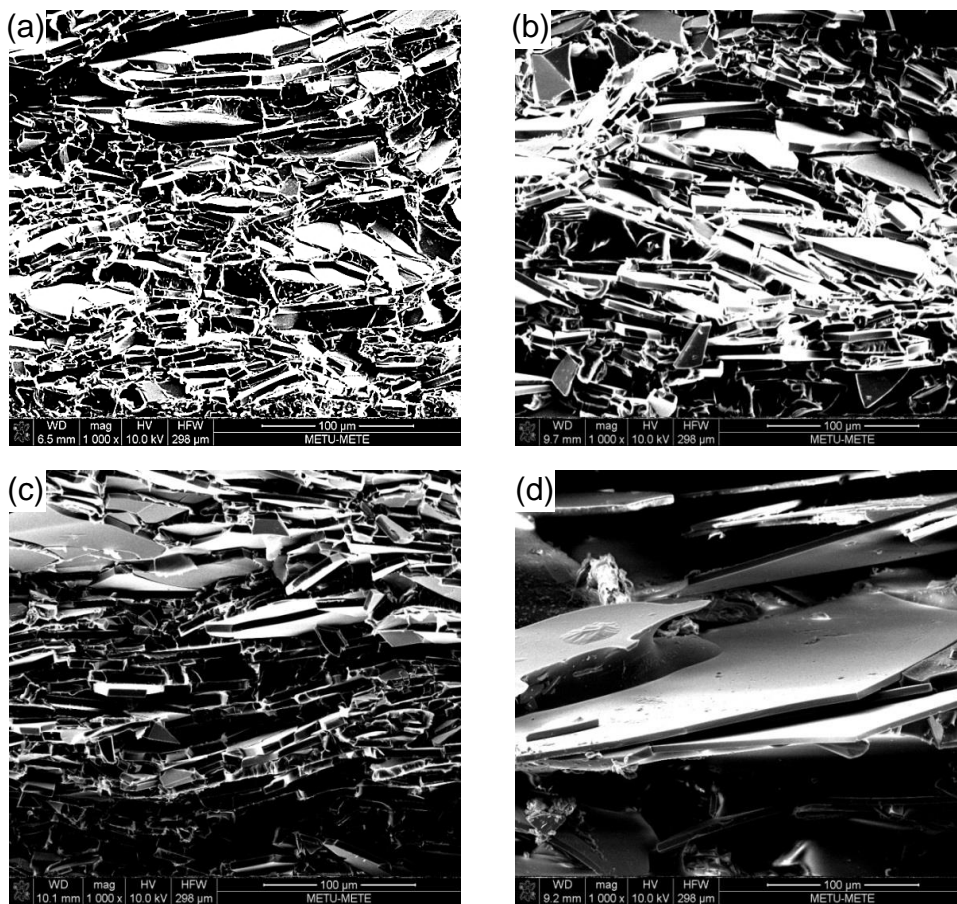


Figure 4.7. Scanning electron microscope images of the fracture surfaces of the three point bending tested PS matrix composites fabricated by (a) AC+HASC, (b) TC+HASC, (c) TC+HP and (d) AC+HP.

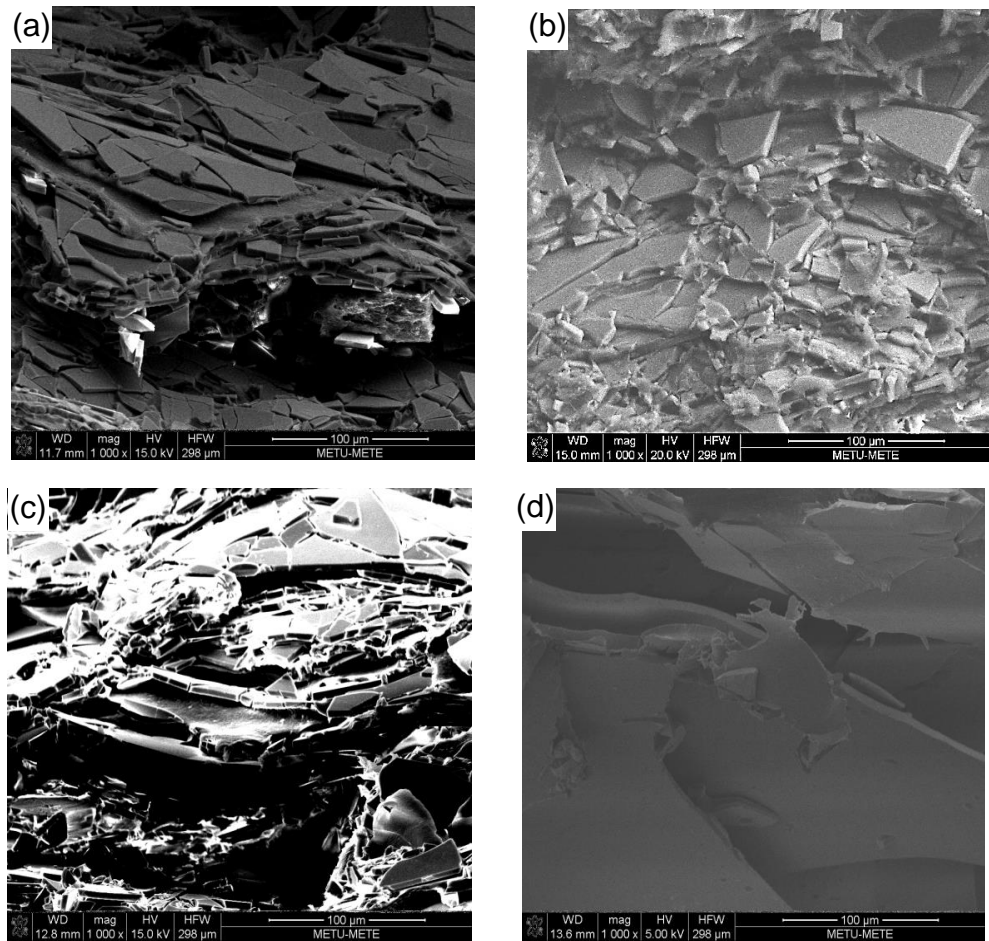


Figure 4.8. Scanning electron microscope images of the fracture surfaces of the three point bending tested ABS matrix composites fabricated by (a) AC+HASC, (b) TC+HASC, (c) TC+HP and (d) AC+HP.

Three point bending test was conducted in all specimens to determine the mechanical behavior of the composites. The results showed that AC+HASC processed composites were superior to the others in terms of flexural strength. The reason why the AC+HASC processed composites has demonstrated superior mechanical characteristics to the others can be explained by the microstructure formation controlled by the flow mechanism of the molten polymer during HASC process.

Three point bending test results revealed that independent of the matrix type HASC processed composites have higher flexural strengths (Figures 4.9 and 4.10) than the HP processed ones mainly due to their lower porosity and higher inorganic content (Table 1). This effect is more pronounced in the case of AC+HASC processed composite compared to the TC+HASC processed one. For PS matrix composites, flexural strength of AC+HASC processed composites is ~21% higher than that of the TC+HASC processed one also due to relatively more efficient alignment of glass flakes as brick and mortar architecture based on the presence of fluid flow during HASC process. For ABS, the increase of the flexural strength was ~5%.

On the other hand, AC+HASC processed PS matrix composites revealed ~31% higher flexural strength compared to ABS matrix composites fabricated by the same method, since strength to weight ratio of PS is 59-72 kN-m/kg while that of ABS is 37kN-m/kg. Consequently, PS matrix composites have higher flexural strength than ABS matrix ones. Furthermore, PS matrix composites have higher elastic modulus values compared to ABS matrix ones because of the lower elasticity of the pristine PS compared to ABS which also reveals itself by the lower flexural strains achieved in PS matrix composites independent of the processing combination applied. Three point bending test results presented in Figure 4.9 and 4.10 show the effectiveness of AC+HASC process combination leading to higher strength composites independent of their thermoplastic polymer matrix mainly due to the microstructural characteristics it generates.

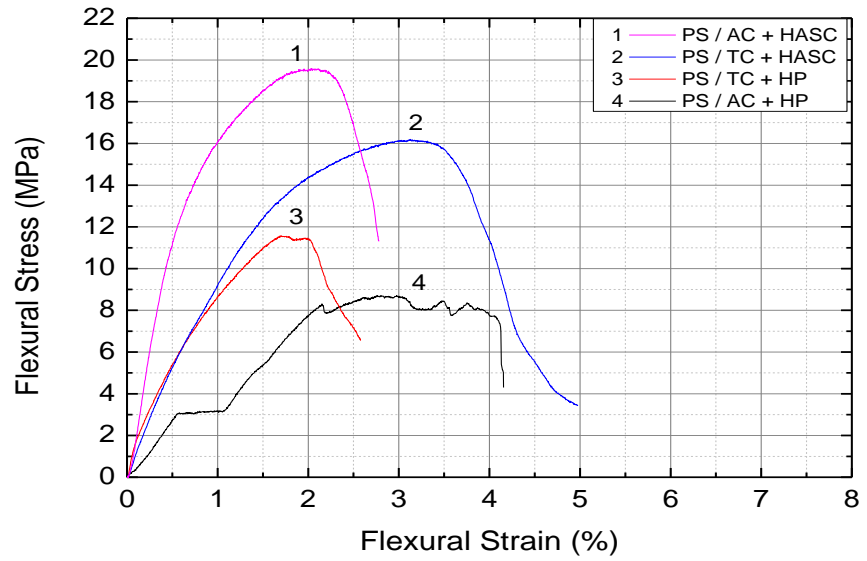


Figure 4.9. Flexural stress vs. strain curves of PS matrix composites fabricated by the four process combinations.

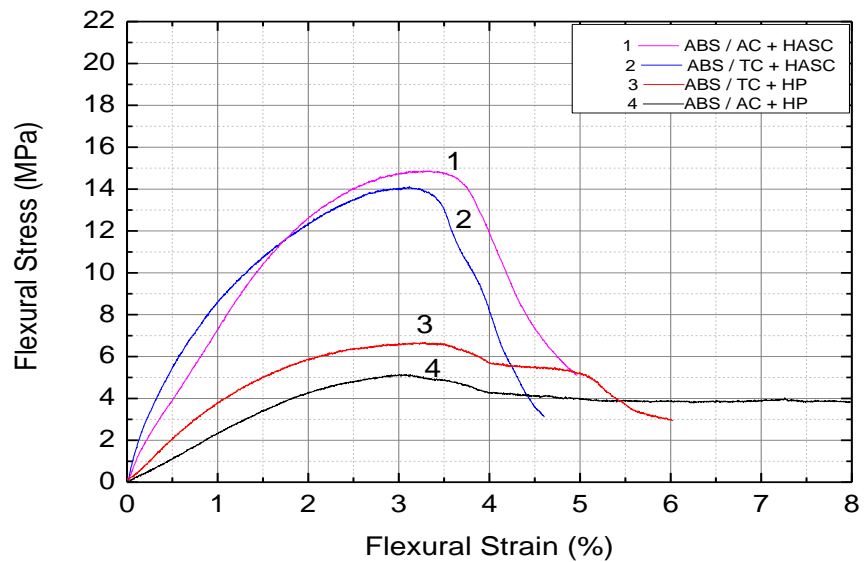


Figure 4.10. Flexural stress vs. strain curves of ABS matrix composites fabricated by the four process combinations.

Three point bending test results indicated that composites with different thermoplastic polymer matrices revealed different mechanical behavior. Two different thermoplastic polymers namely PS and ABS have different number average molecular weight as well as different chemical components and different structural type. All these differences in their inherent characteristics lead to the difference in the mechanical properties of the composites they form. PS granules used in this study have 64946 g/mole number average molecular weight while ABS granules have 28309 g/mole. According to the number average molecular weights the rheology and swelling behavior of polymers are different. Higher number average molecular weight leads to weaker fading response, and hence higher viscosity of the molten polymer. Moreover, the intrinsic viscosities of PS and ABS used in this study were 0.585324 dL/g and 0.406511 dL/g, respectively. This leads to better flow characteristic to ABS during HASC process. Nevertheless, even though packing and inorganic flake alignment during the HASC process might be more efficient in the case of ABS matrix, due to its chemical structure dependent deficient inherent mechanical strength, AC+HASC processed ABS matrix composites reveal lower flexural strength compared to PS matrix one.

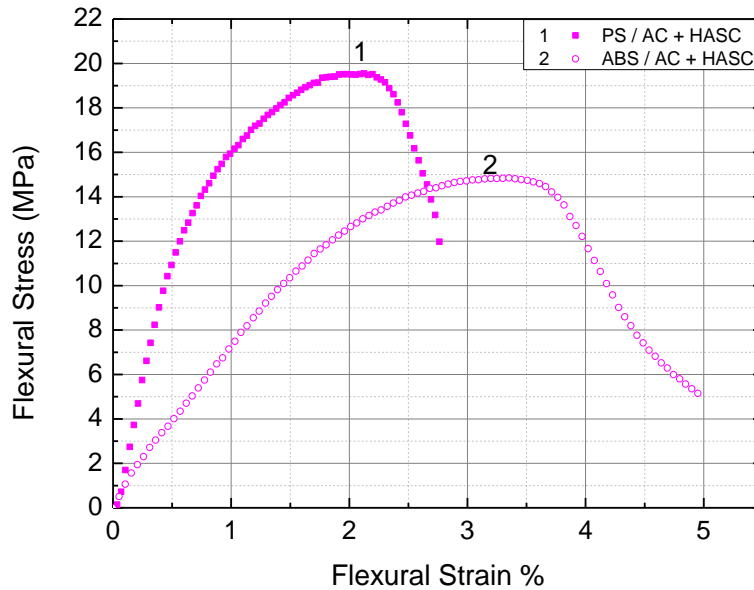


Figure 4.11. Variation in mechanical properties of acrylonitrile butadiene styrene and polystyrene polymer matrices composites fabricated by AC+HASC method.

To improve the interaction between inorganic and organic phases and to investigate the coupling agent effect in the resulting mechanical properties of the composites, glass flake surfaces were treated with aminopropyltriethoxy type organofunctional silane. As it has been mentioned earlier on, silane molecule functions as a chemical bridge bonding to both the inorganic surface and the organic matrix. In the present case there is a weak interaction between the selected silane and both of the thermoplastic polymer used. However, despite this weak interaction silane results in enhanced crosslinking in the polymers [79]. Due to its direct effect on the polymer and bonding to the inorganics surface, silane treatment is expected to improve the mechanical characteristics of the targeted composites.

Silane treated and as-received glass flake surfaces were examined by XPS to observe the attachment of the silane molecules on the inorganic surfaces. In

Figure 4.12 (a) surface chemical composition of as-received glass flakes is given. Peaks at 102, 153, 284-293, 540 and 1071 eV correspond to Si2p, Si2s, C1s, O1s, Na1s, respectively, where peaks at 496, 978 and 999 eV correspond to NaKL1, OKL1 and OKL2 Auger peaks (Figure 4.12 (a)). Peaks at 102, 285, 400 and 532 eV in Figure 4.12 (b) correspond to Si2p, C1s, N1s and O1s, respectively. Presence of N1s peak in the case of the silane treated glass flakes proves the silane attachment to the surface by the applied procedure. The intensity difference in C1s and Si2p peaks in both cases points out to the difference in the chemical bonding and the interaction between the inorganic surface and the silane molecule resulting from the applied surface functionalization.

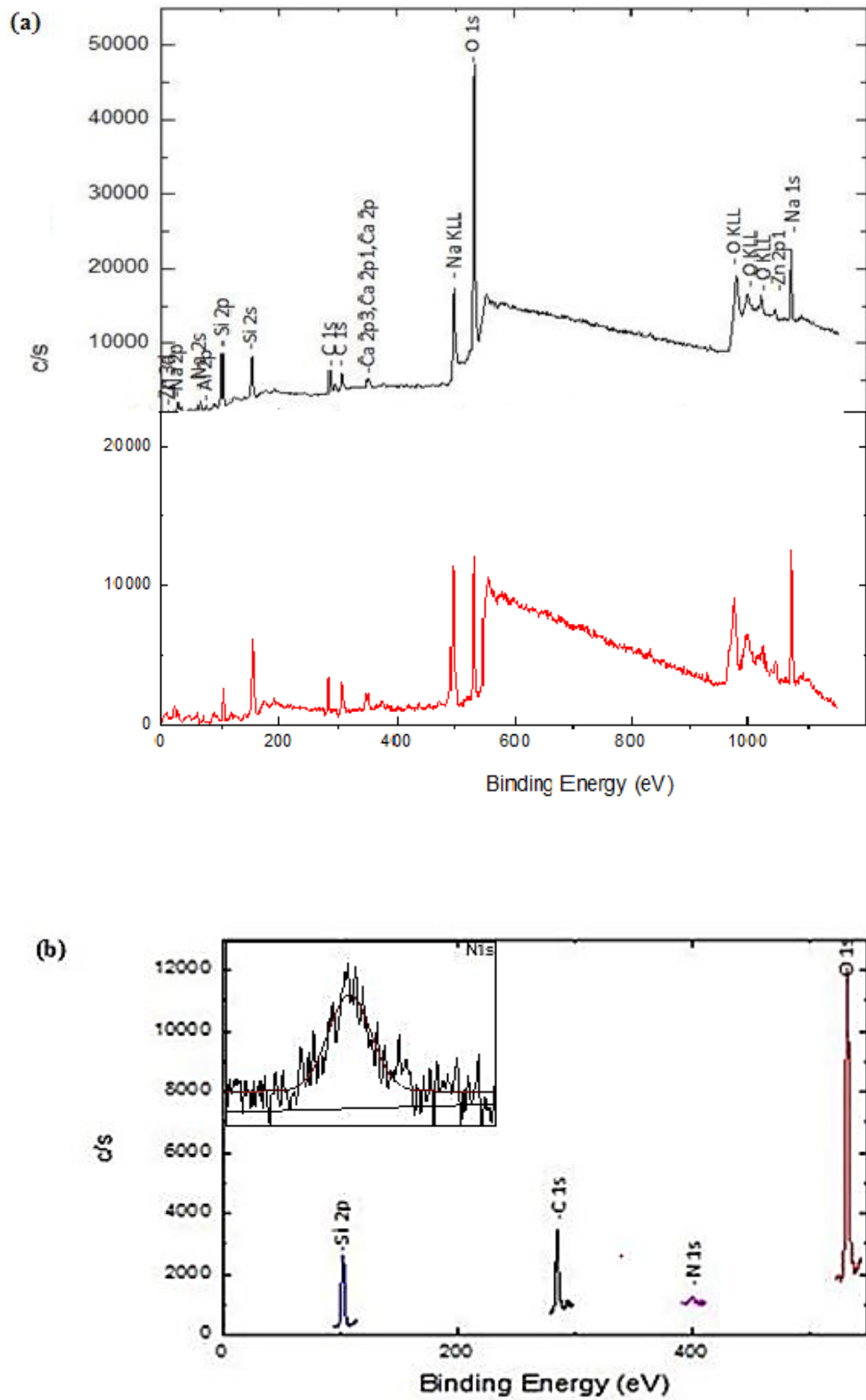


Figure 4.12. XPS spectra of (a) as-received and (b) silane treated glass flakes.

Silane treatment could improve the interaction between the glass flakes surfaces and the organic matrix. However, modification of the glass flake surfaces with aminopropyltriethoxy silane results in differences in the microstructure and chemical structures of the resulting composites. According to the inorganic content and hardness results given in Table 4.2, surface treatment by silane is more effective in PS matrix composites compared to ABS matrix ones due to the interaction difference between the thermoplastic polymer type and the silane used. Modification with silane in PS matrix enhances the interlocking in between the polymer chains leading to enhanced hardness.

Superior molecular attraction between the silane and polystyrene molecules leads to enhanced interaction between the silane attached glass flake and the PS matrix. Therefore, as shown in Table 4.2 there is a remarkable inorganic content difference in PS matrix composites before and after silanization while there is no change in ABS matrix ones. This corresponds to higher interlocking of the PS polymer chains resulting in stronger bonding among the glass flakes leading to higher hardness despite the decrease in the inorganic content. Even though the inorganic content remains unchanged, the increase in hardness in the ABS matrix composites after silanization depends also on the interlocking within the polymer chains despite the molecular interaction between the silane and ABS molecules are weaker compared to that in PS matrix. In addition to these, difference in the HASC process temperatures for PS and ABS matrix composites may also be effective in the resulting properties, as molecular attraction and bonding ability of silane to inorganic surfaces changes with temperature as well as viscosity of the surrounding molten polymer.

Table 4.2. Inorganic content, density, relative density (%) and hardness of AC+HASC processed ABS or PS matrix composites reinforced by as-received or silane treated glass flakes.

	Inorganic Content (wt%)	Density (g/cm ³)	Relative Density (%)	Hardness (HV0.2)
ABS Matrix				
AC+HASC/Silane	52	1.47 ± 0.2	100	20 ± 2.7
AC+HASC	52	1.47 ± 0.1	100	15 ± 1.7
PS Matrix				
AC+HASC/Silane	51	1.39 ± 0.1	93	25 ± 2.4
AC+HASC	55	1.39 ± 0.2	93	20 ± 2.3

In Figures 4.13 and 4.14 microstructures of AC+HASC processed PS matrix composites reinforced by as-received or silane treated glass flakes are shown. According to these microstructures alignment of the flakes seems to have improved with the silane treatment. Silane improves the interlocking of polymer chains limiting the amount of matrix remaining between the glass flakes in order to optimize space filling in the structure. Consequently, organofunctional silane treatment applied on the inorganic flake surfaces has a positive effect on the formation of the desired brick and mortar architecture. The polymer matrix amount remaining in between the glass flakes is indicated by the arrows in Figures 4.13 and 4.14 showing the presence of a more uniformly distributed, thinner matrix layer on the surfaces of silane treated glass flakes. This uniform distribution of the matrix in the structure is based on the molecular interaction between polymer chains and silane affecting the flowing behavior of the molten polymer. Superior alignment along with the uniformly distributed matrix among the reinforcing phase is the key to achieve strengthening and stiffening in the nacre-like bio-inspired composites.

When Figures 4.13 (d) and 4.14 (d) are compared it seems that the alignment of surface treated glass flakes is superior in PS matrix composite compared to that of ABS matrix ones, respectively. The reasons behind this difference can be the better interaction between the silane and the PS as well as the properties of the polymer such as chain length, viscoelastic behavior and monomer. Especially the monomer has a crucial importance on the interaction behavior of the polymer chain with the organofunctional silane.

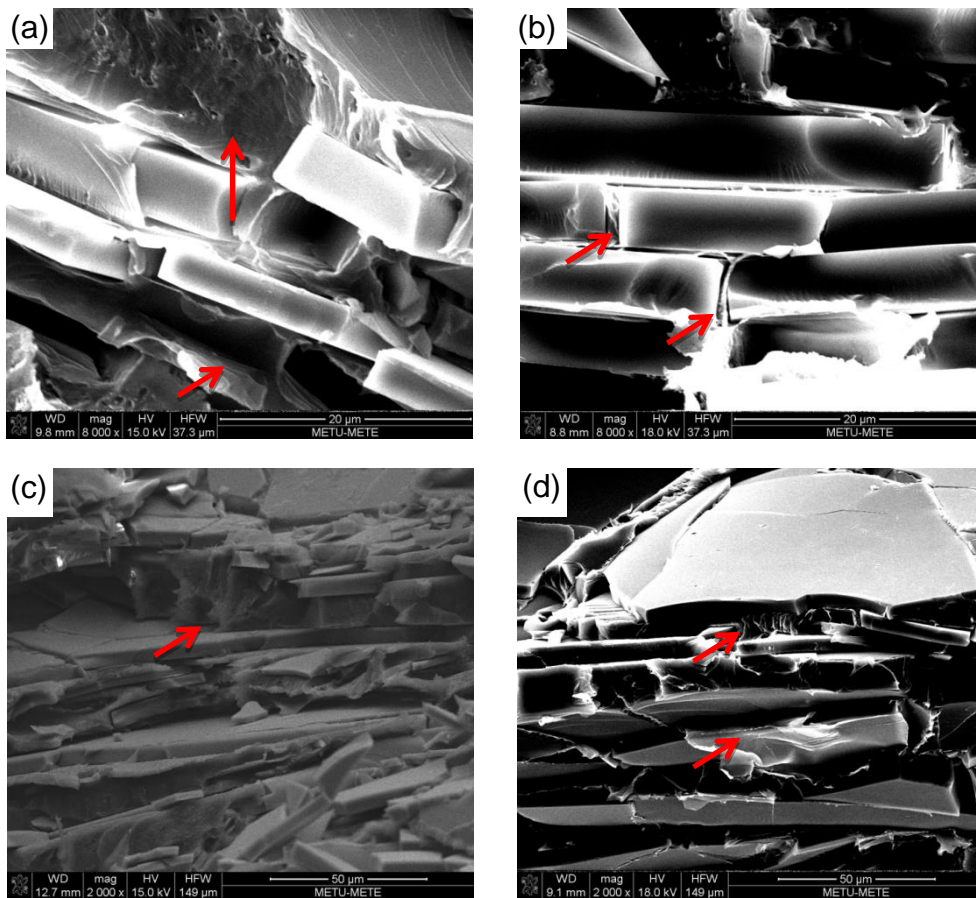


Figure 4.13. Fracture surfaces of three point bending tested AC+HASC processed PS matrix composites reinforced by (a) and (c) as-received and (b) and (d) silane treated glass flakes.

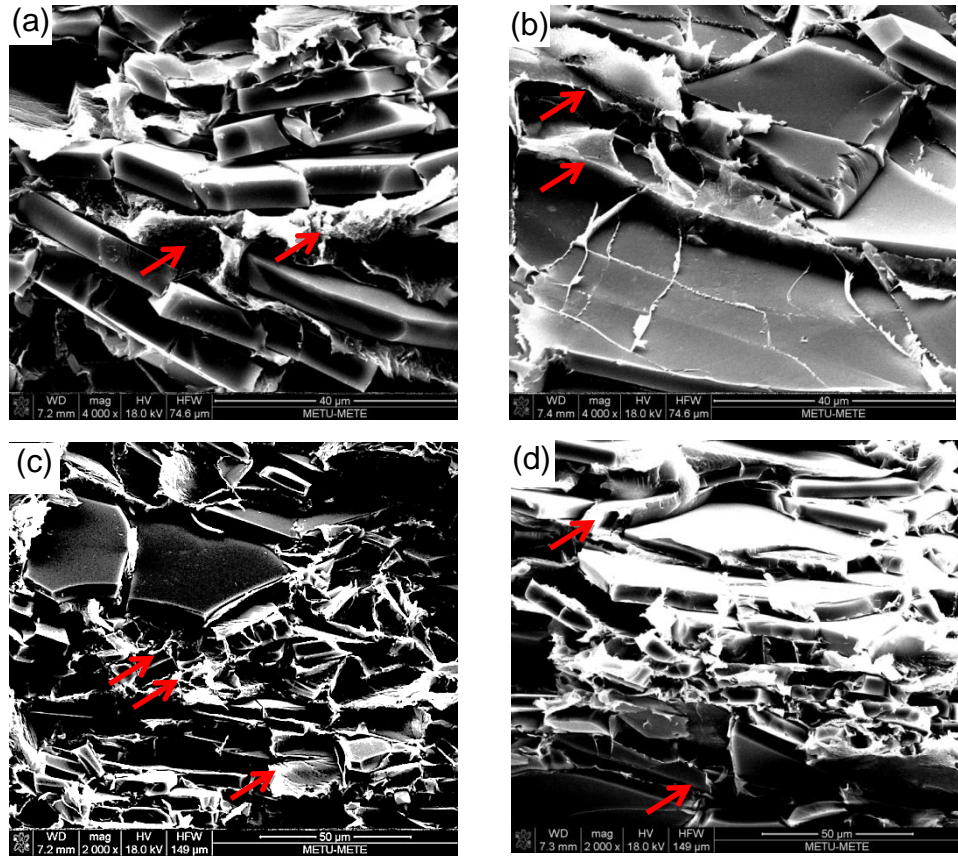


Figure 4.14. Fracture surfaces of three point bending tested AC+HASC processed ABS matrix composites reinforced by (a) and (c) as-received and (b) and (d) silane treated glass flakes.

Flexural stress vs strain curves of AC+HASC processed PS and ABS matrix composites reinforced by as-received and silane treated glass flakes are shown in Figure 4.15. According to these three point bending test results, it is clear that after silane treatment there is a remarkable increase in flexural strength and stiffness for both of the polymer matrices. Results showed that after silane treatment flexural strengths of PS and ABS matrix composites increased by ~34% and ~27%, respectively, compared to their counterparts reinforced by as-received glass flakes. Higher strength and stiffness of PS matrix composites compared to those of ABS matrix ones is also evident in both of the cases.

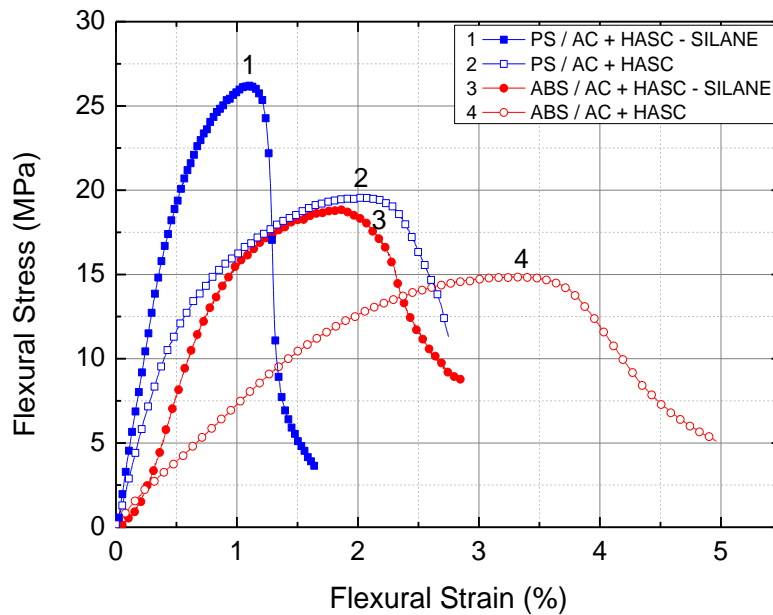


Figure 4.15. Flexural stress vs. strain curves of AC+HASC processed PS and ABS matrix composites reinforced by as-received and silane treated glass flakes.

For both thermoplastic polymer matrices, mechanical response of the fabricated composites has improved when reinforced by silane treated glass flakes revealing itself with increasing flexural strength and stiffness values. This is an expected result of treating inorganic reinforcement surfaces with a proper silane applied with a proper method. Silane treatment could enhance the possible interactions between the polymer chains. However, penetration of polymer chains into the silane structure could be suppressed by the Si-O-Si bonds between the silane molecules and the inorganic surface [79]. In Figure 4.16, the schematic representation of the interaction between the polymer chains and aminopropyltriethoxy silane is illustrated. In this schematic representation, polymer chains interlock with each other, and there is a small attraction between the silane molecules and the polymer chains. Although there is no direct attachment between the silane and polymer molecules, enhanced interlocking of

the polymer chains due to the effect of silane can lead to increase in strength of the composites.

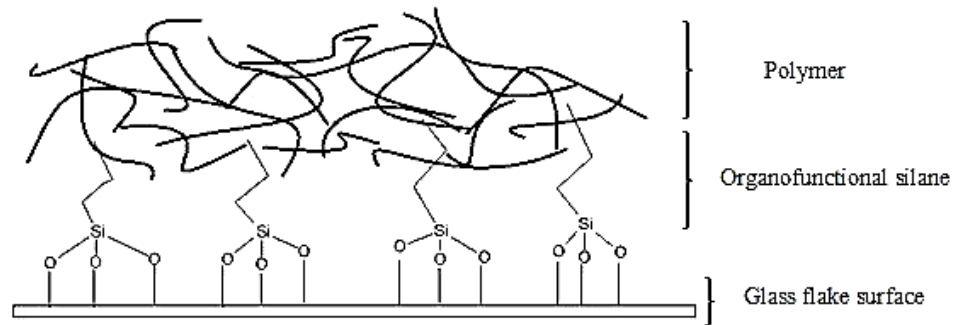


Figure 4.16. Schematic representation of the interaction between aminopropyltriethoxy silane and polymer chains [79].

Effect of silane treatment on the fracture resistance of the AC+HASC processed PS and ABS matrix composites has been investigated by work of fracture tests. Energy absorbed by the material during the growth of a crack has been determined by dividing the area under the Load vs. Extension curves (Figure 4.17) to the fracture surface area of the composite after the test. Although fracture surfaces of composites were tortuous rather than being flat after the work of fracture tests, the area was taken to be smooth as a first approximation, which has also been done in studies reporting about the toughening mechanism of nacre [49].

Results of this test demonstrate the ability to absorb energy during crack propagation, and hence fracture. According to the results presented in Figure 4.17, energy absorption has increased from 171 J/m² to 295 J/m² in AC+HASC processed PS matrix composite after silane treatment. In the case of the AC+HASC processed ABS matrix composite energy absorption has increased from 349 J/m² and 379 J/m² following the silane treatment. As expected, ABS matrix composites show much higher work of fracture

compared to PS matrix once due to their higher inherent elasticity and toughness. However, in the case of the PS matrix composites the improvement in work of fracture was much higher due to the better flake alignment as well as superior interaction between the PS matrix and the applied silane.

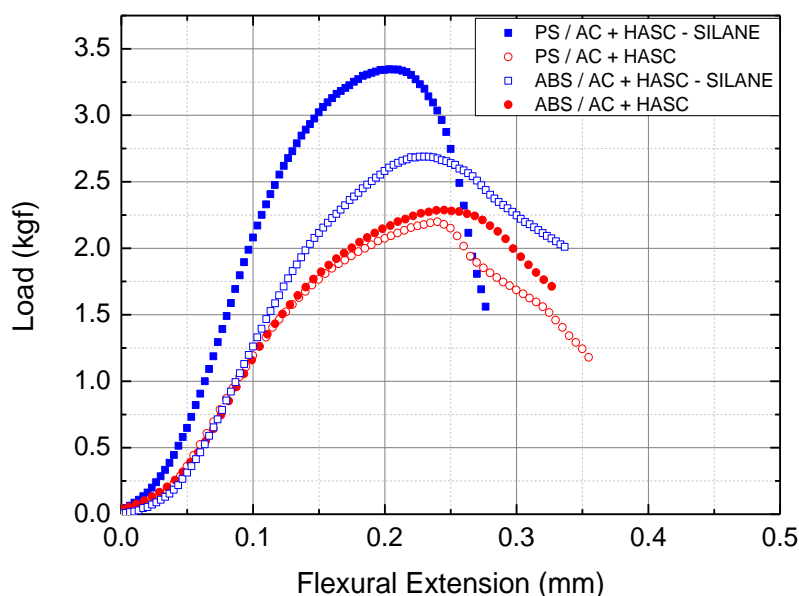


Figure 4.17. Load- extension curves of SENB specimens of AC+HASC processed PS and ABS matrix composites reinforced by as-received and silane treated glass flakes.

4.2 Magnetite Nanoparticle Attached Glass Flake Reinforced Nacre-Like Bulk Lamellar Composites Fabricated by Magnetic Field Assistance

One of the novel approaches proposed for the fabrication of inorganic flake or platelet reinforced nacre-like bio-inspired composites is to include magnetic field assistance in the processing. This includes the alignment of non-magnetic inorganic flakes or platelets with an applied magnetic field which is mainly possible by attaching magnetic particles on the surfaces of

the reinforcing materials. In this scope, within the current study magnetite nanoparticle attached glass flake reinforced nacre-like bulk lamellar composites were fabricated by magnetic field assistance.

Applied procedure comprised of attaching magnetite nanoparticles on as-received glass flake surfaces, aligning these surface modified flakes by a magnetic field supplied using a hard magnet and finally consolidating the dried initial material via hot-pressing to obtain bulk composites. The success of the attachment of magnetite nanoparticles by the applied treatment has been proven by the change in the color of the initially transparent glass flakes to brown which was the color of the used cationic magnetite nanoparticle solution. In Figure 4.18 coloring of the glass flakes with magnetite nanoparticle attachment can be observed both before and after filtration.



Figure 4.18. Color difference between as-received and nanoparticle attached glass flakes before and after filtering the processing solution.

Optical microscope image of magnetite nanoparticle glass flakes placed on the hard magnet shows the effect of magnetic field on these surface modified glass flakes (Figure 4.19). It is clear that surface modified glass flakes align with the magnetic field being their basal planes perpendicular to the magnet surface. The alignment of these flakes could also be observed by naked eye very clearly because of the change in the color of the mass by alignment. With the alignment of the surface modified glass flakes the color of the mass changes from light to dark brown where its brightness decreases at the same time.

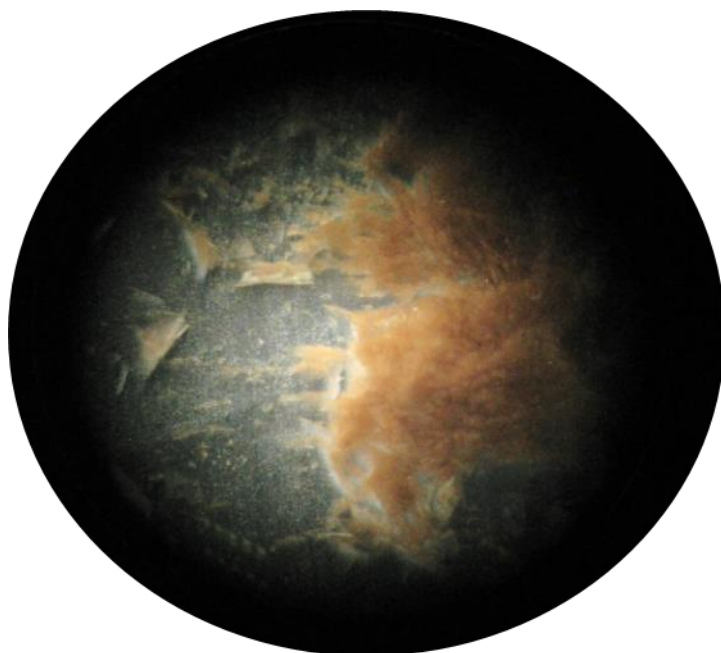


Figure 4.19 Optical microscope image of the surface modified glass flakes aligned on the hard magnet.

To investigate the attachment of magnetite nanoparticles in detail surfaces of as-received and surface modified glass flakes were analyzed by FTIR. As it can be seen in Figure 4.20, acquired FTIR spectra of the as-received and magnetite nanoparticle attached glass flakes show different peak positions and structures caused by the difference in the existing bonds in the two cases. As glass flakes is mainly composed of SiO_2 , there are three different peaks common to both as-received and surface modified glass flakes corresponding to Si-O-Si bond. Peaks at 860-940, at 710-1175 and 415-540 cm^{-1} correspond to Si-O-Si bond stretching, tetrahedral Si-O-Si bonding and Si-O-Si bond bending, respectively. For both of the cases the peaks observed at 1400 cm^{-1} might correspond to Al_2O_3 since the C-type glass flakes contain low amount of aluminum oxide. Peaks present between 800 to 950 cm^{-1} in the FTIR spectrum of the magnetite nanoparticles attached glass flakes (Figure 4.20 (b)) corresponds to Si-O-Fe attachment. In addition

with the applied surface modification, FTIR spectrum peaks of the as-received glass flakes shifted and the area under the peaks changed.

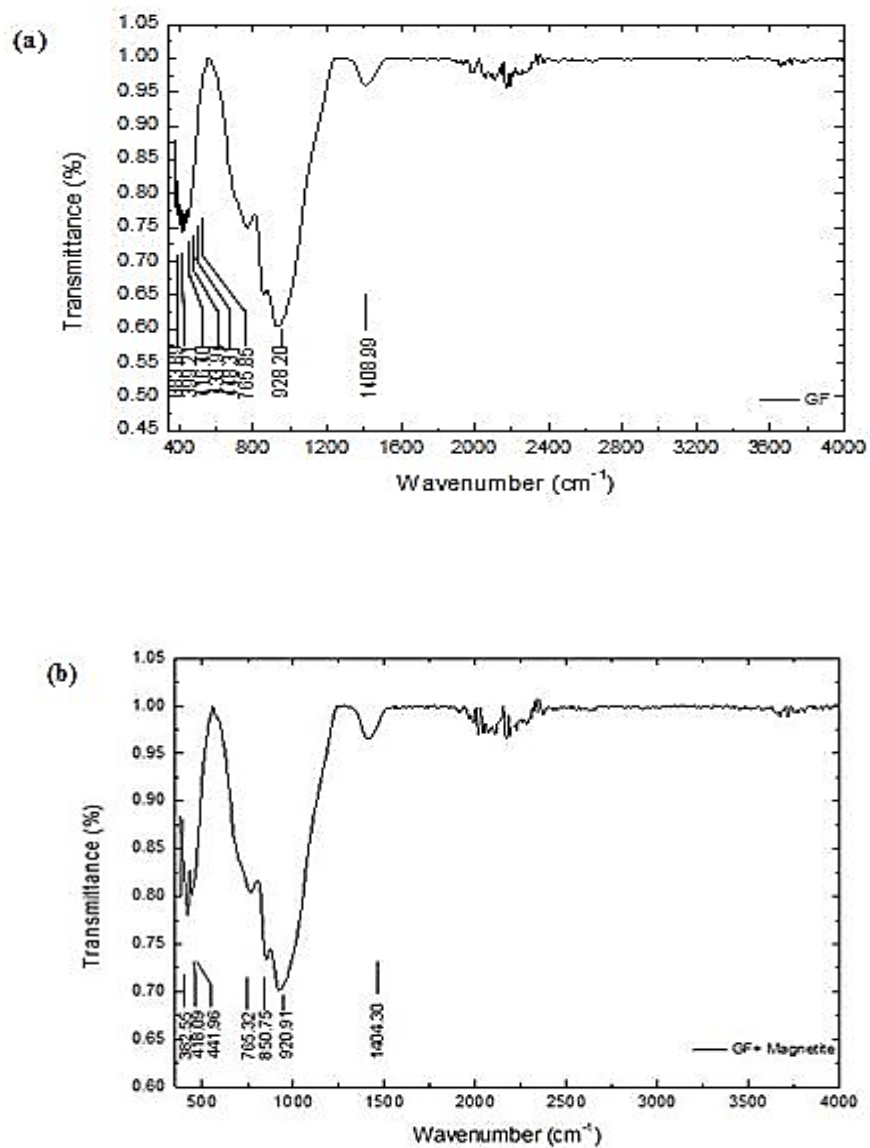


Figure 4.20 FTIR spectra of (a) as-received and (b) magnetite nanoparticle attached glass flakes.

After the alignment of the surface modified glass flakes vertically on the magnet surface, necessary amount of polymer solution was added drop by drop on the aligned glass flakes. Three different polymer solution compositions were used in order to investigate the effect of the amount of the polymer matrix on the resulting properties of the composites. Initial amount of the polymer, which is polystyrene (PS) in the current case, was changed such that the matrix content in the composites before consolidation were 38, 43 and 53 wt%. At this step the critical issue was not to harm the flake alignment supplied by the magnetic field, while increasing the organic matrix content to be added.

After adding different amounts of polymers on the aligned glass flakes for each set, the consolidation of the mass was achieved following its drying by hot-pressing. Hot-pressing method includes melting of the polymer matrix which is under the action of a unidirectional pressure leading to ideally uniform distribution of the organic matrix in all structure. However, although the consolidated composite contained sufficient amount of the polymer matrix, absence of polymer flow, and hence drainage, from the system has led to porosity formation. In Table 4.3, percent relative density for different initial polymer amounts in the composites is shown. According to these results, increase of the initial polymer content resulted in denser composites, i.e. lower amount of residual porosity, since molten polymer can fill in the available gaps in the structure more efficiently and uniformly with increasing amount of liquid polymer in the structure. Microhardness results demonstrated no considerable difference for varying polymer contents. Even though there is ~10% densification difference between the maximum and minimum achieved densities, presence of similar hardness values can be attributed to the locality of the microhardness test applied and the relatively larger pore sizes observed.

Table 4.3. Density, relative density (%) and hardness of the fabricated composites for three different initial polymer contents (wt% PS).

Polymer Content (wt% PS)	Density (g/cm ³)	Relative Density (%)	Hardness (HV0.2)
53	1.31	100	16 ± 3.1
43	1.23	90	15 ± 3.1
38	1.21	89	15 ± 3.0

Alignment of the magnetite nanoparticle attached glass flakes by means of magnetic field application was followed by the HP process as the consolidation process which was mentioned in Chapter 3 in detail. Consequently, microstructure formation in magnetically aligned and hot-pressed composites can be compared to those achieved by the previously discussed process combinations including HP process, namely TC+HP and AC+HP. In this scope, microstructural observation of the composites containing various amounts of polymer matrices revealed that brick and mortar arrangement was achieved in all composites independent of the polymer content (Figure 4.21). Similar nacre-like microstructure has also been achieved by the previously presented PS matrix composites fabricated by HP process containing combinations (Figure 4.7 (c) and (d)).

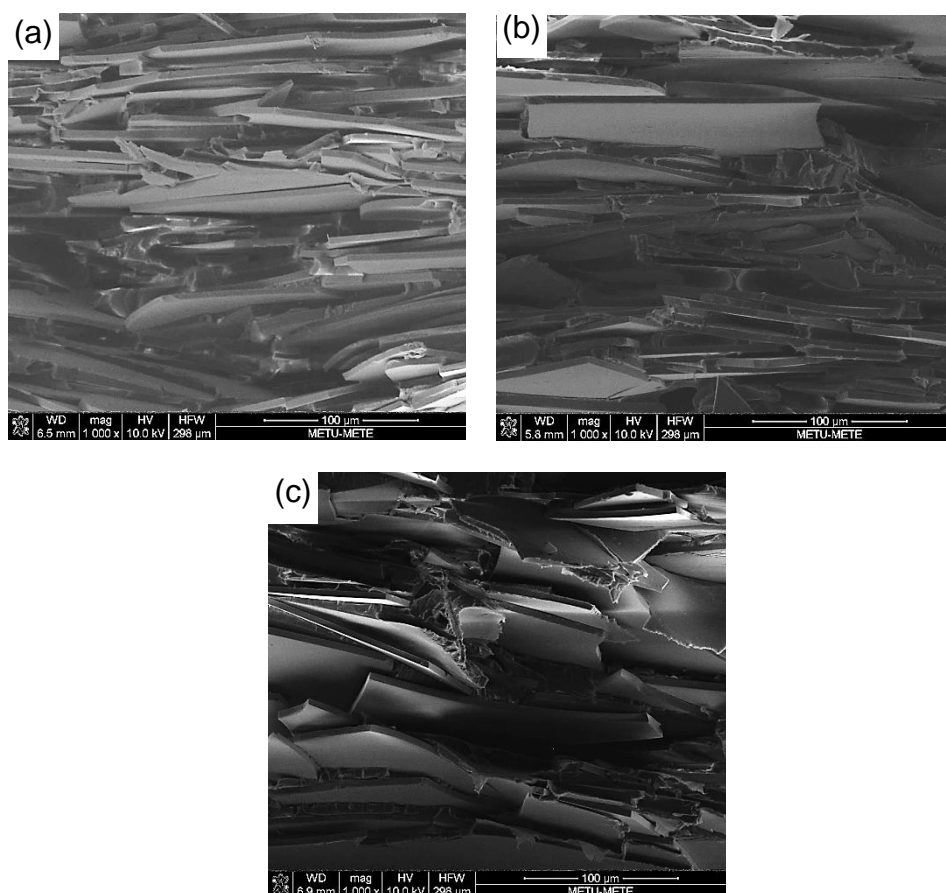


Figure 4.21 Fracture surfaces of the three point bending tested composites fabricated by magnetic field assistance and HP containing (a) 38 wt %, (b) 43 wt % and (c) 53 wt % PS matrix.

To reveal the mechanical properties of composites fabricated by magnetic field assistance method, three point bending test was conducted. Three point bending test results revealed the increase in the flexural strength of the composites with increasing polymer matrix content. The proportionality between the strength and the polymer matrix content can be attributed to the improvement of the interaction between the matrix and the magnetite nanoparticle attached flakes with the help of the efficient distribution of the matrix in the structure. According to the three point bending test results shown in Figure 4.22, composite containing of 53 wt% polymer matrix has ~35% and ~163% higher flexural strength than the composites containing 43 and 38 wt% polymer matrix, respectively. Expectedly, 38 wt% polymer matrix containing composite, which corresponds to the highest amount of

the inorganic phase content, has the highest stiffness, yet both of its flexural stress and failure to strain are the lowest due to the inefficient stress transfer from the matrix to the reinforcement caused by its non-uniform distribution.

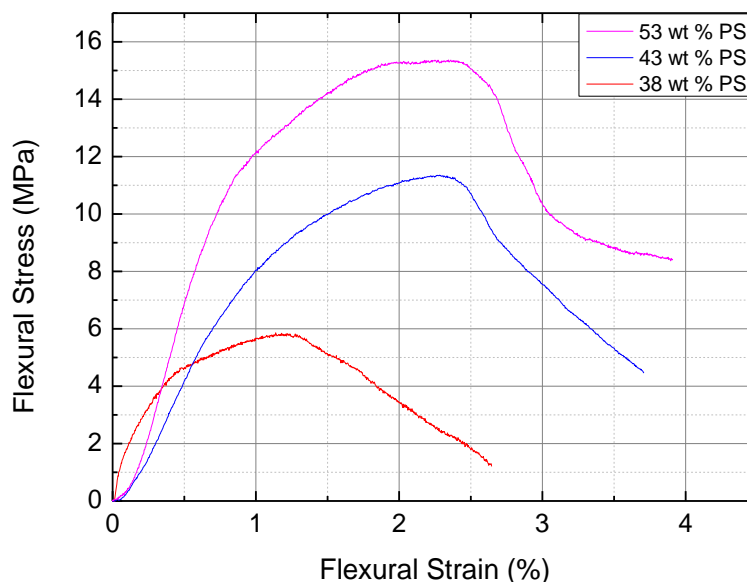


Figure 4.22. Three point bending test data of composites fabricated by magnetic field assistance followed by HP having different amounts of polymer matrix.

The interaction between the PS matrix and the magnetite nanoparticles attached on the glass flake surfaces also have a crucial effect on the resulting mechanical properties in addition to the effect of polymer content and distribution within the composites. The interaction between the PS molecules and the magnetite particles has been schematically illustrated in Figure 4.2, where the magnetite nanoparticles act as an adhesive strongly bonding the organic and inorganic phases. Increasing polymer content resulting in a more uniform distribution in the composites corresponds to higher effectiveness in the interaction between the PS molecules and magnetite nanoparticle attached glass flake surfaces.

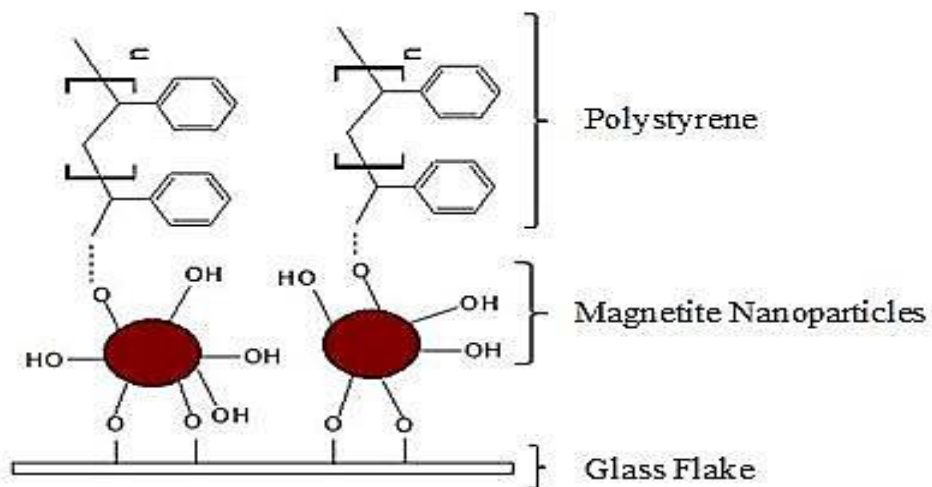


Figure 4.23. Schematic representation of the chemical interaction between the magnetite nanoparticles attached on the glass flake surfaces with polystyrene molecules.

Additionally, in this study magnetite nanoparticle attached glass flake surfaces were also treated by an organofunctional silane called aminopropyltriethoxy silane. The aim of this treatment was to further improve the chemical interaction between the organic and inorganic phases. Since previously presented results clearly indicated that increasing polymer matrix content has led to superior flexural strength, magnetite nanoparticle attached and silane treated glass flakes were used to reinforce 53 wt% polymer containing composites. Microstructural investigation (Figure 4.24) of just magnetite nanoparticle attached and also additionally silane treated glass flake reinforced composites fabricated by magnetic field assistance revealed that both of the composites have brick and mortar architecture, yet the interaction between the polymer matrix and the inorganic surfaces seems to be remarkably improved by the applied silane treatment. In Figure 4.24 (b), improvement in the adhesion of the PS matrix to the silane treated glass flake surfaces was shown by arrows as compared to a lower amount of PS

adhered to only magnetite nanoparticle attached glass flakes again shown by arrows in Figure 4.24 (a).

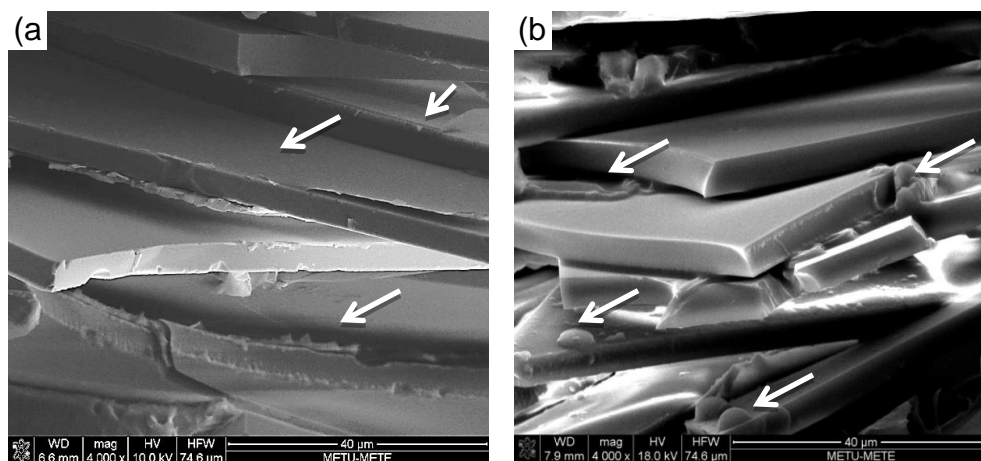


Figure 4.24. Fracture surfaces of the three point bending tested 53 wt% PS matrix containing composites fabricated by magnetic field assistance and HP reinforced by (a) only magnetite nanoparticle attached glass flakes and (b) magnetite nanoparticle attached and then silane treated glass flakes.

Change in the mechanical properties of the 53 wt% PS matrix containing composites by silanization of the magnetite nanoparticle attached glass flake surfaces has been investigated by microhardness measurements and three point bending tests. After silane treatment, the microhardness of the composite increased from ~16 to ~21 HV. In addition to this, three point bending test results revealed that 53 wt% PS matrix containing composite reinforced by silane treated magnetite nanoparticles attached glass flakes have the highest flexural strength and the stiffness compared to the others (Figure 4.25). Increase in hardness, strength and stiffness shows that the interaction and interfacial adhesion between the polymer and the magnetite nanoparticle attached glass flake surfaces have further been enhanced by the organofunctional silane treatment. Furthermore, the results demonstrated that there could be also an interaction between the magnetite nanoparticles

and silane molecules contribution to the improvement in the mechanical characteristics.

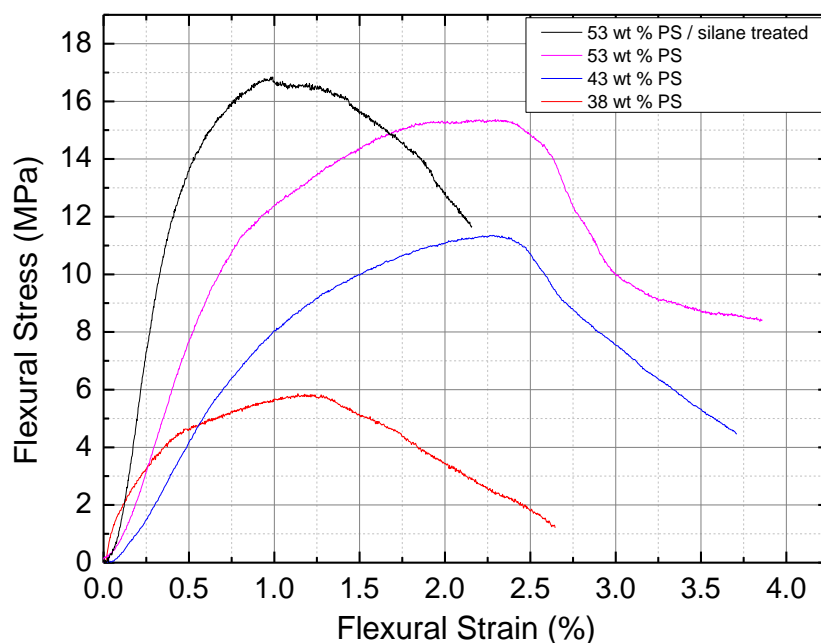


Figure 4.25. Three point bending test data of composites fabricated by magnetic field assistance followed by HP having different amounts of polymer matrix also including the silane treated one.

Fracture resistance of the composites fabricated by magnetic field assistance followed by HP has been investigated via work of fracture tests applied on all composites. As mentioned previously, energy absorbed by the material during the growth of a crack has been determined by dividing the area under the Load vs. Extension curves (Figure 4.26) to the fracture surface area of the composite after the test. Although fracture surfaces of the composites were not smooth rather than being flat after the work of fracture tests, the area was taken to be smooth and flat as a first approximation, which has also been done in studies reporting about the toughening mechanism of nacre

[49]. According to the results presented in Figure 4.26, energy absorption has increased from 181 J/m² to 314 J/m² for 53 wt% PS matrix containing composites after treating the magnetite nanoparticle attached glass flakes with silane. Energy absorption has increased from 156 J/m² to 175 J/m² by increasing the matrix content in the composites from 43 wt% to 38 wt%. Mechanical test results demonstrated increasing the polymer matrix content increases both the strength and fracture resistance of the composites fabricated by magnetic field assistance followed by HP which were further enhanced by the application of silane treatment on the magnetite nanoparticle attached glass flakes. This demonstrates that both strengthening and toughening can be achieved in nacre-like bulk lamellar composites by the proper alignment of the inorganic flakes in the matrix, the usage of the optimum amount of organic-inorganic phase ratio along with the application of an organofunctional silane treatment on the inorganic surfaces.

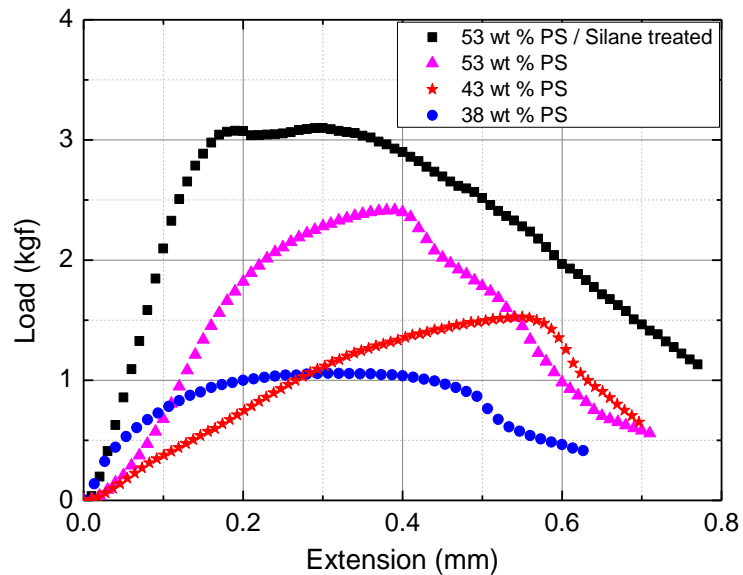


Figure 4.26. Load vs. extension curves of WOF tested composites fabricated by magnetic field assistance followed by HP process having different amounts of polymer matrix also including the silane treated one.

CHAPTER 5

CONCLUSION

In this study, hot-pressing and magnetic field assistance based processing method combinations have been developed in order to fabricate nacre-like bulk lamellar thermoplastic matrix composites reinforced by glass flakes. For both of the processing routes, glass flake surfaces were treated with an organofunctional silane, in order to tailor the interface between the organic and inorganic phases and to achieved strengthening along with improvement in fracture resistance. Following the fabrication steps mechanical properties of the fabricated composites were examined using three point bending, micro hardness and work of fracture tests.

Within the scope of the hot-pressing based methods, four different combinations composed of as-casting (AC) or tape casting (TC) as initial shaping processes followed by hot-pressing (HP) or hot press assisted slip casting (HASC) as consolidation steps were studied. These four combinations were designated as AC +HASC, TC+HASC, AC+HP and TC+HP. Effectiveness of these process combinations in revealing brick and mortar structure similar to that of nacre with enhanced mechanical characteristics has been investigated. According to the findings previously presented in detail, even though all of the four process combinations have led to the nacre-like brick and mortar architecture, this structure could be achieved most properly using AC+HASC where the inorganic content and densification could be maximized.

To control the alignment of the inorganic flakes in reaching to the nacre-like microstructure similar to that of the mollusc shell, magnetic field assistance technique was examined as a novel approach. The interaction with the applied magnetic field was supplied by the attachment of magnetite nanoparticles on non-magnetic glass flake surfaces. The main point in this part was to change the organic to inorganic ratio in the composite and to control the interfacial properties between the two constituent phases. Desired brick and mortar microstructural architecture was obtained by magnetic field alignment followed by hot-pressing for changing organic contents of the composites.

Following points demonstrate the major conclusions drawn at the end of this study:

- Among the hot-pressing based process combinations AC+HASC is more effective in obtaining mechanically superior nacre-like bulk composites with the optimum inorganic content and polymer matrix distribution it provide in the structure.
- Of the two different thermoplastic matrices, PS and ABS, used in the composites fabricated by hot-pressing based process combinations, PS leads to higher mechanical strength and stiffness due to its higher molecular weight and crystalline structure.
- According to the three point bending results PS matrix composite fabricated by AC+HASC method reveals 21% higher flexural strength than the one fabricated by TC+HASC method. In the case of the ABS matrix composites above mentioned difference in the flexural strength is ~32%.
- Even though TC+HASC process combination has also led to brick and mortar architecture with well-oriented glass flakes in the

structure, it revealed deficient mechanical properties compared to AC+HASC mainly caused by the higher porosity content resulting from the inefficient flow of the molten polymer during HASC step.

- Treatment of glass flake surfaces with an organofunctional silane, namely aminopropyltriethoxy silane, improved the interaction between the organic and inorganic phases revealing itself with increased strength values following this surface functionalization.
- For the AC+HASC processed PS and ABS matrix composites flexural strength increased by 34% and 27%, respectively, by the applied surface functionalization using silane.
- Work of fracture test results demonstrated that AC+HASC processed ABS matrix composites have higher fracture resistance due to higher elasticity and toughness of the ABS matrix. However, even though surface functionalization has led to an improvement in the energy absorption capacity of both matrix composites during crack growth, enhancement in the case of PS matrix composites was much more remarkable pointing out to a more effective interfacial characteristic achieved by silanization.
- Magnetite nanoparticles can be attached on glass flake surfaces from a cationic solution effectively in controlled amounts. Magnetite nanoparticle attached glass flakes respond to the applied field and their orientation can be controlled.
- In the case of composites fabricated by magnetic field assistance and hot-pressing, increasing the matrix content in the material has led to higher strength values, where the matrix can be distributed more effectively and uniformly in the structure when its amount is higher.

This shows that rather than maximizing the inorganic reinforcement content its ratio with the matrix should be optimized for optimized mechanical characteristics, and hence for maximized mechanical performance.

- Surface functionalization of magnetite nanoparticle attached glass flake surfaces has led to ~10% increase in flexural strength of composites fabricated by magnetic field assistance.
- The efficiency of the magnetic field assistance in controlling the alignment of the inorganic flakes depends on the strength of the applied magnetic field. Despite this limitation this is a practical method for the fabrication of nacre-like bulk lamellar composites with thermoplastic as well as thermoset polymer matrices.
- The methods mentioned in this dissertation could be applied to various types of thermoplastic polymer matrices. Furthermore, any inorganic material with flake or platelet morphology such as alumina or CaCO_3 etc. can be used as reinforcement in such composites using these methods. Consequently, presented methods are useful and efficient methods for the fabrication of bio-inspired bulk lamellar composites which can make them available for structural engineering applications.

REFERENCES

- [1]. Munch, E., Launey, M. E., Alsem, D. H., Saiz, E., Tomsia, a P., & Ritchie, R. O. (2008). Tough, bio-inspired hybrid materials. *Science (New York, N.Y.)*, 322(5907), 1516–20. doi:10.1126/science.1164865
- [2]. Barthelat, F. (2007). Biomimetics for next generation materials. *Philosophical Transactions. Series A, Mathematical, Physical, and Engineering Sciences*, 365(1861), 2907–19. doi:10.1098/rsta.2007.0006
- [3]. Xia, F., & Jiang, L. (2008). Bio-Inspired, Smart, Multiscale Interfacial Materials. *Advanced Materials*, 20(15), 2842–2858. doi:10.1002/adma.200800836
- [4]. Wegst, U. G. K., & Ashby, M. F. (2004). The mechanical efficiency of natural materials. *Philosophical Magazine*, 84(21), 2167–2186. doi:10.1080/14786430410001680935
- [5]. Ashby, M. F., Gibson, L. J., Wegst, U., & Olive, R. (1995). The Mechanical Properties of Natural Materials. I. Material Property Charts. *Proceedings of the Royal Society A: Mathematical, Physical and Engineering Sciences*, 450(1938), 123–140. doi:10.1098/rspa.1995.0075
- [6]. Katti, K. S., & Katti, D. R. (2006). Why is nacre so tough and strong? *Materials Science and Engineering: C*, 26(8), 1317–1324. doi:10.1016/j.msec.2005.08.013
- [7]. Katti, K. S., Mohanty, B., & Katti, D. R. (2006). Nanomechanical properties of nacre, 58105(August 2005). doi:10.1557/JMR.2006.0147
- [8]. Tushtev, K., Murck, M., & Grathwohl, G. (2008). On the nature of the stiffness of nacre. *Materials Science and Engineering: C*, 28(7), 1164–1172. doi:10.1016/j.msec.2007.10.039
- [9]. Katti, K. S., Katti, D. R., Pradhan, S. M., & Bhosle, A. (2011). Platelet interlocks are the key to toughness and strength in nacre. *Journal of Materials Research*, 20(05), 1097–1100. doi:10.1557/JMR.2005.0171
- [10]. Group, B., Zoology, A., & Materials, W. (1990). Comparison of nacre with other ceramic composites, 25.

- [11]. Oner Ekiz, O., Dericioglu, A. F., & Kakisawa, H. (2009). An efficient hybrid conventional method to fabricate nacre-like bulk nano-laminar composites. *Materials Science and Engineering: C*, 29(6), 2050–2054. doi:10.1016/j.msec.2009.04.001
- [12]. Gurbuz, S. N., & Dericioglu, A. F. (2013). Effect of reinforcement surface functionalization on the mechanical properties of nacre-like bulk lamellar composites processed by a hybrid conventional method. *Materials Science & Engineering. C, Materials for Biological Applications*, 33(4), 2011–9. doi:10.1016/j.msec.2013.01.013
- [13]. Chen, R., Wang, C., Huang, Y., & Le, H. (2008). An efficient biomimetic process for fabrication of artificial nacre with ordered-nanostructure. *Materials Science and Engineering: C*, 28(2), 218–222. doi:10.1016/j.msec.2006.12.008Artificial Carbonate Nanocrystals.pdf. (n.d.).
- [14]. Pandit, A., Ocakoglu, K., Buda, F., van Marle, T., Holzwarth, A. R., & de Groot, H. J. M. (2013). Structure determination of a bio-inspired self-assembled light-harvesting antenna by solid-state NMR and molecular modeling. *The Journal of Physical Chemistry. B*, 117(38), 11292–8. doi:10.1021/jp402210xBioinspired Au TiO₂ photocatalyst derived from butterfly wing (Papilio Paris).pdf. (n.d.).
- [15]. Libanori, R., Erb, R. M., & Studart, A. R. (2013). Mechanics of platelet-reinforced composites assembled using mechanical and magnetic stimuli. *ACS Applied Materials & Interfaces*, 5(21), 10794–805. doi:10.1021/am402975a
- [16]. Luz, G. M., & Mano, J. F. (2009). Biomimetic design of materials and biomaterials inspired by the structure of nacre. *Philosophical Transactions. Series A, Mathematical, Physical, and Engineering Sciences*, 367(1893), 1587–605. doi:10.1098/rsta.2009.0007
- [17]. Katti, D. R., Katti, K. S., Sopp, J. M., & Sarikaya, M. (2001). 3D finite element modeling of mechanical response in nacre-based hybrid nanocomposites, *11.25th Anniversary Article*
- [18]. Kakisawa, H., & Sumitomo, T. (2011). The toughening mechanism of nacre and structural materials inspired by nacre. *Science and Technology of Advanced Materials*, 12(6), 064710. doi:10.1088/1468-6996/12/6/064710
- [19]. Luz, G. M., & Mano, J. F. (2010a). Mineralized structures in nature: Examples and inspirations for the design of new composite materials and biomaterials. *Composites Science and Technology*, 70(13), 1777–1788. doi:10.1016/j.compscitech.2010.05.013

- [20]. Tang, Z., Kotov, N. a, Magonov, S., & Ozturk, B. (2003). Nanostructured artificial nacre. *Nature Materials*, 2(6), 413–8. doi:10.1038/nmat906
- [21]. Barthelat, F., Li, C., Comi, C., & Espinosa, H. D. (2006). Mechanical properties of nacre constituents and their impact, *3111*(July 2005), 1977–1986. doi:10.1557/JMR.2006.023
- [22]. Mukherjee, A. (Ed.). (2010). *Biomimetics Learning from Nature* . InTech.doi:10.5772/198
- [23]. Thomas, S., Ninan, N., Mohan, S., & Francis, E. (2012). *Natural Polymers, Biopolymers, Biomaterials, and Their Composites, Blends, and IPNs* (Vol. 2). Apple Academic Press
- [24]. DeMouthe J.F. (Ed.) Elsevier.(2006). *Natural Materials Sources, Properties and Uses*.
- [25]. Jiang, L.,Feng L.(2010). BIOINSPIRED INTELLIGENT NANOSTRUCTURED INTERFACIAL MATERIALS. Chemical Industry Press.
- [26]. Mohanty, A. K., Drzal, L. T., & Group, F. (2005). *NATURAL FIBERS , BIOPOLYMERS , AND BIOCOMPOSITES*.
- [27]. Baker, A., Dutton, S., & Kelly, D. (2004). *Composite Materials for Aircraft Structures* . American Institute of Aeronautics and Astronautics.
- [28]. Chung, D.L.D.(2010). *Composite Materials Second Edition*. Springer. doi:10.1007/978-1-84882-831-5
- [29]. Wallenberger,F.T.,Bingham,P.A.(2010). *Fiberglass and Glass Technology Energy Friendly Compositions and Applications* .Springer.doi:10.1007/978-1-4419-0736-3
- [30]. Thomas, S., Joseph, K., Malhotra, S. K., & Goda, K. (n.d.). *Edited by Related Titles Nanocomposites Wood-Plastic Composites Rubber Nanocomposites Flame Retardant Polymer Nanocomposites Polyolefin Blends and Composites Advances in Bioceramics and Biocomposites II , Ceramic Engineering and Science Polyolefin Composi*.
- [31]. Liu, K., & Jiang, L. (2011). Bio-inspired design of multiscale structures for function integration. *Nano Today*, 6(2), 155–175. doi:10.1016/j.nantod.2011.02.002

- [32]. Lee, Y., Chung, H. J., Yeo, S., Ahn, C.-H., Lee, H., Messersmith, P. B., & Park, T. G. (2010). Thermo-sensitive, injectable, and tissue adhesive sol–gel transition hyaluronic acid/pluronic composite hydrogels prepared from bio-inspired catechol-thiol reaction. *Soft Matter*, 6(5), 977. doi:10.1039/b919944f
- [33]. Tampieri, A., Celotti, G., Landi, E., Sandri, M., Roveri, N., & Falini, G. (2003). Biologically inspired synthesis of bone-like composite: self-assembled collagen fibers/hydroxyapatite nanocrystals. *Journal of Biomedical Materials Research. Part A*, 67(2), 618–25. doi:10.1002/jbm.a.10039
- [34]. Porter, B. M. M., & Mckittrick, J. (n.d.). It's tough to be strong : Advances in bioinspired based materials, 93(5).
- [35]. Haldar, S., & Bruck, H. a. (2014). Mechanics of composite sandwich structures with bioinspired core. *Composites Science and Technology*, 95, 67–74. doi:10.1016/j.compscitech.2014.02.011
- [36]. Ji, B., & Gao, H. (2004). Mechanical properties of nanostructure of biological materials. *Journal of the Mechanics and Physics of Solids*, 52(9), 1963–1990. doi:10.1016/j.jmps.2004.03.006
- [37]. Liu, K., Yao, X., & Jiang, L. (2010). Recent developments in bio-inspired special wettability. *Chemical Society Reviews*, 39(8), 3240–55. doi:10.1039/b917112f
- [38]. Yao, H.-B., Tan, Z.-H., Fang, H.-Y., & Yu, S.-H. (2010). Artificial nacre-like bionanocomposite films from the self-assembly of chitosan-montmorillonite hybrid building blocks. *Angewandte Chemie (International Ed. in English)*, 49(52), 10127–31. doi:10.1002/anie.201004748
- [39]. Feng, X.-Q., Gao, X., Wu, Z., Jiang, L., & Zheng, Q.-S. (2007). Superior water repellency of water strider legs with hierarchical structures: experiments and analysis. *Langmuir: The ACS Journal of Surfaces and Colloids*, 23(9), 4892–6. doi:10.1021/la063039b
- [40]. Chen, J., Su, H., Song, F., & Moon, W. (2012). Bio inspired Au/TiO₂ photocatalyst derived from butterfly wing (Papilio Paris). *Journal of Colloid and Interface Science* Retrieved September 15, 2014 from <http://www.sciencedirect.com/science/article/pii/S002197971101544X>
- [41]. Meyers, M. A., Lin, A. Y.-M., Chen, P.-Y., & Muiyco, J. (2008). Mechanical strength of abalone nacre: role of the soft organic layer. *Journal of the Mechanical Behavior of Biomedical Materials*, 1(1), 76–85. doi:10.1016/j.jmbbm.2007.03.001

- [42]. Barthelat, F., Tang, H., Zavattieri, P., Li, C., & Espinosa, H. (2007). On the mechanics of mother-of-pearl: A key feature in the material hierarchical structure. *Journal of the Mechanics and Physics of Solids*, 55(2), 306–337. doi:10.1016/j.jmps.2006.07.007
- [43]. Currey, J. D. (1977). Mechanical Properties of Mother of Pearl in Tension. *Proceedings of the Royal Society B: Biological Sciences*, 196(1125), 443–463. doi:10.1098/rspb.1977.0050
- [44]. Luz, G. M., & Mano, J. F. (2010b). Mineralized structures in nature: Examples and inspirations for the design of new composite materials and biomaterials. *Composites Science and Technology*, 70(13), 1777–1788. doi:10.1016/j.compscitech.2010.05.013
- [45]. Stempflé, P., Pantalé, O., Rousseau, M., Lopez, E., & Bourrat, X. (2010). Mechanical properties of the elemental nanocomponents of nacre structure. *Materials Science and Engineering: C*, 30(5), 715–721. doi:10.1016/j.msec.2010.03.003
- [46]. Rousseau, M., Lopez, E., Couté, A., Mascarel, G., Smith, D. C., Naslain, R., & Bourrat, X. (2005). Sheet nacre growth mechanism: a Voronoi model. *Journal of Structural Biology*, 149(2), 149–57. doi:10.1016/j.jsb.2004.09.005
- [47]. Espinosa, H. D., Rim, J. E., Barthelat, F., & Buehler, M. J. (2009). Merger of structure and material in nacre and bone – Perspectives on de novo biomimetic materials. *Progress in Materials Science*, 54(8), 1059–1100. doi:10.1016/j.pmatsci.2009.05.001
- [48]. Lin, A., & Meyers, M. A. (2005). Growth and structure in abalone shell. *Materials Science and Engineering: A*, 390(1-2), 27–41. doi:10.1016/j.msea.2004.06.072
- [49]. Jackson, A. P., Vincent, J. F. V., & Turner, R. M. (1988). The Mechanical Design of Nacre. *Proceedings of the Royal Society B: Biological Sciences*, 234(1277), 415–440. doi:10.1098/rspb.1988.0056
- [50]. Meyers, M. A., Chen, P.-Y., Lin, A. Y.-M., & Seki, Y. (2008). Biological materials: Structure and mechanical properties. *Progress in Materials Science*, 53(1), 1–206. doi:10.1016/j.pmatsci.2007.05.002
- [51]. Chen, P.-Y., McKittrick, J., & Meyers, M. A. (2012). Biological materials: Functional adaptations and bioinspired designs. *Progress in Materials Science*, 57(8), 1492–1704. doi:10.1016/j.pmatsci.2012.03.001

- [52]. Cartwright, J. H. E., & Checa, A. G. (2007). The dynamics of nacre self-assembly. *Journal of the Royal Society, Interface / the Royal Society*, 4(14), 491–504. doi:10.1098/rsif.2006.0188
- [53]. Meyers, M. A., Chen, P.-Y., Lin, A. Y.-M., & Seki, Y. (2008). Biological materials: Structure and mechanical properties. *Progress in Materials Science*, 53(1), 1–206. doi:10.1016/j.pmatsci.2007.05.002
- [54]. Nudelman, F., Gotliv, B. A., Addadi, L., & Weiner, S. (2006). Mollusk shell formation: mapping the distribution of organic matrix components underlying a single aragonitic tablet in nacre. *Journal of Structural Biology*, 153(2), 176–87. doi:10.1016/j.jsb.2005.09.009
- [55]. Li, X. (2007). Nanoscale structural and mechanical characterization of natural nanocomposites: Seashells. *Jom*, 59(3), 71–74. doi:10.1007/s11837-007-0043-2
- [56]. Chen, P.-Y., Lin, a Y. M., Lin, Y.-S., Seki, Y., Stokes, a G., Peyras, J., ... McKittrick, J. (2008). Structure and mechanical properties of selected biological materials. *Journal of the Mechanical Behavior of Biomedical Materials*, 1(3), 208–26. doi:10.1016/j.jmbbm.2008.02.003
- [57]. Huang, S., Phua, S. L., Liu, W., Ding, G., & Lu, X. (2014). Nacre-like composite films based on mussel-inspired “glue” and nanoclay. *RSC Advances*, 4(3), 1425. doi:10.1039/c3ra45793a
- [58]. Cheng, Q., Jiang, L., & Tang, Z. (2014). Bioinspired layered materials with superior mechanical performance. *Accounts of Chemical Research*, 47(4), 1256–66. doi:10.1021/ar400279t
- [59]. Wang, J., Cheng, Q., & Tang, Z. (2012). Layered nanocomposites inspired by the structure and mechanical properties of nacre. *Chemical Society Reviews*, 41(3), 1111–29. doi:10.1039/c1cs15106a
- [60]. Wei, H., Ma, N., Shi, F., Wang, Z., Zhang, X., December, R. V., February, V. (2007). Artificial Nacre by Alternating Preparation of Layer-by-Layer Polymer Films and CaCO₃ Strata, (5), 1974–1978. doi:10.1039/b61559.(15)
- [61]. Bonderer, L. J., Studart, A. R., & Gauckler, L. J. (2008). Bioinspired design and assembly of platelet reinforced polymer films. *Science (New York, N.Y.)*, 319(5866), 1069–73. doi:10.1126/science.1148726
- [62]. Sarikaya, M., Fong, H., Frech, D. W., & Humbert, R. (1999). Biomimetic Assembly of Nanostructured Materials. *Materials Science Forum*, 293, 83–98. doi:10.4028/www.scientific.net/MSF.293.83

- [63]. Yao, H.-B., Tan, Z.-H., Fang, H.-Y., & Yu, S.-H. (2010). Artificial nacre-like bionanocomposite films from the self-assembly of chitosan-montmorillonite hybrid building blocks. *Angewandte Chemie (International Ed. in English)*, 49(52), 10127–31. doi:10.1002/anie.201004748
- [64]. Libanori, R., Münch, F. H. L., Montenegro, D. M., & Studart, A. R. (2012). Hierarchical reinforcement of polyurethane-based composites with inorganic micro- and nanoplatelets. *Composites Science and Technology*, 72(3), 435–445. doi:10.1016/j.compscitech.2011.12.005
- [65]. Coupling, S., & Guide, A. (n.d.). Silane coupling agent guide.
- [66]. Ch, C. H., & H, S. O. C. (n.d.). Silane Coupling Agents :
- [67]. Search, P. (n.d.). APPLYING A SILANE COUPLING AGENT.
- [68]. Choi, S.-H., & Zhang Newby, B. (2006). Suppress polystyrene thin film dewetting by modifying substrate surface with aminopropyltriethoxysilane. *Surface Science*, 600(6), 1391–1404. doi:10.1016/j.susc.2006.01.050
- [69]. Flewitt, P. E. J., & Wild, R. K. (2003). Physical Methods for Materials Characterisation. doi:10.1887/0750308087
- [70]. Awaja, F., Gilbert, M., Kelly, G., Fox, B., & Pigram, P. J. (2009). Adhesion of polymers. *Progress in Polymer Science*, 34(9), 948–968. doi:10.1016/j.progpolymsci.2009.04.007
- [71]. C.Riviere, J., & Myhra, S. (2009). *Surface and Interface Analysis-Methods for problem -solving* . CRC Press Taylor & Francis Group.
- [72]. Silverstein ,webster and kiemle Spectroscopy Chemistry NMR FTIR MS - Silverstein.pdf. (n.d.).
- [73]. S.Nikolic, G. (2011). Application of Fourier Transform Mid-Infrared Spectroscopy (FTIR) for Research into Biomass Feed-Stocks. In *FOURIER TRANSFORMS -NEW ANALYTICAL APPROACHES AND FTIR STRATEGIES* (pp. 71-85). InTec
- [74]. Teraoka, I. (2002). *An Introduction to Physical Properties* (Vol. 3).
- [75]. Sanchez, I. C., & Lacombe, R. H. (1978). Statistical Thermodynamics, *11*(6), 1145–1156.
- [76]. Dobry, A., & Physico-chimique, I. D. B. (1946). Phase Separation in Polymer Solution, 90–100.

[77]. Beek, G. P. Van Der, Stuart, M. A. C., Fler, G. J., & Hofman, J. E. (2001). A Chromatographic Method for the Determination of Segmental Adsorption Energies of Polymers . Polystyrene on Silica, (5), 1180–1186.

[78]. Irgens, F. (2014). Rheology and Non-Newtonian Fluids. Cham: Springer International Publishing. doi:10.1007/978-3-319-01053-3

[79]. Choi, S.-H., & Zhang Newby, B. (2006). Suppress polystyrene thin film dewetting by modifying substrate surface with aminopropyltriethoxysilane. Surface Science, 600(6), 1391–1404. doi:10.1016/j.susc.2006.01.050